REPORT UAG - 9

WORLD DATA CENTER A

Upper Atmosphere Geophysics

DATA ON COSMIC RAY EVENT OF NOVEMBER 18, 1968 AND ASSOCIATED PHENOMENA

April 1970

WORLD DATA CENTER A

National Academy of Sciences

2101 Constitution Avenue, N. W. Washington, D. C. U.S.A., 20418

World Data Center A consists of the Coordination Office

and eight subcenters:

World Data Center A
Coordination Office
National Academy of Sciences
2101 Constitution Avenue, N.W.
Washington, D.C., U.S.A. 20418
Telephone (202) 961-1404

Solar and Interplanetary Phenomena, Ionospheric Phenomena, Flare-Associated Events, Aurora, Cosmic Rays, Airglow:
World Data Center A:
Upper Atmosphere Geophysics
Environmental Science Services Administration
Boulder, Colorado, U.S.A. 80302
Telephone (303) 447-1000 Ext. 3381

Geomagnetism, Seismology, Gravity and Tsunami:
World Data Center A:
Geomagnetism, Seismology, Gravity & Tsunami
Environmental Data Service, ESSA
Rockville, Maryland, U.S.A. 20852
Telephone (301) 496-8160

Glaciology:
World Data Center A:
Glaciology
American Geographical Society
Broadway at 156th Syreet
New York, New York, U.S.A. 10032
Telephone (212) 234-8100

Longitude and Latitude:
World Data Center A:
Longitude & Latitude
U.S. Naval Observatory
Washington, D.C., U.S.A. 20390
Telephone (202) 698-8422

Meteorology (and Nuclear Radiation):
World Data Center A:
Meteorology
National Weather Records Center
Asheville, North Carolina, U.S.A. 28801
Telephone (704) 253-0481

Oceanography:
World Data Center A:
Oceanography
Building 160
Second and N Streets, S.E.
Washington, D.C., U.S.A. 20390
Telephone (202) 698-3753

Rockets and Satellites:
World Data Center A::
Rockets and Satellites
National Academy of Sciences
2101 Constitution Avenue, N.W.
Washington, D.C., U.S.A. 20418
Telephone (202) 961-1404

Upper Mantle Project:
World Data Center A:
Upper Mantle Project
Lamont Geological Observatory
Palisades, New York, U.S.A. 10964
Telephone (914) 359-2900 Ext. 209

Notes:

(1) World Data Centers conduct international exchange of geophysical observations in accordance with the principles set forth by the International Council of Scientific Unions. WDC-A is established in the United States under the auspices of the National Academy of Sciences.

(2) Communications regarding data interchange matters in general and World Data Center A as a whole should be addressed to: World Data Center A, Coordination Office (see address above).

(3) Inquiries and communications concerning data in specific disciplines should be addressed to the appropriate subcenter listed above.

WORLD DATA CENTER A

Upper Atmosphere Geophysics

REPORT UAG - 9

DATA ON COSMIC RAY EVENT OF NOVEMBER 18, 1968 AND ASSOCIATED PHENOMENA

compiled by

J. Virginia Lincoln

WDC-A, Upper Atmosphere Geophysics

Boulder, Colorado

Prepared by Research Laboratories, ESSA, Boulder, Colorado
and published by

U.S. DEPARTMENT OF COMMERCE
ENVIRONMENTAL SCIENCE SERVICES ADMINISTRATION
ENVIRONMENTAL DATA SERVICE
ASHEVILLE, NORTH CAROLINA, USA 28801

April 1970

SUBSCRIPTION PRICE: $9.00 a year; $2.50 additional for foreign mailing; single copy price varies.* Checks and money orders should be made payable to the Superintendent of Documents. Remittance and correspondence regarding subscriptions should be sent to the Superintendent of Documents, Government Printing Office, Washington, D.C. 20402.

*Price of this issue 55 cents.

FOREWORD

This report is one of a series of special data compilations and discussion on solar-terrestrial events of special interest, and collects in one place more data and more detailed data than normally appear in the scientific literature. Cosmic ray increases at sea level are relatively rare phenomena and there has been an informal consensus among cosmic ray scientists that such a compilation should be made for the event of November 18, 1968.

Actually this report is an outgrowth of the preceding one in this series, UAG-8 "Data on Solar-Geophysical Activity October 24 - November 6, 1968." That report was compiled to fulfill a recommendation of the Inter-Union Commission on Solar-Terrestrial Physics and was the result of the more than 50 replies providing detailed data or discussions of observations. In these replies, many cosmic ray workers in particular included data and discussion through November 18, commenting that this was a very significant phenomenon and from the standpoint of their discipline much more interesting than the phenomena associated with the solar activity of the preceding weeks. Rather than have UAG-8 include data and discussions on the November 18 event from some authors but not others, it was decided to prepare this separate report from this volunteered information supplemented by the results of a new request to the other contributors to UAG-8.

This is a truly international effort as can be seen by the list of contributors, acknowledgment of whose participation is implicit. The solar-terrestrial scientific community is indebted to the compilers and editors of this report, the staff of World Data Center-A, Upper Atmosphere Geophysics, Miss J. Virginia Lincoln, Director. The provision of these special data reports, however, is still an experiment in communication within the scientific community and the reactions of the community to this approach will determine the future course of these efforts.

A. H. Shapley, Chairman
IUCSTP Working Group 1,
Monitoring of the Solar-
Terrestrial Environment

TABLE OF CONTENTS

	Page
FOREWORD A. H. Shapley	1
1. INTRODUCTION AND BACKGROUND DATA J. Virginia Lincoln	5
2. SOLAR REGION	
"Preceding Changes in the Active Region" (Constance Sawyer and Sara F. Smith)	9
"Data Concerning November 18, 1968, in Addenda to 'Solar Circumstances at the Cosmic Ray Decrease on January 28, 1967'" (Helen W. Dodson and E. Ruth Hedeman)	13
3. SOLAR RADIO EVENTS	
"On the Type IV Burst of November 18, 1968" (A. Krüger)	14
"An Outstanding mm-Radioburst Observed November 18, 1968" (G. Feix)	17
"The Radio Outburst of November 18, 1968 at 1026 UT Observed at Metric Waves with High Temporal Resolution" (A. Abrami)	20
4. SOLAR X-RAYS	
"Solar X-Ray Emission on November 18, 1968" (D. M. Horan and R. W. Kreplin)	23
"Solar Cosmic-Ray Event on 18 November 1968" (Stephen Pintér)	26
5. SPACE OBSERVATIONS	
"Editorial Comments" (J. Virginia Lincoln)	30
"Explorer 34 Solar Proton Monitoring Experiment, Ep >10 Mev, November 17 - 28, 1968" (C. O. Bostrom, D. J. Williams and J. F. Arens)	31
"Energetic Proton Flux (5-70 Mev) at Synchronous Orbit November 11 - December 8, 1968" (G. A. Paulikas)	32
"Protons, Alpha Particles, and Electrons Resulting from the 18 November 1968 Solar Flare" (L. J. Lanzerotti)	34
"Pioneer 9 Solar Wind Velocity and Electric Field Data 8 November 1968 to 4 January 1969" (Ira M. Green and F. L. Scarf)	40
6. COSMIC RAYS	
"Tabulations and Selected Graphs of Neutron Monitor Observations November 18, 1968" (J. Virginia Lincoln)	43
"Scintillation Monitor Bologna, Italy 15-minute Observations" (M. Galli)	64
"Events of November 15 to November 22, 1968" (John F. Steljes)	66
"Asymptotic Directions of Approach Appropriate for the High Energy Solar Proton Event of November 18, 1968" (M. A. Shea and D. F. Smart)	68
"Investigations of Cosmic Ray Intensity Variations in Antarctica" (M. A. Pomerantz and S. P. Duggal)	81

Table of Contents (Continued)

Page

7. IONOSPHERE
"Observations in the Arctic and Antarctic of the 18 November 1968 Solar Cosmic Ray Event" 83
(A. D. Goedeke and A. J. Masley)
"Comparison of Transpolar VLF Measurements with Riometer Measurements Made Within the Polar Cap During the PCA Event November 18, 1968" 86
(K. Rinnert)
"Ionospheric Absorption Around November 18, 1968" 88
(H. Schwentek)
"Radio Propagation Quality Indices November 15-30, 1968" 89
(B. Beckmann)

8. GEOMAGNETIC ACTIVITY
"Note on 'On the Solar and Geomagnetic Events of October-November 1968' by M. C. Ballario in World Data Center A - Upper Atmosphere Geophysics Report UAG-8, March 1970" 90
(J. Virginia Lincoln)
"Equatorial Dst" 91
(M. Sugiura and S. J. Cain)
"Geomagnetic Disturbances During the Period November 16-21, 1968 Associated with the McMath Plage Regions 9760, 9772 and 9780" 92
(K. Kawasaki and S.-I. Akasofu)

1. INTRODUCTION AND BACKGROUND DATA

by

J. Virginia Lincoln
Space Disturbances Laboratory
ESSA Research Laboratories, Boulder, Colorado

As stated in the foreword, this report has resulted from the several contributions suggested for study of the cosmic ray ground level event of November 18, 1968. As with other reports in this series, each person's contribution has been prepared without the benefit of seeing the others. This naturally leads to some repetition, but from different viewpoints.

General Activity

The general solar situation on November 18, 1968 is indicated in Fig. 1 which is a reprint of the solar charts and maps for November 18, 1968 as published in "Solar-Geophysical Data", Number 293, issued January 1969. The most likely flare to associate with this event occurred in McMath Region 9760. Table 1 presents this region's history in the manner now used in "Solar-Geophysical Data." The calcium plage data are from McMath-Hulbert Observatory or Catania if in parentheses; the sunspot magnetic field data from Mt. Wilson Observatory; the area, count and Zürich classification from Sacramento Peak Observatory, or Boulder or Culgoora if in parentheses; and the 9.1 cm data from Stanford University. The units are explained in "Solar-Geophysical Data Descriptive Text."

Table 1

McMATH REGION 9760 CMP DATE 11.5								RETURN OF REGION 9736								ROTATION 2	
CALCIUM PLAGE DATA								SUNSPOT DATA								9.1 CM	
NOV.	MC NO.	LAT	CMD	L	AREA	INT	MW NO.	LAT	CMD	L	MAG	H	AREA	CNT	C	INT	FLUX
4	9760	N18	E88	359	200	1.0										9	
5	9760	N19	E83	346	1500	2.0	17045	N19	E80	346	(βp)	3	(50)	3	D	18	11
6							17045	N19	E64	346	(βp)	2	73	12	J	14	5
7	(11)	(N20)	(E55)	349	(4503)	(4.3)	17045	N19	E53	346	(βγ)	3	113	16	D	16	6
8	9760	N19	E38	348	3000	3.5	17045	N18	E40	346	(δ)	5	(500)	27	D	24	8
9	(11)	(N17)	(E26)	349	(2847)	(3.6)	17045	N18	E24	346	(δ)	5	614	12	H	28	12
10	9760	N18	E11	352	3000	3.5	17045	N19	E14	346	(δ)	5	574	9	H	38	15
							17056	N17	E05	355	(βp)	2					
11	9760	N18	W01	350	3000	4.0	17045	N19	E02	345	δ		563	26	H	-	-
							17056	N17	W07	354	βp						
12	9760	N18	W13	349	3000	3.5							566	34	H	36	17
13	9760	N17	W26	349	3200	3.5							596	16	H	34	12
14	(11)	(N20)	(W39)	352	(6600)	(4.2)							(470)	15	C	30	12
15	(11)	(N18)	(W50)	349	(5653)	(5.2)							(620)	19	G	30	10
16	(11)	(N20)	(W62)	348	(5606)	(3.4)	17045	N20	W66	348	δ		(450)	14	C	26	10
17							17045	N20	W76	344	(δ)	4	(450-600)	4	H	23	9
18	9760	N19	W90	345	1000	3.5										19	9

The final Zürich relative sunspot numbers, Rz, and the 2800 MHz solar flux, S, associated with the period are given below; there was no outstanding change on November 18:

	Rz	S		Rz	S
Nov. 16	84	130.5	Nov. 20	92	142.5
Nov. 17	82	143.8	Nov. 21	84	137.1
Nov. 18	77	151.5	Nov. 22	81	134.4
Nov. 19	80	144.8	Nov. 23	76	135.7

Events

For convenience of the user some of the data as published in "Solar-Geophysical Data" are repeated here. At the time of the cosmic ray event there was a confirmed grouped flare, number 19246. The flare had two maxima as follows:

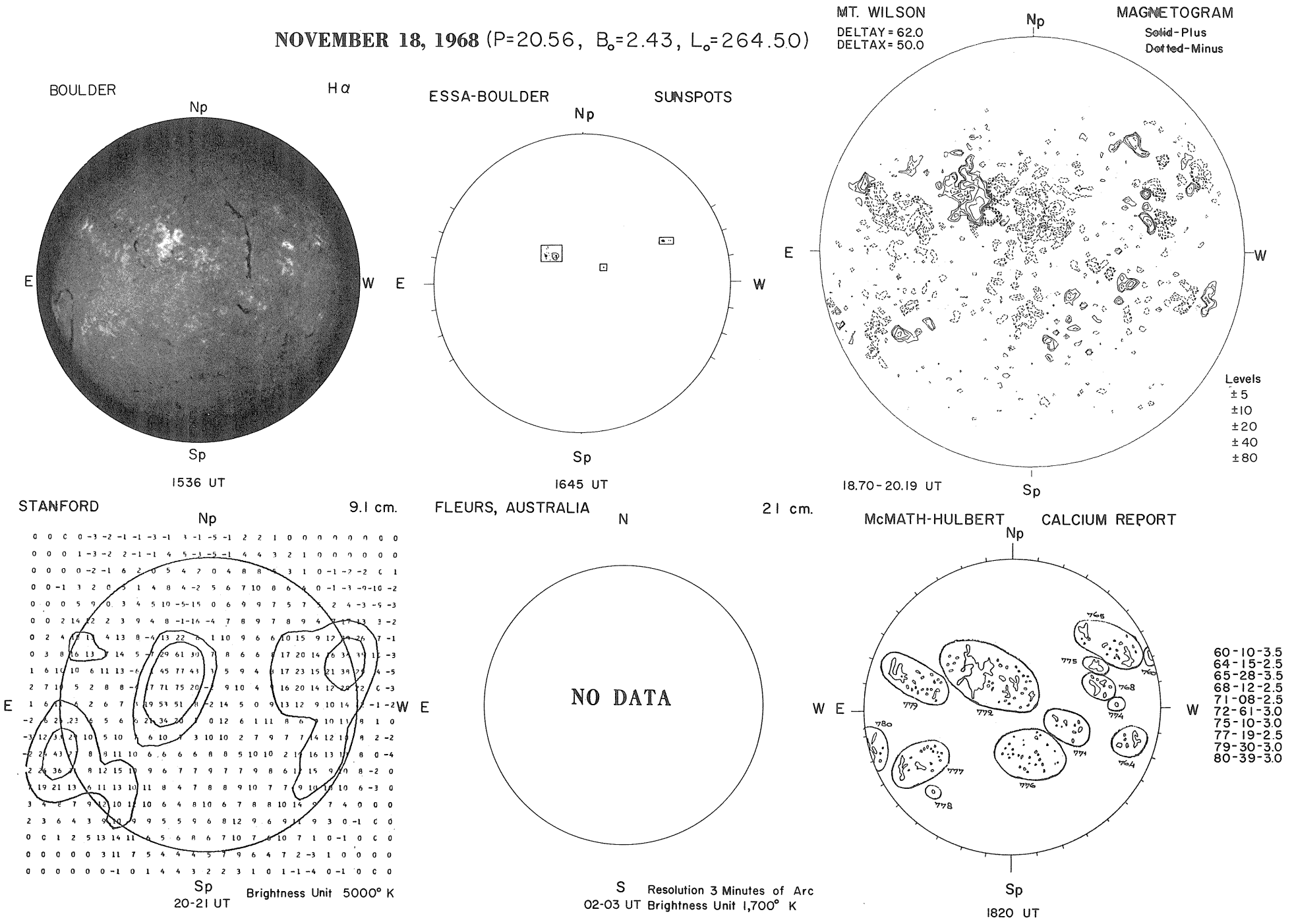

Fig. 1. General solar situation November 18, 1968.

Universal Time			Location						
Start	End	Max Phase	Lat	Approx. Mer Dist.	Central Distance	Duration Min	Importance	Meas. Area Sq. Deg.	Remarks
1017	1127	1033	N21	W87	0.998	70	1B	2.07	A 3335
1026	1235	1058	N20	W90	1.000	129	1B	1.66	AHVY 4116

Remarks

A = Eruptive prominence, base at >90° V = Occurrence of an explosive phase
H = Flare with high velocity dark surge Y = Onset of a system of loop-type prominences

The first number is the number of stations reporting the individual maximum and not necessarily the total number of stations reporting some part of the flare event. (For this flare there were 6 stations in the latter category.) The second number is the number of values entering the average importance, the third the number of values entering the average measured area and the last number the number of stations reporting at the time of the individual maximum and not necessarily the total number of stations observing during the flare event.

The sudden ionospheric disturbance events during the time of the flare were:

Universal Time				Wide Spread Index	Number of Station Reports by Type						
Start	End	Max	Imp.		SWF	SCNA	SEA	SPA	LF-SPA	SES	SFD
1026	1220	1050	3	5	3	1	3	2	2	3	
1114	1236	1135	2	5				1	1	1	

The worldwide solar radio emission outstanding occurrences were not published in "Solar-Geophysical Data" for this period. The events of November 18, 1968 are therefore given in Table 2 in the format in which they are now published. The spectral data were published and are repeated here:

STATION	DECIMETRIC BAND START UT	END UT	INT.	TYPE	METRIC BAND START UT	END UT	INT.	TYPE
WEISSENAU	1026.5	1034	3	IIIGG				
	1026.5	1050	3	IV				
	1026.5	1105	3	II				
					1045	1104	2	IIIGG,DP
	1122.5	1126	1	III				

The magnetic activity throughout the period is indicated in Fig. 2 which presents the 27-day musical-note diagram of Kp. There is an sc on November 20 at 0904 UT reported by 49 stations (ssc: 44 [A: 23; B: 21]; si: 4; pi2: 1) but the storm which followed was of short duration and of only moderate intensity.

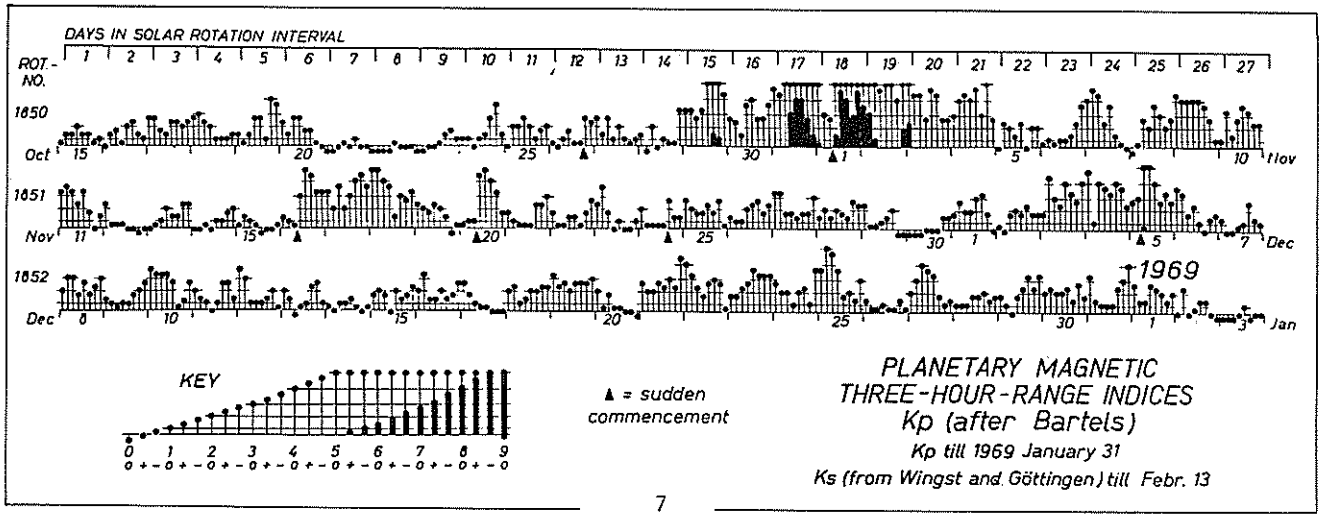

Table 2

SOLAR RADIO EMISSION
OUTSTANDING OCCURRENCES

NOVEMBER 1968

NOV 1968	FREQUENCY	STATION	TYPE	STARTING TIME UT	TIME OF MAXIMUM UT	DURATION MINUTES	FLUX DENSITY $10^{-22} Wm^{-2} Hz^{-1}$ PEAK	MEAN	INT	REMARKS
18	9400	TYKW	5	0327	0329.2	6	7.0	2.0		
	8800	MNL	4	0359.7	0401.5	3.7	39.3	19.7		
	4995	MNL	4	0359.7	0401.5	3.7	8.9	4.4		
	8800	MNL	29	0403.4	0403.4	13.6	15.3	4.3		
	4995	MNL	29	0403.4	0403.4	26.4U	4.4	1.5		
	8800	MNL	28	0419.8	0422.8	4.2	11.0	4.3		
	4995	MNL	28	0419.8	0423.1	4.2	13.3	5.9		
	9400	TYKW	45	0400	0426.7	110	55.0	10.0		
	3750	TYKW	45	0405	0426.7	100	20.0	3.0		
	2695	MNL	22	0420.5	0426.8	22.5	9.9	3.3		
	2000	TYKW	45	0420	0426.5	90	5.0	2.0		
	8800	MNL	4	0424	0426.8	4.2	50.3	24.0		
	4995	MNL	4	0424	0426.8	4	43.0	20.7		
	17000	TOKO	45	0425.9	0426.5	1.2	15.0			
	8800	MNL	29	0428.2	0428.2	55.8	13.1	2.2		
	4995	MNL	29	0428	0428	51	11.8	3.5		
	200	GORK	41	0613.2	0614.5	1.8	75.0			
	100	GORK	41	0644.1	0646.1	2.8	40.0D			
	9100	GORK	1	0746.8	0748	3.4	13.0	2.7		
	9139	NEUS	20	0926.5E	0926.5		5.5			
	19000	SLOU	46	1025.8	1030	26	1970.0			
	9500	NERA	47	1025.4	1027.2	31				
	9139	NEUS	47	1025.5	1027	15 U	2600.0			
	9100	GORK	47	1025.5	1027	35.5	2970.0	910.0		
	3100	CRIM	47	1025	1029	160	770.0			
	225	HARS	45	1025.5	1031	25	375.0D	60.0U		
	15000	KISV	47	1026	1030	34.5	2755.0U	815.0U		
	6100	KISV	47	1026	1045	38.5	945.0	43.0U		
	3000	NERA	47	1026	1029.7	40	1400.0	600.0		
	2950	GORK	45	1026	1027.9U	37.3U	720.0			
	2950	GORK		1026	1029.7		920.0			
	2950	GORK		1026	1044.8		825.0			
	2920	BERL	47	1026	1029.5	214 U				
	2800	SLOU	45	1026	1029.5	22	1220.0			
	1500	NEUS	47	1026.5	1030	210 D	1091.0			
	1420	KIEL	45	1026	1031	44	900.0	350.0		
	930	BORD	45	1026	1029.4	66	1200.0	69.0		SLOW DECLINE
	808	ONDR	45	1026		34.5				
	650	GORK	45	1026.4	1032.4	35	540.0			
	650	GORK		1026.4	1040.5		172.0			
	420	KIEL	45	1026	1029	67	400.0D	300.0		
	260	ONDR	45	1026.5		34	85.0D			
	240	KIEL	45	1026	1030	24	15000.0D	600.0		
	234	POTS	45	1026 U	1031.5	174	2000.0	18.0		
	200	NERA	47	1026.6	1032.1	9	3500.0	1500.0		
	200	GORK	48	1026.7	1032.1	9.2	4000.0D			
	111	POTS	45	1026.5U	1034 U	51.5	8000.0	60.0		
	100	GORK	49	1026.9	1034.2U	60	100000.0D			
	100	GORK	48	1026.9	1034.2	9.1	100000.0D			
	536	ONDR	45	1027	1034	75	325.0			
	202	IZMI	45	1027	1032	9	2000.0	300.0		
	100	GORK	49	1036	1049.1U	50.9	2700.0			
	23	POTS	45	1040 U	1048 U	25	4000.0	1200.0		
	9139	NEUS	29	1025.5	1044.5		1950.0			
	2920	BERL	29	1026	1044.5					
	1500	NEUS	29	1026.5	1044.5		284.0			
	2800	SLOU	29	1048	1048	114	550.0			
	19000	SLOU	29	1052 U	1052 U	60	160.0			
	3800	GORK		1055 E		75 E				
	9500	NERA	29	1056.7		73				
	3000	NERA	29	1056.1		274 D	65.0			
	9100	GORK	29	1100	1100	76	163.0	73.0		
	1500	BERL	46	1120	1121	6	10.5	1.7		
	260	ONDR	5	1135	1135	1	15.0			
	1500	NEUS	46	1145	1154.2	10	9.0	1.3		
	15400	SGMR	3	1501	1504	7.1	14.3	5.8		
	4995	SGMR	3	1502.9	1503.5	16	15.0	5.2		
	8800	SGMR	3	1503.2	1503.9	2.9	11.3	5.0		
	2800	OTTA	23	1745	1830	110	5.0	2.5		
	2800	OTTA	1	1804	1805	2.5	2.2	1.1		
	2800	OTTA	1	1813	1814	3	3.4	1.7		

2. SOLAR REGION

"Preceding Changes in the Active Region"

by

Constance Sawyer
Space Disturbances Laboratory
ESSA Research Laboratories, Boulder, Colorado

and

Sara F. Smith, Lockheed Solar Observatory
Rye Canyon Research Center of Lockheed
Saugus, California

ABSTRACT

The sunspot group that produced the flare of 1968 November 18 showed three features that have been described as characteristic of energetic active regions: one part of the region grew as another part seemed to decay [Martres et al., 1968]; the line of magnetic polarity reversal lay nearly parallel to the solar equator; and the transition from the normal, north-south orientation appeared as a counterclockwise rotation in this northern-hemisphere region [Sakurai, 1967]. The polarity reversal line appeared to rotate by about 30° per day from November 14 to 17.

The primary data used in this study are derived from Lockheed Solar Observatory's filter magnetograms. This technique for observing magnetic fields is described and illustrated by Ramsey [1969] and is similar in principle to the methods employed by Leighton [1959] and Harvey [1963]. Briefly, the method of obtaining the magnetic field information is as follows. Half-second exposures are taken through a filter having a bandpass of .15Å centered .15Å into the blue wing of the FeI line at 5324Å. A 1/4 λ analyzer is rotated 90 degrees between successive frames of film exposed at 10-second intervals. By this technique frames of film containing righthanded circularly polarized light (negative polarity) are alternated between frames containing lefthanded circularly polarized light (positive polarity). The intensity of the polarized component of light is related to the strength of the line-of-sight magnetic fields. When the film is projected an obvious flickering in intensity occurs at locations where the line-of-sight components of magnetic field are strong. Areas of opposite polarity are readily distinguished because they flicker out of phase. Lines where the flicker changes phase, therefore, correspond to the boundaries where the polarity reverses. It should be noted that the intensity of the flicker varies greatly with changing image quality and with distance from the center of the solar disk as well as with the strength of the magnetic field components being observed. In this contribution, however, we are primarily concerned with the qualitative use of these films for determining the configuration of the line-of-sight components of the magnetic field rather than quantitative values of field strength.

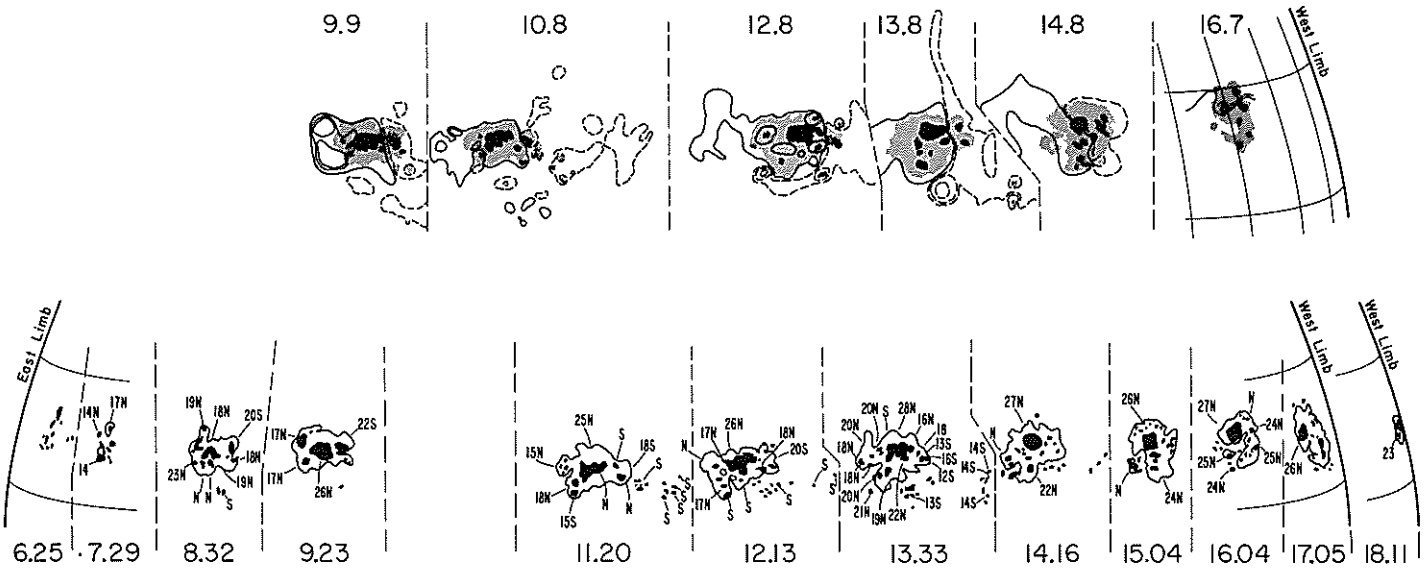

Fig. 1. Upper line: The sunspot group and magnetic fields as seen on filter magnetograms in the period preceding the flare of November 18, 1968. Lower line: sunspot drawings and magnetic fields from Solnechnye Dannye. The region is shown on successive days as it rotated across the disk.

The upper row of sketches in Figure 1 shows characteristic features identified in these flickering FeI films. The outer contour encloses the region where the flicker is more prominent than the squirming motion of the quiet chromosphere. With good observations this region corresponds to the Hα plage. The second contour defines regions of stronger flicker (and brighter plage). In a few cases a third contour is shown where the region appears bright relative to its surroundings on one frame, and relatively dark on the next frame; these small regions seem to correspond to the transition between plage and visible sunspot on the Hα films. Well developed sunspot umbras are underexposed on these films but strong flicker is usually present in the surrounding penumbra. Comparing these contours to a Sacramento Peak high resolution (5 arc sec) magnetogram kindly provided by David Rust, we can guess that the three contour levels correspond roughly to 40, 60 and 160 gauss as measured by a conventional magnetograph with square aperture 5 arc sec on each side. However, because of small-scale structure associated with the flicker, the 5324Å FeI filtergram films are thought to flicker only where the line-of-sight field exceeds 100 gauss. This region was one of the first observed at Lockheed with the FeI filter, under far less than optimum conditions. Consequently, day-to-day changes in areas of the contoured regions in the sketches in Figure 1 probably depend as much on observing conditions as on the actual evolution of the magnetic region. Also, the detection and interpretation of line-of-sight fields becomes uncertain as a region approaches the limb. Picturing magnetic lines of force arching between a western leader spot and an eastern follower, one can see that as solar rotation carries the region from east limb to west limb, the line of polarity reversal, where the observer's line-of-sight is normal to the field direction, will move from west to east across the region. Also, the polarity closer to the limb is undetectable when the opposite polarity is identifiable. Examples of this may be seen in the Mount Wilson magnetograms published in "Solar-Geophysical Data."

An eastward drift of the polarity reversal line from November 10 to 14 is probably caused by solar rotation. The change in direction of the polarity reversal line is not so readily explained. Observations on November 13 show this line to be typically oriented, more or less parallel to the meridian. But on November 16, regions of opposite polarity are separated by a boundary running more nearly parallel to the equator.

Photographs and drawings in "Solar-Geophysical Data" show that during this period, from November 13 to 17, spots and plage develop northward from the largest spot while the eastern part of the region appears to decay (at least partly because of its approach to west limb). Thus the "center of gravity" of leader spots, of leader plage, and of magnetic field of leading polarity all swing around from east of the large follower spot to north of it. With some faith and imagination in identifying individual spots from day to day, apparent rotation can be seen also in the daily sunspot drawings published in Solnechnye Dannye. These are reproduced in the lower line of Figure 1.

From these discontinuous data we can neither identify individual spots surely from one day to the next, nor establish proper motions. The appearance of many small spots north of the large spot on the 15th, and the parallel development of bright Hα plage in this region, lead us to believe that the most significant change is the growth of this northern region, accompanied by decay of the eastern region, much as described for the general case by Martres et al. On the other hand, Sakurai [1967] describes the east-west direction of the line of polarity reversal, and the rotation that leads to this orientation, as characteristic of regions that produce ground-level cosmic ray events (GLE). He finds that, with few exceptions, the line separating the two magnetic polarities in these sunspot groups rotates in the direction that initially brings the leader spot to the poleward side of the follower. Sakurai proposes that exceptionally strong magnetic buoyancy in these regions leads to rotation that twists the magnetic lines of force into a configuration that is particularly effective for storing energetic charged particles.

A quantitative estimate of the rate of rotation of the line of polarity reversal seen on the filter magnetograms was made by measuring on successive days its inclination to the meridian that passes through the sunspot group (see the inserted sketch in Figure 2). Because of the apparent curvature of meridians near the limb, the actual measurements on the Lockheed films were made with the geographic north-south line as reference. These were reduced by subtraction of the angle P_o (taken from the American Ephemeris and Nautical Almanac) changing the reference line to the solar rotation axis. If, in heliographic coordinates, B_o is the latitude of the center of the solar disk, β the latitude of the sunspot group, and λ its central meridian distance, the angle M from the rotation axis to the tangent to the meridian through the group is defined by:

$$\tan M = \frac{\sin \beta \sin \lambda}{\cos \beta \cos B_o + \sin \beta \cos \lambda \sin B_o}$$

We used $B_o = 3°$, $\beta = 19°$, and $\lambda = \frac{360°}{27^d.3}$ (time of observation - $11^d.8$) to find the value of M for each measurement. This was subtracted from the reduced measured angle to get the inclination of the line of polarity reversal to the meridian, plotted in Figure 2 as solid line and crosses.

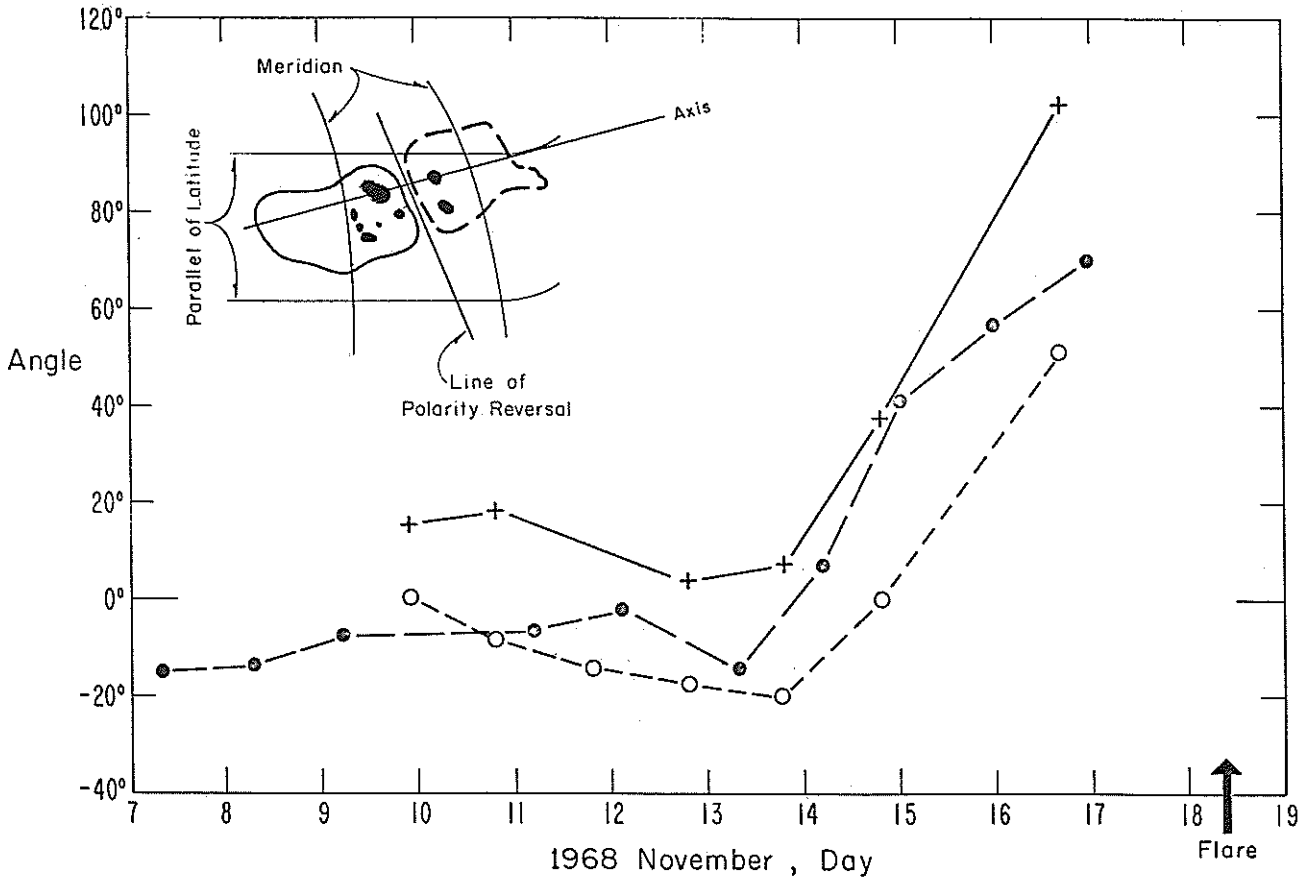

Fig. 2. Rotation of the sunspot group prior to the flare of 1968 November 18. The inset sketch shows schematically the heliographic meridians and parallels of latitude, along with line of polarity reversal, which separates regions of opposite polarity, and the magnetic axis, joining the leader and follower sunspots.

+ ——— + Angle from meridian to line of polarity reversal, measured on Lockheed filter magnetograms.
○ ----- ○ Angle from parallel of latitude to magnetic axis, measured on Lockheed filter magnetograms.
● — — ● Angle from parallel of latitude to magnetic axis, measured on drawings from Solnechnye Dannye.

We also measured on the Lockheed FeI films the direction of the magnetic axis, the line joining the follower and leader sunspots. The angle, plotted as open circles and dashed line in Figure 2, is the inclination of the axis to the parallel of latitude through the sunspot group. The inclination P of the parallel of latitude is found from: $\tan P = \tan \lambda \sin B_o$. The systematic difference between the two angles just shows that the line of polarity reversal is not exactly normal to the magnetic axis.

Finally, the inclination of the magnetic axis was measured for the published sunspot drawings taken from Solnechnye Dannye. These values are plotted as solid circles and dashed line in Figure 2. The rather erratic variation of the angle measured from the published data may arise from uncertainty in identifying the main leader spot. Each set of measurements shows the same trend: the angle changes little until late on the 13th, then increases at a fairly steady rate, between 25° and 35° per day. If we extrapolate this curve to the time of the flare, at November 18.4, we would guess that the angle attains a value of about 135°; this would put the original leader spot of south polarity behind the original follower, and closer to the equator, with the magnetic axis inclined at about 45° to the equator. Of course, there is no evidence that the apparent rotation continues at this rate. The direction of the apparent rotation is that expected from differential rotation; if the leading spot is at higher latitude than the follower, faster solar rotation nearer the equator will carry the follower toward and past the leader. The actual motion is much faster than the difference in solar rotation rate for these close pairs of spots, so this observation is probably irrelevant except as a mnemonic for the direction of rotation.

The November 18 flare can be added to Sakurai's list of flares with GLE in regions that showed an anomalous orientation of the leader and follower polarities and that reached this configuration by an apparent rotation that initially carries the leader spot to higher latitude. We can mention some further examples that showed at least one of these conditions. The region of the flare of 1966 July 6 occurred along a line of polarity reversal that was nearly parallel to the equator, with the spots of leader polarity on the poleward side. This region included two bipolar pairs, each born with the leader spot at higher latitude than the follower [Svestka, 1967]. The region of 1966 August gave a strong impression of rapid rotation [McIntosh, 1966]. From Sacramento Peak films we estimate that the spots rotated through about 50° in the two days before the August 28 flare. The triple flare of 1967 May 23 occurred in a region in which apparent rotation accompanied approach of spots of opposite polarity [McIntosh, 1969].

Negative examples, of changing anomalously oriented regions from which no energetic-particle emission was detected, and of GLE flares not preceded by this behavior, are not hard to find. Further study may determine whether the apparent rotation is itself important to acceleration and storage of energetic charged particles, or if unusual orientation or great complexity of the sunspot group is equally effective when achieved through development of new spots or through merging of groups.

REFERENCES

HARVEY, J. W.	1963	Solar Magnetograph, Sky & Telescope, 26, 196-197.
LEIGHTON, R. B.	1959	Observations of solar magnetic fields in plage regions, Astrophys. J., 130, 366-380.
MC INTOSH, P.	1966	Private communication.
MC INTOSH, P.	1969	Sunspots associated with the proton flare of 23 May 1967, World Data Center A - Upper Atmosphere Geophysics Report UAG-8, ESSA, Boulder, Colorado, 22-29.
RAMSEY, H.	1969	Detecting solar magnetic fields by filter photography, American Astronomers Report, Sky & Telescope, 37, No. 6.
SAKURAI, K.	1967	Solar cosmic-ray flares and related sunspot magnetic fields, Rept. Ionospheric and Space Res. in Japan, 21, 113-124.
SOLNECHNYE DANNYE	1969	Magnitnye polja solnechnyh pjaten, Akad. Nauk. SSSR., Noyabra 1968, Leningrad.
SVESTKA, Z.	1968	Proton flare, in Structure and Development of Solar Active Region, K. O. Kiepenheuer, ed., Springer-Verlag, New York, 517.
THE AMERICAN EPHEMERIS AND NAUTICAL ALMANAC	1968	U. S. Govt. Printing Office, Washington, D. C., 1966, 307.

"Data Concerning November 18, 1968, in Addenda to 'Solar Circumstances at the Cosmic Ray Decrease on January 28, 1967'"

by

Helen W. Dodson and E. Ruth Hedeman
McMath-Hulbert Observatory, The University of Michigan

[Permission has been given by the authors and the publisher to reprint portions of the article appearing in Solar Physics, 9, 278-295.]

The following paragraphs and figures are from the Addenda of the article.

In recent months two additional, well defined enhancements of cosmic rays have been detected by ground-based equipment: 1968, November 18 and 1969, February 25. According to information currently available to us consideration of solar circumstances associated with these new events does not modify evaluations expressed in the body of this paper.

On November 18, 1968 the cosmic ray enhancement was in appropriate time association with a flare at the west limb for which initial reports indicate importance 1 in Hα. Accompanying ionospheric and radio frequency phenomena suggest that the flare was a major solar event. Preliminary data show that this cosmic ray flare occurred in a region that had been only moderately flare-rich in its transit across the solar disk even though the plage contained a γ-δ type spot with maximum area ~800 millionths of the hemisphere. Three days prior to the cosmic ray flare of the 18th, spot area had diminished markedly to ~200 millionths. When the region reappeared at the east limb in December, it had declined in activity. The spot area was still ~200 millionths of the hemisphere and the plage was of only average size and brightness. The only known major event in the region in December was a flare of importance 3 at the east limb on December 2. Polar Cap Absorption followed this flare. The flare on December 2 apparently was another case of an 'isolated' major flare in the late and declining phase of a region associated with energetic cosmic rays (see Figure 2).

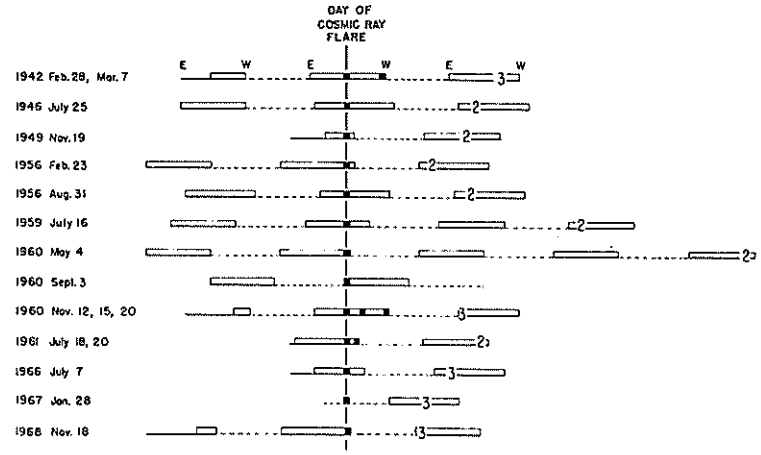

Fig. 2. Schematic presentation of information relating to all known regions in which energetic cosmic ray flares occurred, 1942–1968. The slender rectangles represent passage across the solar disk of regions in which energetic cosmic ray flares occurred. Dashes indicate transit of the invisible hemisphere. The days on which energetic cosmic ray flares occurred are shown by black squares. Numerals 2 and 3 indicate the importance and approximate time of 'isolated major flares' in subsequent rotations. Data more than one rotation prior to cosmic ray flares have been omitted.

The foregoing ground-level enhancements of energetic cosmic rays in 1968 and 1969, coming as they do near the probable time of maximum in the solar cycle, constitute departures from the pattern of solar cycles 18 and 19 in which such increases were not observed during the years of solar maximum. The detection of energetic cosmic ray increases in 1968 and 1969 may be a further indication that solar-terrestrial circumstances in the present solar cycle are somewhat different from those that prevailed during the two preceding cycles.

3. SOLAR RADIO EVENTS

"On the Type IV Burst of November 18, 1968"

by

A. Krüger
Central Institute for Solar-Terrestrial Physics (HHI)
Berlin-Adlershof, G.D.R.

The type IV burst of 18 November 1968 was a somewhat late and isolated event in an active region which had had a δ-configuration since November 8, 1968. The flux ratio of the s-component S_{9400}/S_{1500} was greater than 1.5 from November 9, 1968. Perhaps these circumstances contributed, too, to the outstanding energy output of this event.

Selected records of the radio burst observed at the HHI are shown in Fig. 1. Because of the position of the source region on the very western limb of the sun only those burst components could be observed, which were not subject to a large center-to-limb variation. Therefore, large parts of the type IVmB burst are expected to be missing. In this way, the burst does not exhibit such long duration and high intensities as it might be expected from the associated proton event. Nevertheless, the right-handed polarization of the burst components at 40 MHz indicated an emission of the ordinary component of the magneto-ionic theory, if the leading spot hypothesis is accepted, so that to a certain extent, in this frequency region type IVmB components were recorded. At shorter wavelengths also moderate type IVmA components and the type IVcm burst have been observed. Type IVdm emissions which are characteristic for low-energy events are not present here [cf. Böhme and Krüger, 1969; Castelli and Aarons, 1968]. A spectral diagram of the event is given in Figure 2. From this picture the main components of the burst again can be seen.

Acknowledgement

The assistance of Mr. K. H. Fricke for the construction of the spectral diagram is gratefully acknowledged.

REFERENCES

BÖHME, A. and A. KRÜGER 1968 HHI Suppl. Ser. Solar Data, Vol. I, No. 3.

CASTELLI, J. P. and J. AARONS 1968 Astrophys. J., 153, 267.

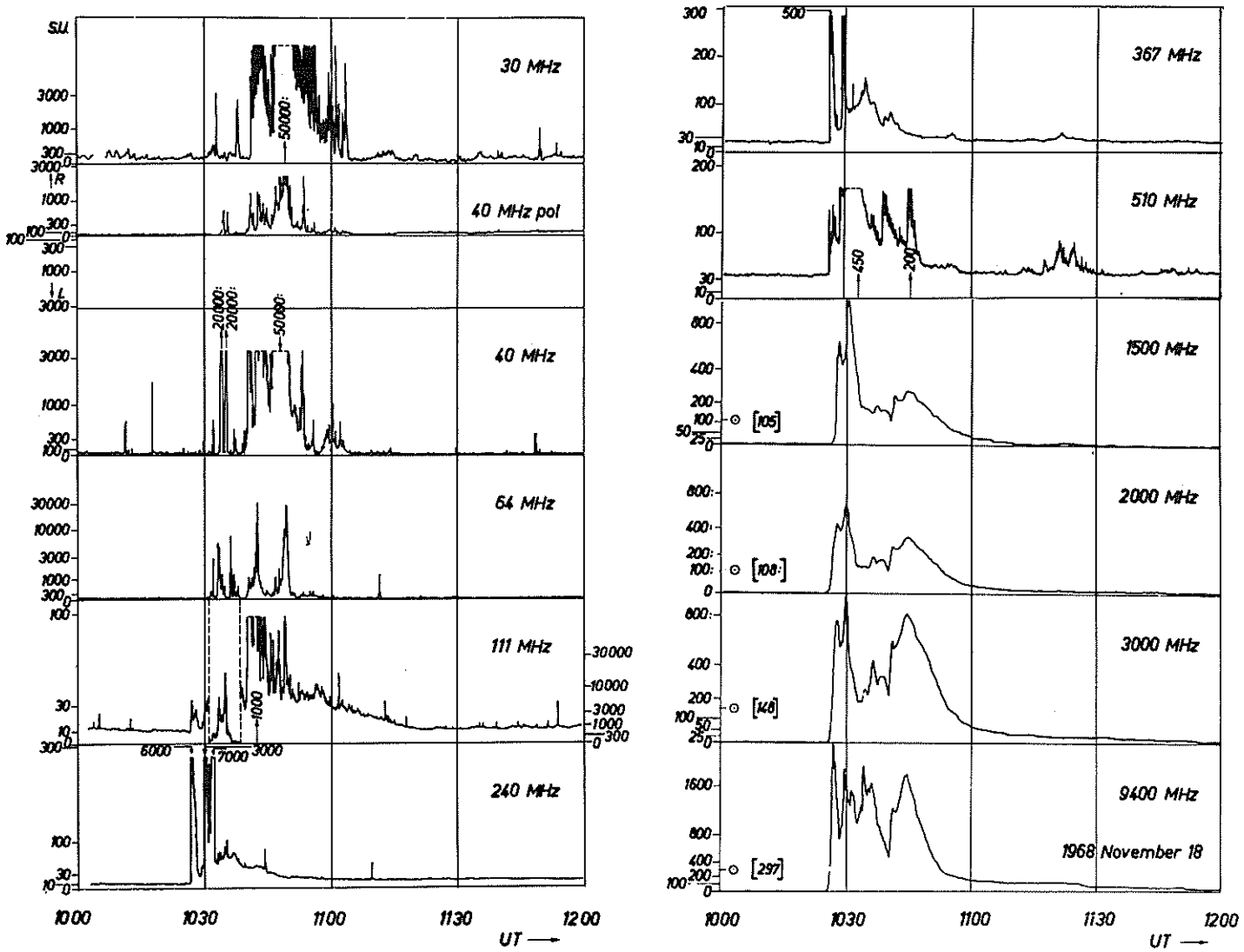

Fig. 1a and 1b. HHI-records of the radio event of November 18, 1968.

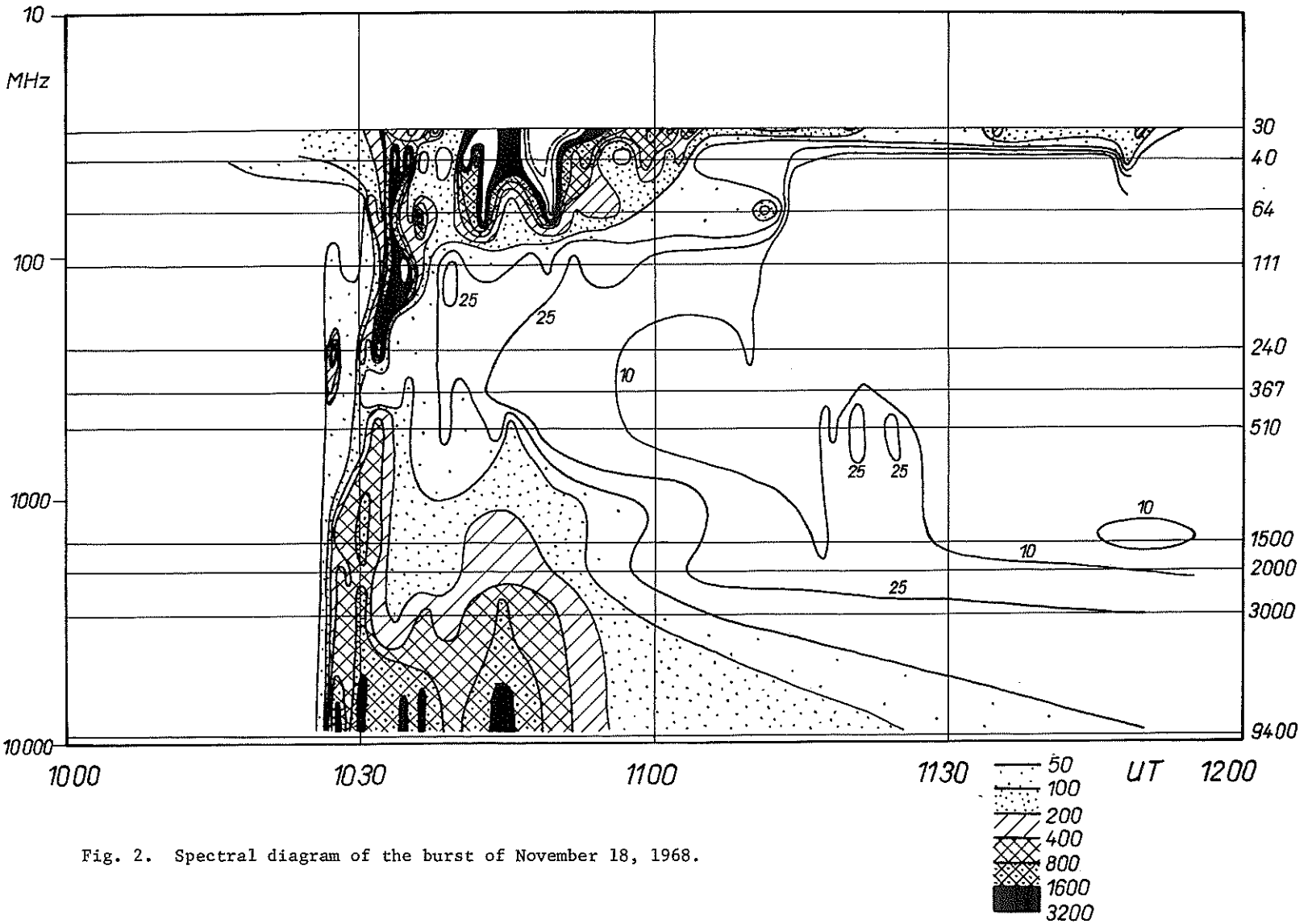

Fig. 2. Spectral diagram of the burst of November 18, 1968.

"An Outstanding mm-Radioburst Observed November 18, 1968"

by

G. Feix
Astronomical Institute of University of Bochum, G.F.R.

[Permission has been given by the author and the publisher to use portions of the article "Solar Bursts at Millimeter Wavelengths", J. Geophys. R., 75, 211-218, 1970.]

The author submitted Figure 1 which shows an outstanding limb flare-burst event. The time of maximum was 1031 UT reaching an intensity of 5000 x $10^{-22}Wm^{-2}Hz^{-1}$. The observations at 36 GHz were made at the Stockert Radio Observatory (N50°34'14") by an equatorially mounted paraboloid antenna 10 m in diameter. The following paragraphs, as well as Tables 1 and 2 are reproduced from the quoted article:

3. Spectra

Violent outbursts that are associated with a flare event have been chosen for a special consideration and are listed in Tables 1 and 2. The observed radio spectrum of these events is given in Figure 3. In comparing the spectra of limb bursts and of selected strong disk bursts (Figure 4) there appears to be an unusual increase of intensity at the mm-wavelength region for limb bursts. This comparison is, of course, restricted only to a small number of identified limb sources. A comparison between the spectral curves of Figure 3 and those of disk bursts originating from the same plage indicate this trend even more. Table 3 shows a few bursts produced by the McMath plage No. 8740, whose active center was identical with the source of the limb event ESSA No. 4771 of Table 1. If these events are considered to be typical for this center of activity, we should find values of 8–13 × 10^{-22} W/m² Hz for all bursts originating from plage No. 8740 on the disk. Continuing these investigations to the plages 9760 and 9503 of Table 1, one would obtain the same results.

For example, (1) The active center of the event described on July 6 became visible July 7, 1968. After July 6 no outstanding event was detectable at 36 GHz from this plage. At the time of the central meridian passage, as shown by Figure 5, on July 12, 1968, the solar drift curve represents the radiation of a common plage during its passage across the disk. (2) The limb burst of April 1, 1967, as shown in Figure 2 has a radio output of about 4000 flux units; this plage exhibited only events with flux units lower than 100 × 10^{-22} W/m² Hz at 36 GHz during its passage across the disk.

If this trend is substantiated it may prove that the line of sight may play an important role for the reception of microwave bursts.

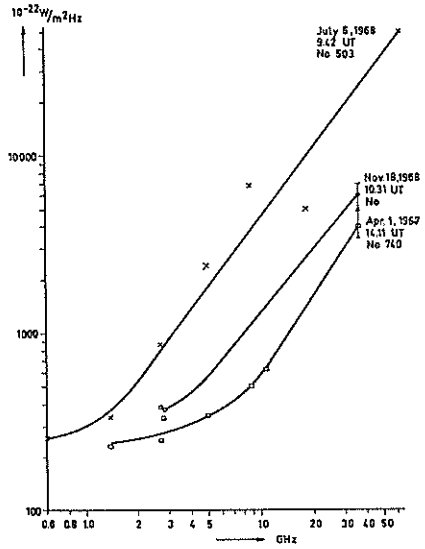

Fig. 3. Power spectra of limb bursts at microwavelengths. Data: Radio and Space Research Station, Ditton Park, Slough, England; Solar-Geophysical Data, ESSA, Boulder, Colorado; Stockert Radio Observatory, Bonn, Germany. Addenda: HHI, Berlin, Germany, received November 18, 1968: At 1027 UT, 9.4 GHz, maximum flux units were 2600; at 1030 UT, 1.5 GHz, maximum flux units were 1090.

TABLE 1. Limb-Flare Characteristic

Date	Position	McMath Plage No.	Central Distance Maximum	Optically Observed Area, Maximum	Estimated Flux Units at 36 GHz, 10^{-22} W/m² Hz	ESSA Flare No.	Remarks*
April 1, 1967	N19–20; W75–85	740	0.992	120	4000	4771	*A*; *H*
July 6, 1968	N12–23; E85–90	503	1.000	220	24000	16373	*A*; *H*; *X*
Nov. 18, 1968	N21–23; W85–90	760	0.999	310	6500		*A*

* *A* = Eruptive prominence, base at > 90°.
H = Flare with high velocity dark surge.
X = Unusually wide H-alpha emission.

TABLE 2. Temperatures and Densities of Limb Bursts at 36 GHz

Date	McMath Plage No.	ESSA Flare No.	Temperature, °K	Flux Units, 10^{-22} W/m² Hz at 36 GHz	Area*
April 1, 1967	8740	4771	1.2×10^6	4000	120
July 6, 1968	9503	16373	3.9×10^6	24000	220
Nov. 18, 1968	9760		0.7×10^6	6500	310
Mean			2×10^6		

* Optically observed area (maximum) in 10^{-6} of the solar disk.

5. Interpretation

The fact that the abnormal bursts at the limb originate from regular plage regions indicates that these bursts are normal ones. It remains to be explained why flares observed in profile present higher intensities than flares facing the observer. If it is assumed that the gaseous envelope rises ahead of the flare and becomes more tenuous with distance from the base of the flare, we have to consider the radiation of a thin layer at different points on the solar disk, namely cos $\delta = 0$ to 1, where δ is the angle between the normal and the line of sight to the observer. The contribution of a thin layer with optical thickness $d\tau$ at the optical depth τ is given by *Unsöld* [1955]

$$I = \text{constant}\, e^{-\tau \sec \delta}\, d\tau \sec \delta \qquad (3)$$

Normalized to unity at $\delta = 0$ this function shown in Figure 7 gives the contribution of the intensity of a thin layer versus the distance from the center of the sun expressed in terms of cos δ. For layers $\tau \leq 0.001$ it is seen that the intensity at the limb is at least 100 times greater than at the center. Thus we receive at millimeter wavelengths the full brightness of the sporadic condensation shell at the limb. Owing to the fact that the optical thickness depends on the wavelength, the lower curves represent the situation at centimeter wavelengths and longer.

The experimental observations indicate that limb bursts exhibit, if at all, only weak post-burst components [*Feix*, 1969]. If the apparent center of the burst activity is slightly behind the solar limb, it is interesting that the burst is only impulsive. This suggests that the source of post-burst radiation is situated at layers around 10,000 km. We find a similar situation for the slowly varying component, i.e. the radiation of a plage at millimeter wavelengths. In Figure 7 the average values P of the relatively strong plage 8742 are graphed. According to the flat layer model, τ must be between 1 and 2. The darkening of a plage near the limb was investigated in many cases and seems to be a common feature. These and other data [*Nagnibeda*, 1967] point to a flat source of considerable optical thickness. The MM-burst data suggest a similar model for the post-burst component as well.

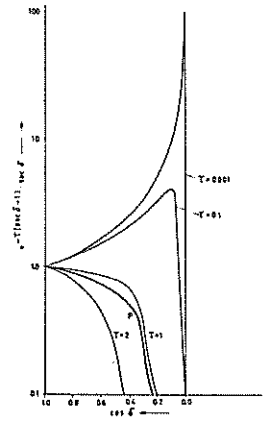

Fig. 7. Normalized contribution of a thin layer versus cos δ; P, daily average values of the millimeter intensity of McMath plage no. 8818.

6. Conclusion

The radio burst at millimeter wavelengths is believed to be produced by two components: (1) By a component originating from an optically thick layer located at the height of the flare base. This component is responsible for the gradual rise and fall as well as for the post-increase phase of a burst. Estimated temperatures after the impulsive component may be in the range 30,000°K to 80,000°K, (2) By an impulsive component due to an optically thin shock front of the mean temperature 2×10^6°K rising ahead of the chromosphere into the corona.

References

Feix, G., MM-Burst observations by a pencil beam-research note, *Solar Phys.* (in press), 1969.

Nagnibeda, V. G., Properties of sources of the slowly varying component of 2 cm solar radio

Unsöld, A., *Physik der Sternatmosphären*, p. 113, Springer-Verlag, Berlin, 1955.

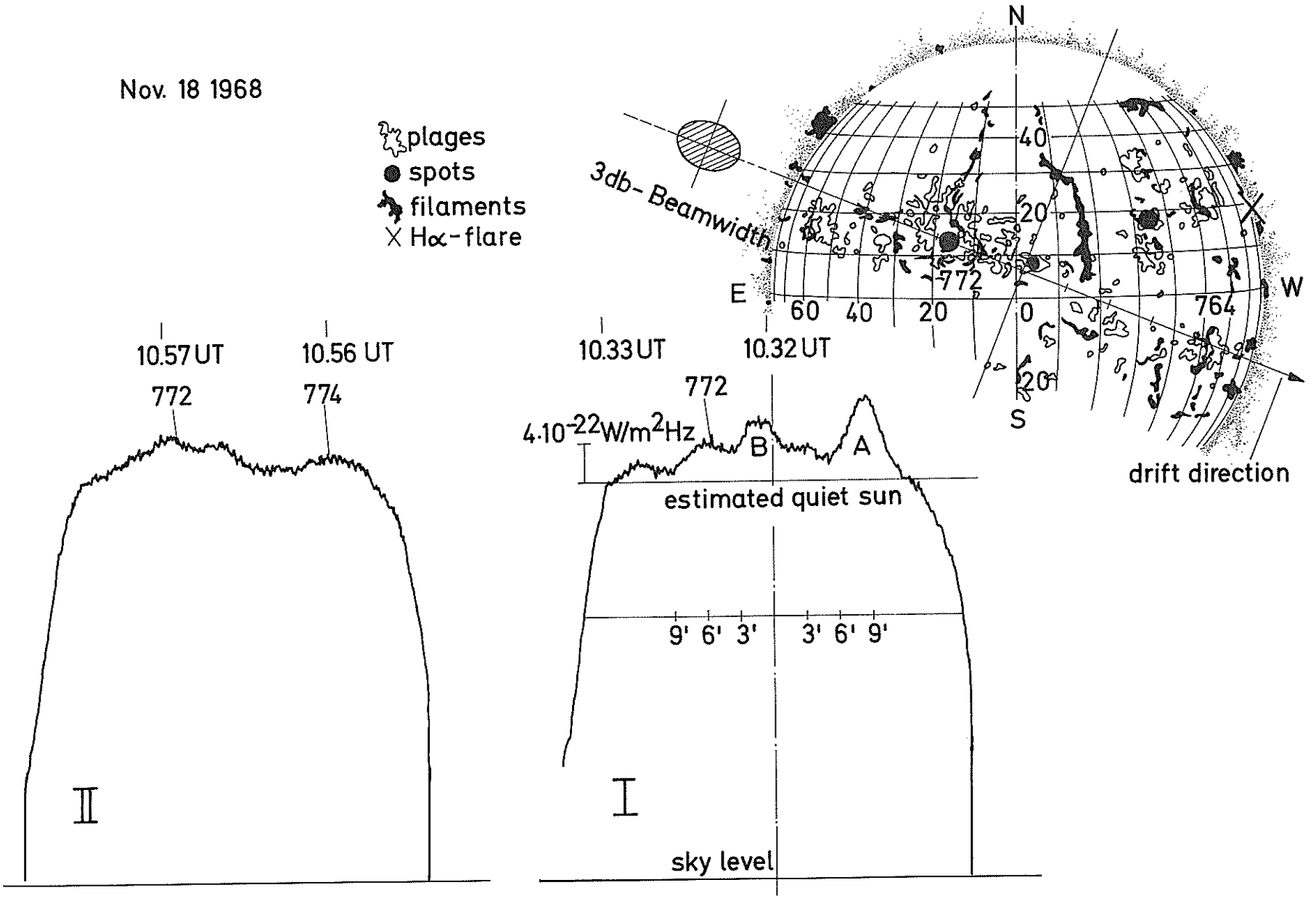

Fig. I Sidelobe reception of an outstanding limb flare-burst event. I drift curve around the burst maximum. II drift curve for noise trace comparison after the burst. A & B are 25 to 30 dB down from the main beam level.

"The Radio Outburst of November 18, 1968 at 1026 UT Observed at Metric Waves with High Temporal Resolution"

by

A. Abrami
Astronomical Observatory, Trieste, Italy

The radio outburst occurred at 1026 UT on November 18, 1968 and was associated with the secondary maximum of an optical flare of importance 1b, which started at 1026 UT at position N20 W90. It has been observed at the Trieste Astronomical Observatory with the metric waves radiometer (239 MHz) and the high temporal resolution recording equipment already described in a preceding report of this series [ABRAMI, 1970].

The time profile of the event is presented here in two separate diagrams ranging from $10^h26^m0^s$ to $10^h29^m6^s$ and from $10^h29^m0^s$ to $10^h32^m36^s$ UT (Figure 1) obtained from the original records by means of the same reduction technique already quoted [loc. cit.]. These diagrams represent the initial more variable phase of the phenomenon. Its whole evolution is sketched in the diagram of Figure 2 obtained from the measures of the enhanced background made at low resolution. In this figure the part of the diagram observed at high resolution is underlined.

The more relevant data obtained from these profiles are as follows:

Starting time	earlier than	$10^h26^m37^s$ UT
Time of the first maximum		$10^h26^m45^s \pm 8^s$
Time of the second maximum		$10^h29^m45^s \pm 1^s$
Time of the third maximum		$10^h31^m54^s \pm 5^s$
Duration	about	39^m
Peak flux density	greater than	$1600 \times 10^{-22} Wm^{-2}Hz^{-1}$
Total energy emitted until $10^h32^m36^s$	greater than	15×10^{-18} $Jm^{-2}Hz^{-1}$

REFERENCE

ABRAMI, A. 1970 Some radio bursts in the period October 29 - November 3, 1968 observed at metric waves with high temporal resolution. World Data Center A - Upper Atmosphere Geophysics Report UAG-8, ESSA, Boulder, Colorado, 163-168.

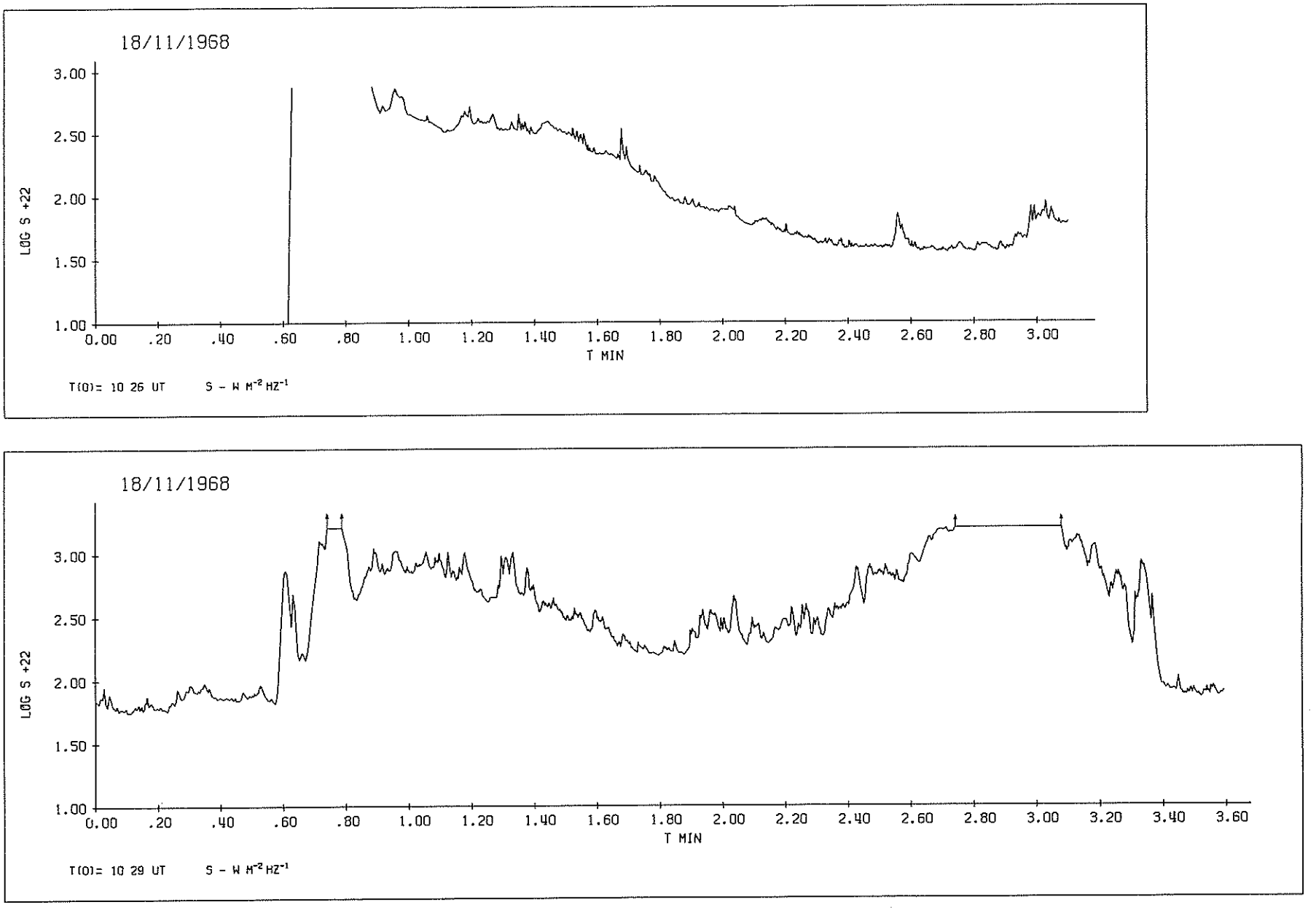

Fig. 1. Detailed time profiles of 239 MHz burst, Trieste Astronomical Observatory, beginning at 1026 UT and at 1029 UT November 18, 1968

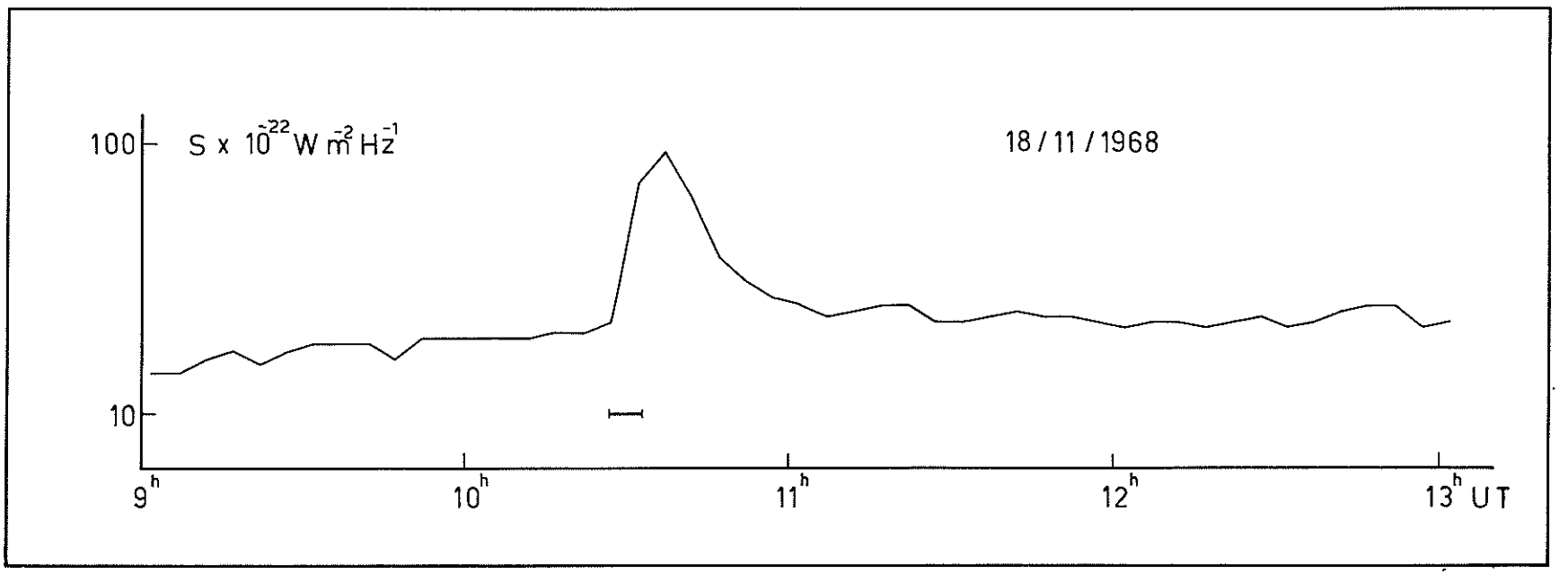

Fig. 2. Low resolution tracing of 239 MHz burst, Trieste Astronomical Observatory, November 18, 1968.

4. SOLAR X-RAYS

"Solar X-Ray Emission on November 18, 1968"

by

D. M. Horan and R. W. Kreplin
E. O. Hulburt Center for Space Research
Naval Research Laboratory
Washington, D. C. 20390

ABSTRACT

Solar x-ray data, obtained by the Naval Research Laboratory's SOLRAD 9 satellite during the proton flare of November 18, 1968 are presented. Presence of high energy proton flux in the vicinity of the earth is indicated by charged-particle interference with the satellite's x-ray sensors at lower altitudes and higher latitudes after the flare.

Measurements of solar x-ray emission on November 18, 1968, Figure 1, by sensors aboard the Naval Research Laboratory's SOLRAD 9 satellite (Explorer 37, 1968-17A) show the Class 1B proton flare to be the predominant x-ray event of the day. The top curve on the plot represents the solar x-ray emission in the 8 to 20A band, and the next lower curve represents solar x-ray emission in the 1 to 8A band. In both cases a gray body solar emission spectrum [Kreplin, 1969] with a 2 x 10^6 K color temperature was assumed in converting from detector current output to energy flux units. The third curve from the top represents emission in the 0.5 to 3A band assuming a gray body spectrum with a 10 x 10^6 K color temperature for the emitting solar region. Since solar emission in the 0.5 to 3A band is usually below the threshold level of the detector, the curve representing these data is quite intermittent prior to the flare.

The x-ray emission is plotted in units of ergs/cm^2/sec on a logarithmic scale. The abscissa is linear with the integers denoting hours in Universal Time (UT). Charged-particle interference with x-ray detectors, which can cause the plotted flux levels to be higher or lower than the actual flux, is indicated by the lowest data curve. The ionization chamber current caused by the charged-particle background is digitized and recorded as a "count". The number of "counts" is linearly related to the current generated in the 0.5 to 3A ionization chamber by penetrating charged-particles when the detector is facing away from the sun. Counts of 10 to 15 indicate no particle interference with the detectors. Counts of 20 to the maximum value of 127 indicate increasing amounts of particle interference.

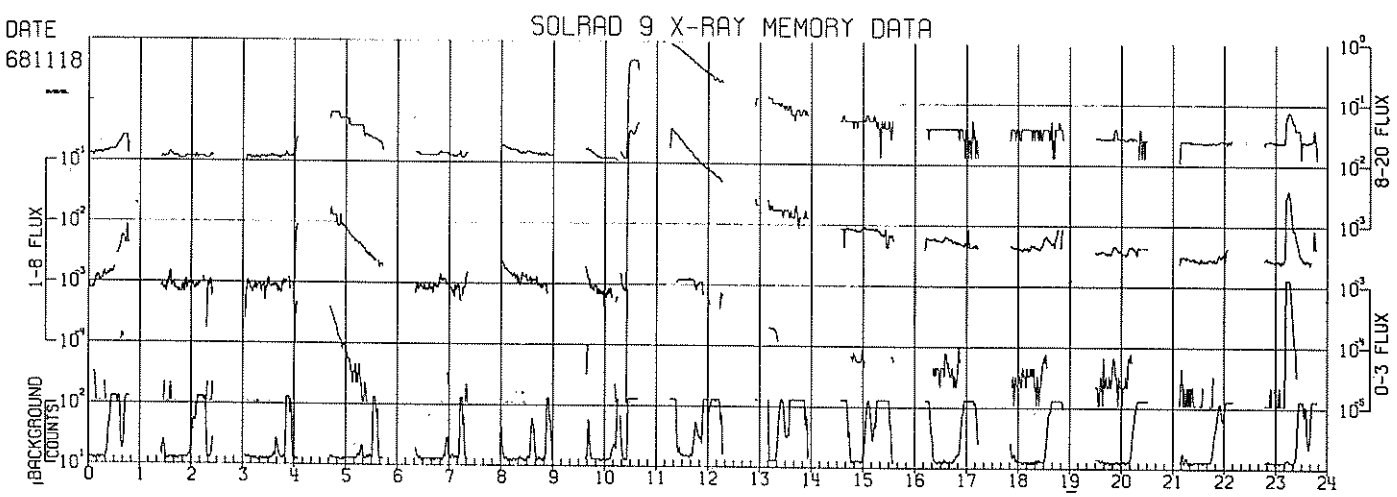

Fig. 1. Solar X-ray Emission November 18, 1968.

During the first ten hours of November 18, Figure 1, background solar x-ray emission in the 1 to 8A and 8 to 20A bands was steady at high values. Two small x-ray events occurred with peak flux levels of the first at 0040 UT and peak levels of the second hidden by satellite night but occurring after 0405 and before 0441 UT. These events correspond to an unconfirmed normal subflare at 0036 UT*, and two unconfirmed Class 1 flares and a normal subflare whose maximum phases occurred at 0426, 0431, and 0444 UT, respectively. A third small event may have attained peak values between 0722 and 0759 UT. This would correspond in time to a confirmed faint subflare with a maximum phase at 0750 UT.

Sharply rising flux levels marking the beginning of the proton flare were first observed at 1026 UT. A small peak in the 1 to 8A band emission occurred at 1029 UT. The principal optical maximum phase was observed at 1033 UT. A second, larger x-ray peak occurred between 1039 and 1115, but the exact time is unknown because of satellite night. A secondary optical maximum phase was observed at 1058. The x-ray emission from the event decayed quite steeply between 1115 and approximately 1400 where a more gradual decay commenced. The x-ray emission from the proton flare does not merge with background x-ray levels until approximately 0500 UT on 19 November, Figure 2. A sharp x-ray event which peaked at 2315 on November 18, corresponds to an unconfirmed brilliant subflare with a maximum phase observed at 2312 UT.

Since the predominant event of the day is known to be a proton flare, the behavior of the lowest data curve on the plots is especially interesting. The plot for November 17, 1968, Figure 3, shows the preflare behavior of this data curve, which indicates charged-particle intereference with the 0.5 to 3A ionization chamber when the detector is facing away from the sun. Note that the duration of charged-particle interferences during the first 14 hours of the day was approximately ten minutes, but during the final ten hours of the day it increased to 20 to 30 minutes. This increase in the time during which charged-particle interference occurred is associated with the passage of the satellite through a larger portion of the South Atlantic anomaly. The same pattern is observed in the plot for November 18, Figure 1. However, the plot for November 19, Figure 2, does not show the same pattern of charged-particle interferences.

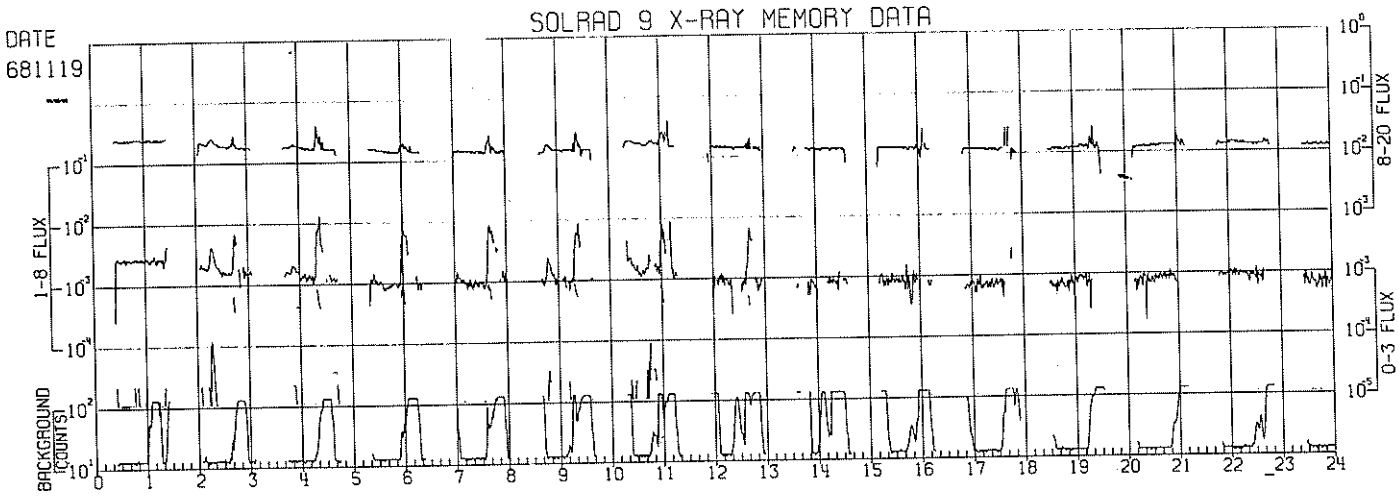

Fig. 2. Solar X-ray Emission November 19, 1968.

*All references to Flare Class were obtained from "Solar-Geophysical Data", IER-FB-297, May 1969, published by ESSA Research Laboratories, Department of Commerce.

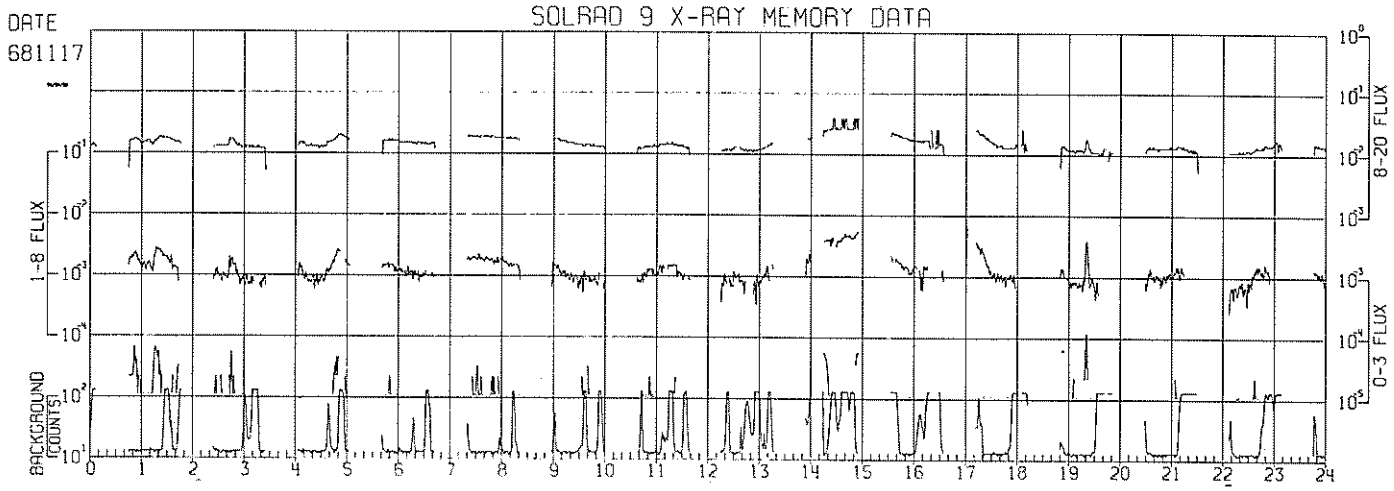

Fig. 3. Solar X-ray Emission November 17, 1968.

Instead, the traces show that charged-particle interferences endured for approximately 20 to 30 minutes throughout the day. The charged-particle interferences during the first half of the day lasted longer than those observed at similar times on November 17 and 18. Satellite orbit data show that the longer duration charged-particle interferences occurred, because, after the flare, the satellite encountered interfering charged-particles at lower altitudes and closer to the South Pole between 50° and 180° East longitude. The additional particles encountered were probably high energy protons coming directly from the sun and not trapped particles. The effect is not clearly discernible on the plots prior to about 16 hours after the proton flare started. However, it is quite possible that the increased proton flow began before it first becomes noticeable, because, during the time intervening between flare occurrence and the clear evidence of increased charged-particle interference, the satellite's path did not cross regions where differences in preflare and postflare conditions in the southern hemisphere would be noticeable in the SOLRAD data. Changes in the North Polar region were not observed, because the satellite usually crossed these regions during periods of satellite night when the data memory system was not operating.

REFERENCES

KREPLIN, R. W. 1961 Ann. Geophys., 17, 151-161.

"Solar Cosmic-Ray Event on 18 November 1968"

by

Stephen Pintér
Geophysical Institute of the Slovak Academy of Sciences
Hurbanovo, Czechoslovakia

A sudden enhancement of cosmic radiation was observed at many terrestrial observatories on 18 November 1968. Cosmic-ray events were connected with the flare which appeared near west limb at the position 18N 84W.

Most of the observatories classified the flare as one with importance 1b in the Hα line. Accompanying phenomena such as the radio bursts in the different wavelengths, x-ray bursts and SID effects connected with them show that it was a large energetic solar event. The relative low degree of the importance of the flare in Hα-line can be explained with respect to its limb position.

The flare appeared in McMath plage region 9760 which was visible on the solar disk from 4 November until 18 November. The active region was created by a great group of spots with a configuration typical of proton active regions. The maximum area of spots reached approximately 800-millionths of the hemisphere. According to "Solar-Geophysical Data", there were 73 confirmed flares in the studied region, none of which had greater importance than that of 18 November. Since the proton eruption appeared close to the limb we can study the spatial evolution of the flare in connection with the x-rays in more detail.

The cosmic-ray flare began in Hα light at 1026 UT in the form of a mound. The evolution of this limb phenomenon is visible on the sequence of the photographs from the Hα Cinematographic Flare Patrol made at the Cape of Good Hope Observatory, thanks to the Royal Observatory of England.

One minute after the commencement of the flare at 1027 UT there appeared an explosive phase, during which the above cited mound suddenly expanded in the north-south direction along the limb.

In this manner an emission filament was created which had the form of a string of pearls (according to Křivský) where each pearl had increased intensity. During the time from 1028 to 1033 UT the "string of pearls" expanded moderately, and its intensity in Hα increased. At 1034 UT expansion in the vertical plane began, i.e. one part of the flare went over the solar limb. Maximum of the flare is ascribed to the time 1035 UT. On Figure 1 we can see the beginning phase of the separation of the emitting region at 1040 UT meanwhile a flare channel was created in the center. We can see the creation of the loop structure. Twenty minutes later, i.e. at 1100 UT, the expansion and elevation continued meanwhile a very bright strand developed on the top of the loop structure of the flare channel.

At about 1115 UT the loop structure reached maximum intensity and maximum height. Then the loop structure collapsed. A detailed study of this proton limb phenomenon was carried out by Křivský and Švestka [1969].

As is seen, on the basis of the behavior of the flare in Hα-line, the most probable phase of the acceleration process occurred during the time interval 1027-1035 UT. Figure 2 shows the time intensity profile of the soft x-ray burst in the wave ranges 1 - 8 Å and 8 - 20 Å, respectively, measured by the satellite Explorer 37 [Kreplin, 1968]. The beginning of the x-ray burst at 1026 UT coincides with the time of the beginning of the Hα flare.

Impulsive increase of the flux level 1 - 8 Å and 8 - 20 Å x-ray emission began at 1027 UT at the time of the explosive flare phase and lasted to 1031 UT, i.e. 4 minutes. During this interval of 4 minutes, the flux level 1 - 8 Å of x-ray emission increased from 7.7×10^{-4} erg cm^{-2} sec^{-1} to 3.4×10^{-1} erg cm^{-2} sec^{-1}.

The time of the implusive increase of the level of x-rays defines the acceleration time of the particles in the flare region. Unfortunately at the time of the maximum phenomenon x-ray detectors aboard Explorer 37 were saturated.

Very long exponential decay time (24 hours) of the soft x-rays, which is shown in Figure 2, is typical for the great bursts connected with proton flares.

During this solar cosmic-ray event a soft 2 - 12 Å x-ray burst was registered by Explorers 33 and 35 [Van Allen, 1967]. The maximum flux F (2 - 12 Å) = 0.25 erg cm^{-2} sec^{-1} was recorded at 1057 UT after which followed a moderate decay of intensity.

The crochet (SFE) was observed at the Hurbanovo Observatory. The beginning of the crochet was at 1026 UT; the impulsive increase of the horizontal intensity of the geomagnetic field occurred during the interval 1027 to 1030 UT. This agrees well with the explosive phase and with the impulsive increase of the soft x-rays.

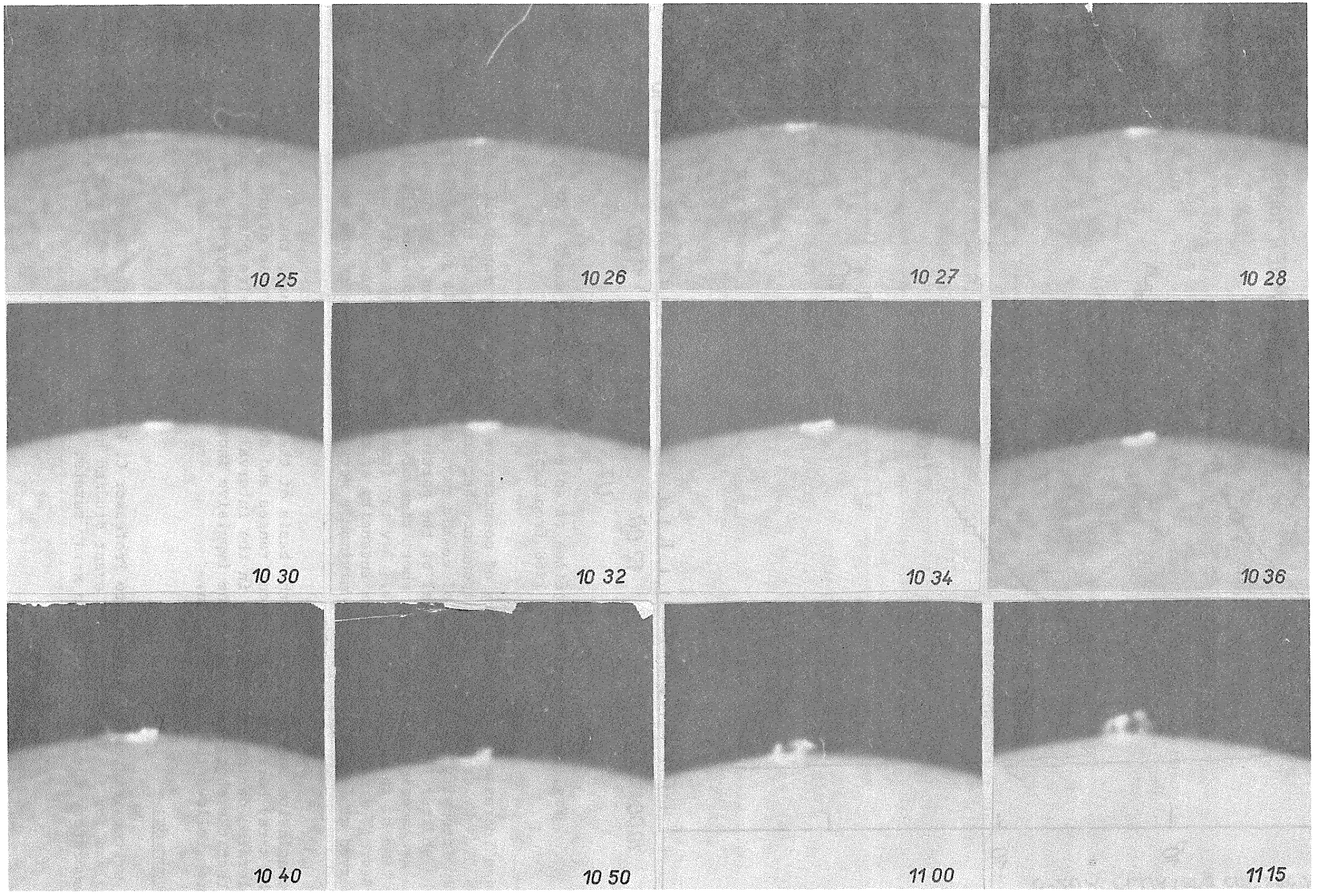

Fig. 1. Hα flare patrol Royal Observatory Capetown, Cape of Good Hope, South Africa, 1025-1115 UT, November 18, 1968.

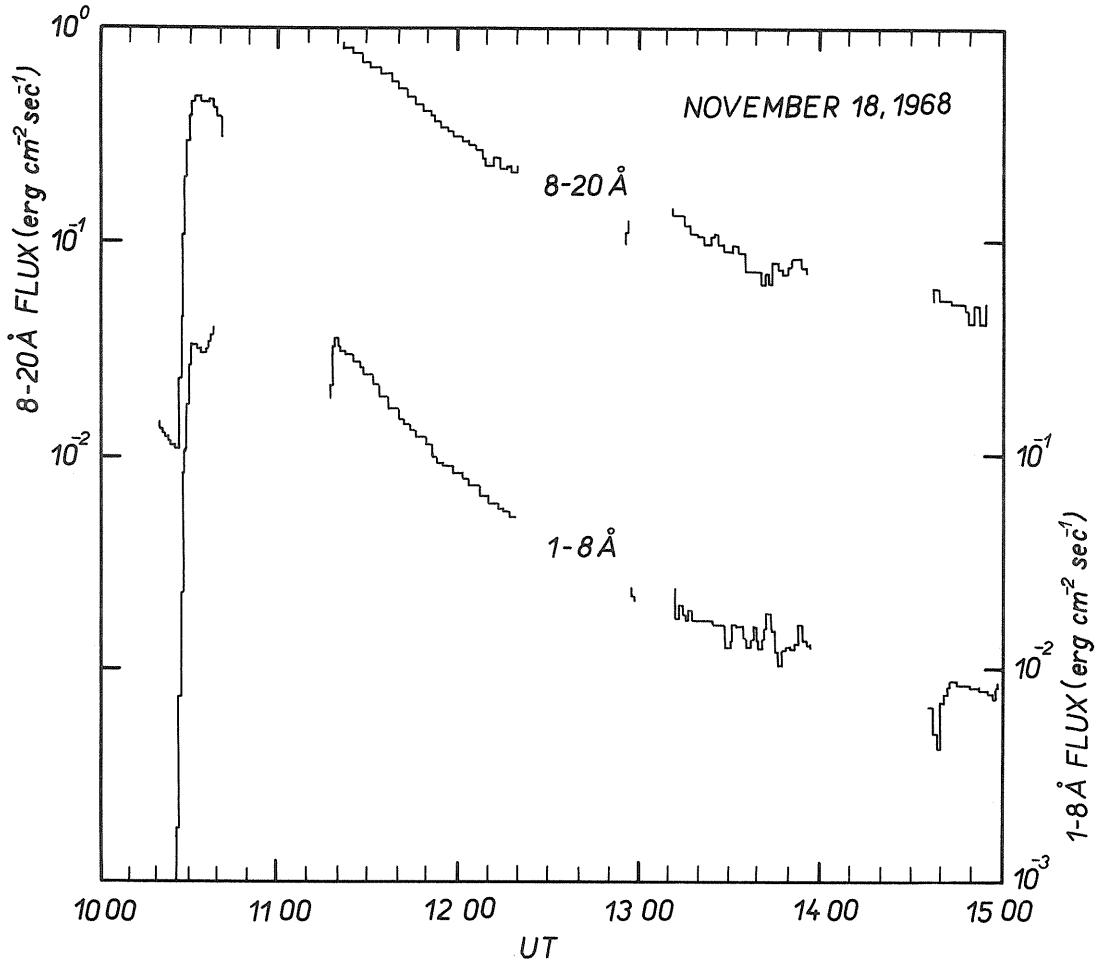

Fig. 2. Intensity profiles of soft x-rays 1 - 8 Å and 8 - 20 Å, November 18, 1968 from Explorer 37.

Sudden increase of the intensity of cosmic-rays in the energy range 0.0 - 5.0 Bev began at 1040-1055 UT. We can see the time dependence between the beginning of the sudden increase of the cosmic-ray intensity and the energy of cosmic rays in Figure 3. It is clear that the greater the energy the shorter the time of arrival of the particles from the sun. Supposing that all the particles are accelerated during the short time of the explosive phase of the flare we can judge that the time of the arrival of the 4.4 Bev ray from the sun to the earth was 13 minutes and for the 1.0 Bev, 18 minutes. The maximum intensity of cosmic-rays at the Deep River Observatory was 12%, observed at 1052 UT. After the maximum a very quick decrease of the intensity of cosmic-rays followed.

In conclusion we can judge, on the basis of the obtained values, that the energetic particles due to the x-ray burst in the different ranges and due to the increase of the solar cosmic-rays are accelerated during some minutes, in the interval of the explosive phase of the flare. It is obvious that the short interval of the impulsive increase of the x-rays is of non-thermal origin after which follows thermal radiation.

Acknowledgements

The writer is greatly indebted to Professor C. W. Allen from the University of London Observatory, England for the Hα film of the event studied here and to Mr. D. H. Horan from the Naval Research Laboratory for the material on x-ray bursts.

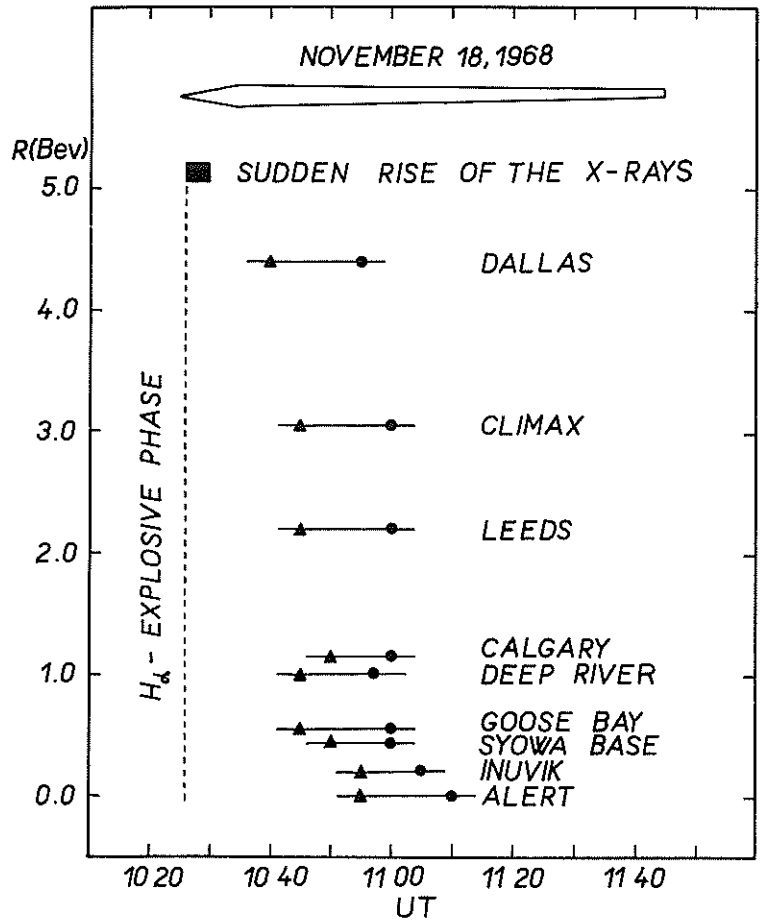

Fig. 3. Onset times of cosmic-ray increases by energy range compared to Hα explosive phase and sudden rise of x-rays, November 18, 1968.

REFERENCES

VAN ALLEN, J. A.	1967	J. Geophys. Res., 72, 5903.
KŘIVSKÝ, L. and Z. ŠVESTKA	1969	Private communication.

5. SPACE OBSERVATIONS

"Editorial Comments"

by

J. Virginia Lincoln
Space Disturbances Laboratory
ESSA Research Laboratories, Boulder, Colorado

In Report UAG-8 two of the articles included data for the period of this report. These were "Explorer 35 University of California Energetic Particles Experiment October 26 - November 22, 1968" by Robert B. Lin, and "Response of Electrons ($E_e \geq 0.28$ Mev) at $1.2 \leq L \leq 1.3$ to the November 1968 Magnetic Storm" by J. C. Armstrong, C. O. Bostrom and D. S. Beall. The former paper presents data for >45 kev electrons, >22 kev electrons, >0.3 Mev protons and ≥15 Mev protons together with the galactic cosmic ray background levels. The latter paper presents data for the count rates of electrons ≥0.28 Mev at L = 1.2. A general feature of these electrons in this region of space is their response to even modest geomagnetic activity.

"Explorer 34 Solar Proton Monitoring Experiment, Ep >10 Mev, November 17 - 28, 1968"

by

C. O. Bostrom
Johns Hopkins University, Applied Physics Laboratory
and
D. J. Williams and J. F. Arens
NASA Goddard Space Flight Center

[The compiler has prepared the following paragraph and figure from the data routinely published in "Solar-Geophysical Data".]

In Figure 1 the proton intensities in the energy range Ep ≥10 Mev from the Solar Proton Monitoring Experiment (SPME) are presented for the period November 17 to 28, 1968. These data are from "Solar-Geophysical Data", No. 300, Part II, p. 91. The Descriptive Text issued as IER-FB 294 (Supplement) to "Solar-Geophysical Data" describes these measurements on pages 64-69. An outstanding event begins on November 18, and full recovery does not take place until November 26, 1968.

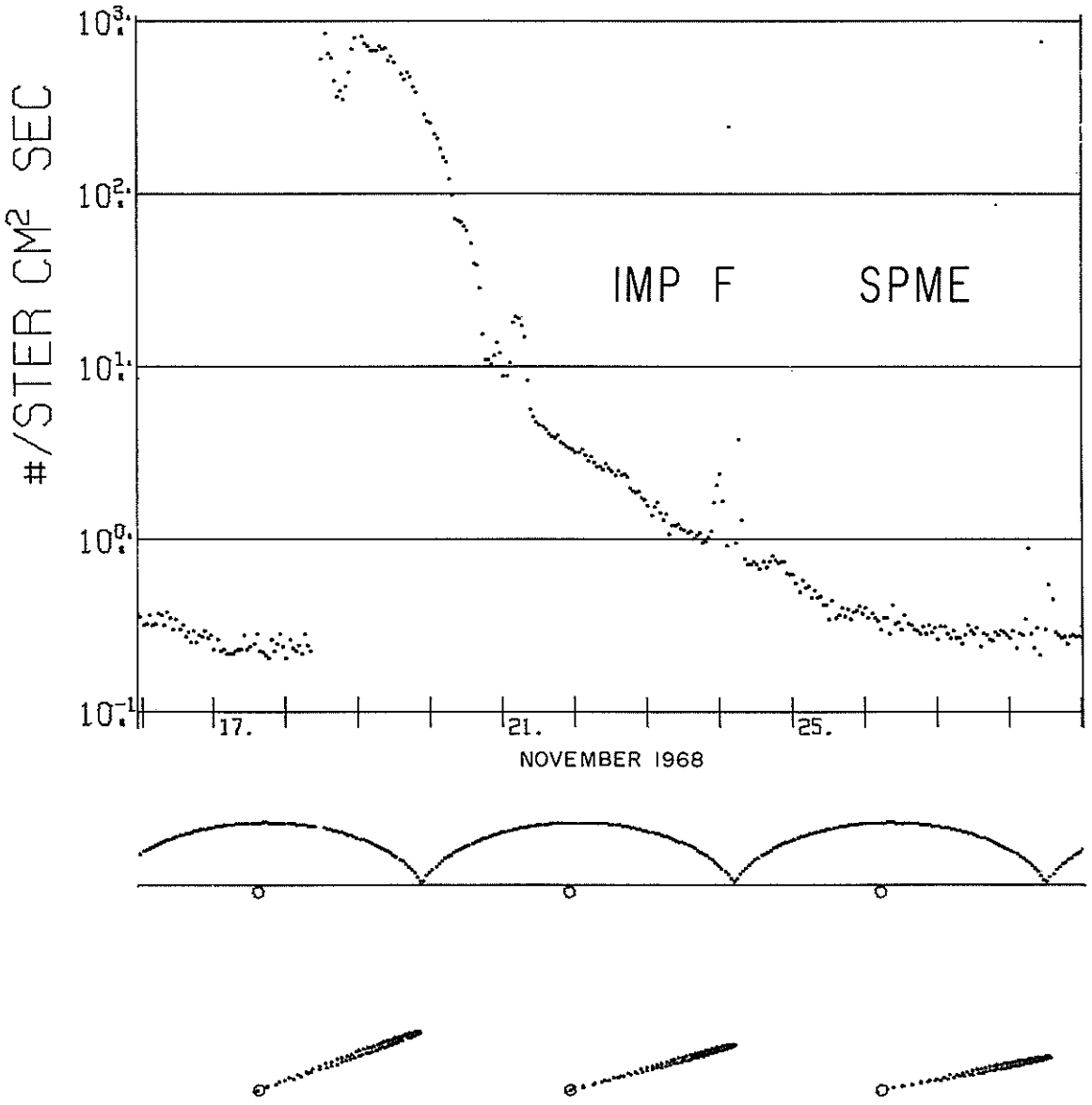

Fig. 1. Ep >10 Mev Hourly Averages.

"Energetic Proton Flux (5-70 Mev) at Synchronous Orbit November 11 - December 8, 1968"

by

G. A. Paulikas
Space Physics Laboratory
The Aerospace Corporation, Los Angeles, California

The data in Figure 1 on the 5-70 Mev proton flux were obtained aboard the ATS-1 satellite. The 21-70 Mev flux at this orbit appears to be identical to the interplanetary flux. The 5-21 Mev flux departs in a complex way from the interplanetary flux because the measurement is made inside the magnetosphere. The flux may be attenuated by up to a factor of 10 for measurements near local noon and magnetic quiet. For other local times and disturbed magnetic conditions the flux of 5-21 Mev protons measured at ATS-1 approaches the interplanetary flux.

The measurements were made with an omnidirectional spectrometer. This instrument contains shielded solid state detectors. Pulse height analysis discriminates electrons from protons and, together with the shield thickness, determines the energy bites of the instrument.

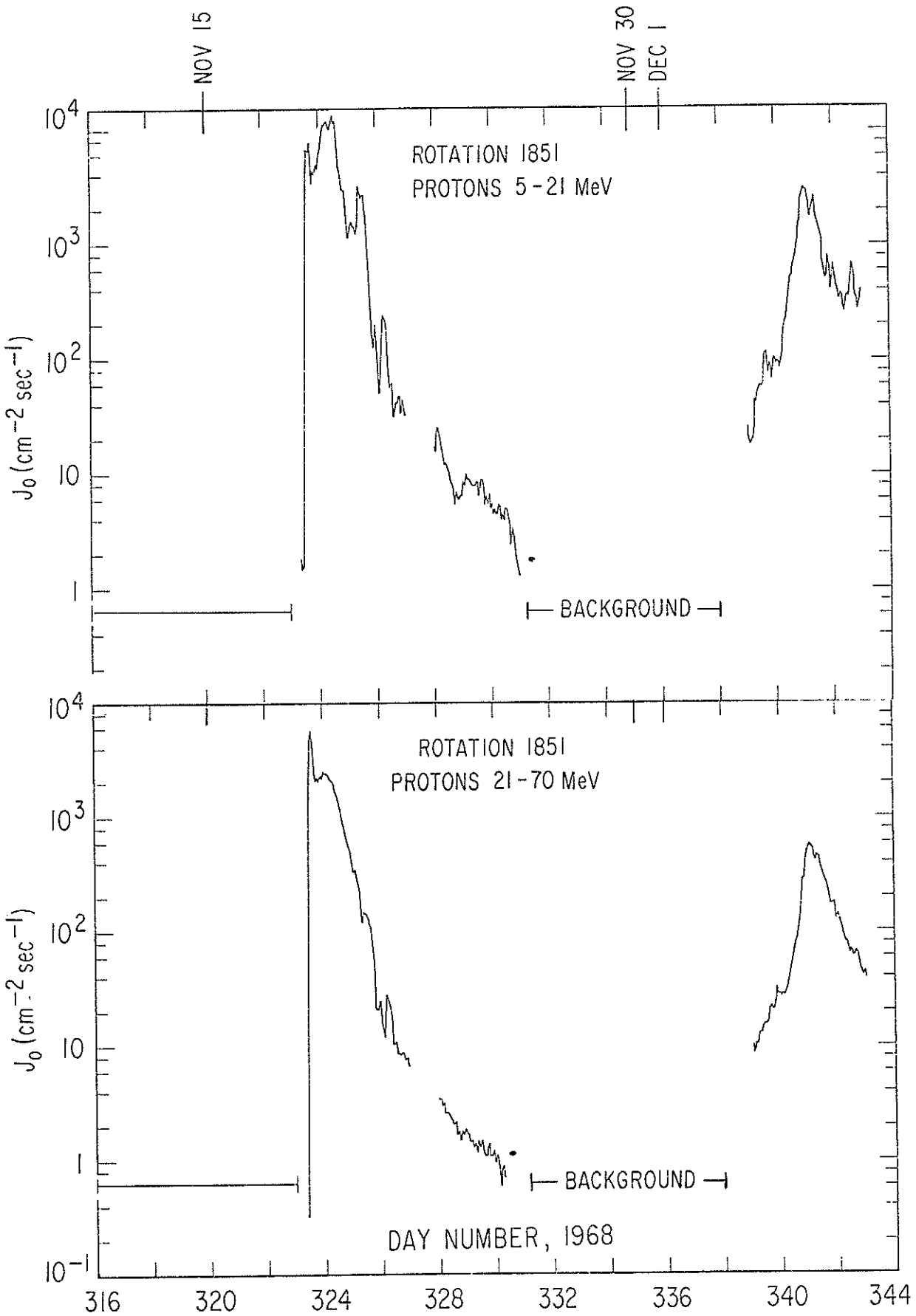

Fig. 1. ATS-1 Energetic proton flux November 11 - December 8, 1968.

"Protons, Alpha Particles, and Electrons Resulting from the 18 November 1968 Solar Flare"

by

L. J. Lanzerotti
Bell Telephone Laboratories
Murray Hill, New Jersey

This report presents the data on the solar proton, alpha particles, and electron fluxes measured by an instrument on the Explorer 34 (IMP F) satellite following the extreme west hemisphere (N21 W87) 1B solar flare of November 18, 1968. The Bell Telephone Laboratories instrument on Explorer 34 has been previously reported in the literature [Lanzerotti et al., 1969]. The data measurements will be described below; a more complete discussion of the observations and their implications for solar particle propagation is in preparation [Lanzerotti and Graedel, to be published].

Proton Observations

Figure 1 contains the hourly average solar proton fluxes measured in the eight energy channels of the experiment. Plotted at the bottom of the figure are the hourly counting rates of the Alert neutron monitor. The ground level high energy particle enhancement from the flare is clearly observed. Also indicated in the neutron monitor plot is the time of the sudden commencement magnetic storm at 0904 UT on November 20.

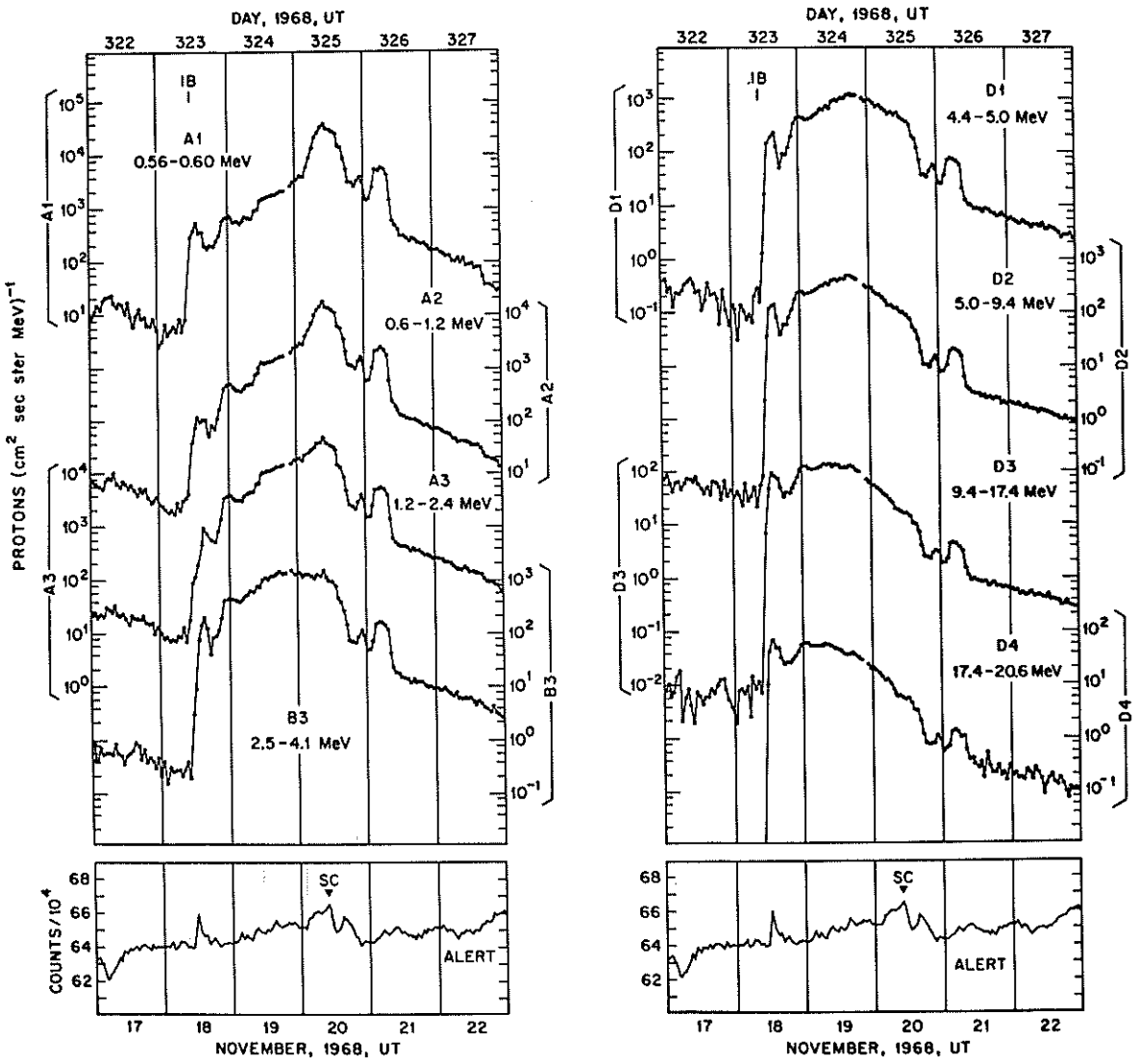

Fig. 1. Solar proton data following the 18 November 1968 solar flare. Plotted below the proton fluxes are the hourly neutron monitor rates from Alert.

The fast time resolution data (not shown) indicates that all of the proton energy channel counting rates increased at approximately the same time (±~10 minutes). The counting rates increased rapidly to a peak and then decreased to a minimum approximately seven to eight hours after the onset. The fluxes in the higher energy channels increased after the initial peak and then decreased steadily while the fluxes in the lower energy channel continued to increase steadily until the time of the sudden commencement. It is interesting to note that an initial peak in the proton fluxes after the particle onset was also observed after another extreme west hemisphere solar flare on 10 September 1961 [Bryant et al., 1965].

After the sudden commencement the fluxes in all proton channels decreased. Two subsequent enhancements were seen prior to a rather steady, exponential decay of the fluxes. The time constant of this decay, beginning at approximately 1200 UT on November 21, was approximately independent of proton energy [Lanzerotti and Graedel, to be published].

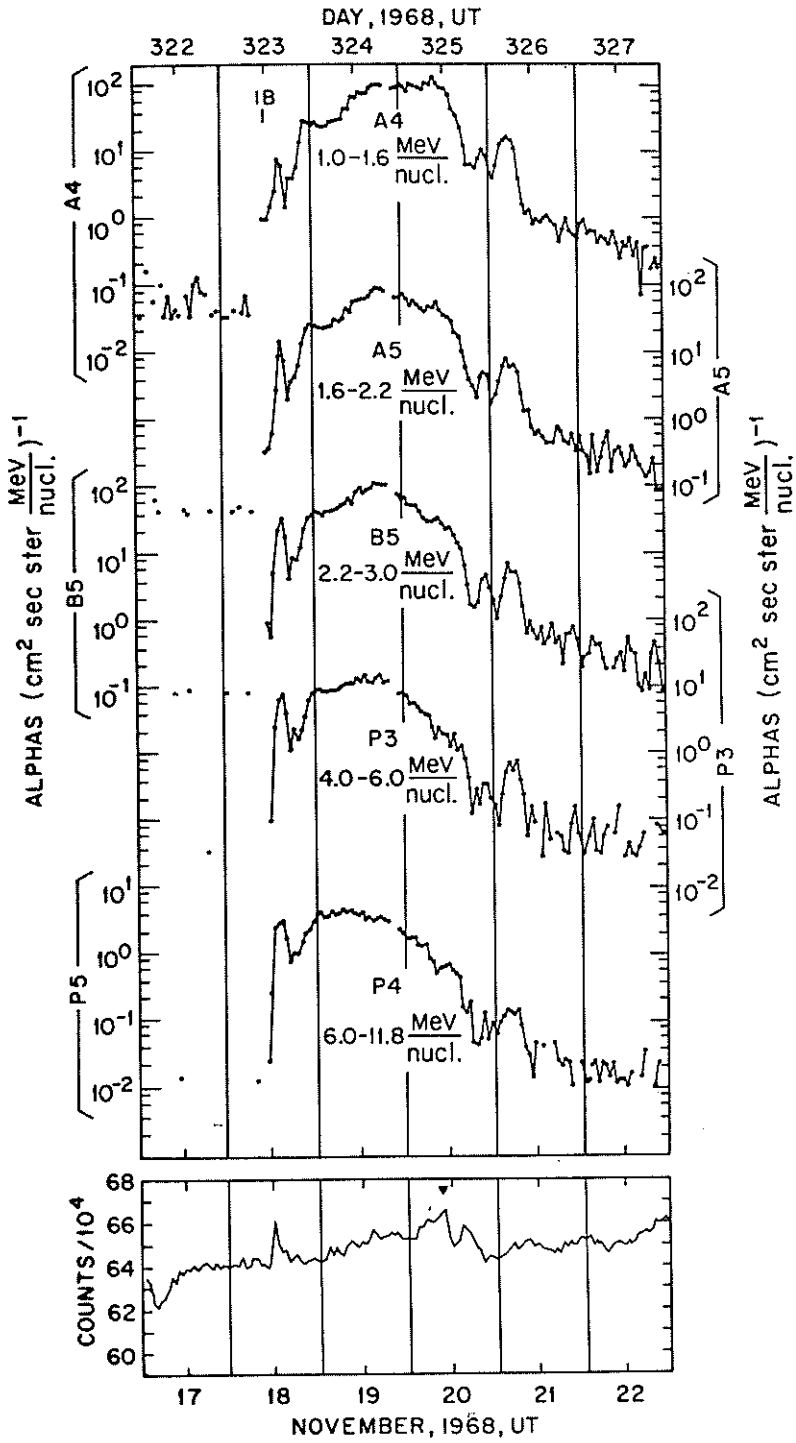

Fig. 2. Alpha particle data following the 18 November 1968 solar flare.

Alpha Particle Observations

The hourly average alpha particle fluxes measured following the 18 November flare are plotted in the Figure 2. The onset times of the alpha particles were also approximately energy independent and equal to the proton onset times. With the major exception that the initial particle peak following the onset appears narrower for the alphas than for the protons, the general flux-time profiles for the alphas and the protons are similar. The approximately exponential decay times beginning on 21 November were approximately energy independent and equal to the proton decay times [Lanzerotti and Graedel, to be published].

The alpha to proton ratios for particles compared as to equal energy (equal rigidity), equal energy per charge ($E_\alpha = 2E_p$) and equal energy per nucleon are plotted in Figure 3. For protons and alphas of equal energy, the alpha to proton ratios increase steadily to the time of the sudden commencement. Following two subsequent enhancements of the ratios, corresponding to the two flux enhancements observed in all energy channels on November 20 and 21, the equal energy ratios remained approximately constant, indicative of the energy-independent decay times beginning on 21 November.

The constant energy per nucleon alpha to proton ratios ($v_\alpha = v_p$) decreased steadily from the flux peaks following the particle onsets to the time of the sudden commencement. After an initial enhancement in the ratios following the particle onsets, the constant energy per charge alpha to proton ratios were essentially constant during the entire period when the particles were observed at the earth.

The alpha to proton ratio data of Figure 3 suggests that the initial enhanced spike of particle fluxes following the particle onsets at the earth was enriched with alpha particles from the flare. Following this enhancement, however, the three sets of alpha to proton ratios had time behaviors quite similar to those observed following the east hemisphere solar event of 23 May 1967 [Lanzerotti and Robbins, 1969]. These similarities and their implications for solar particle propagation are included in a paper in preparation [Lanzerotti and Graedel, to be published].

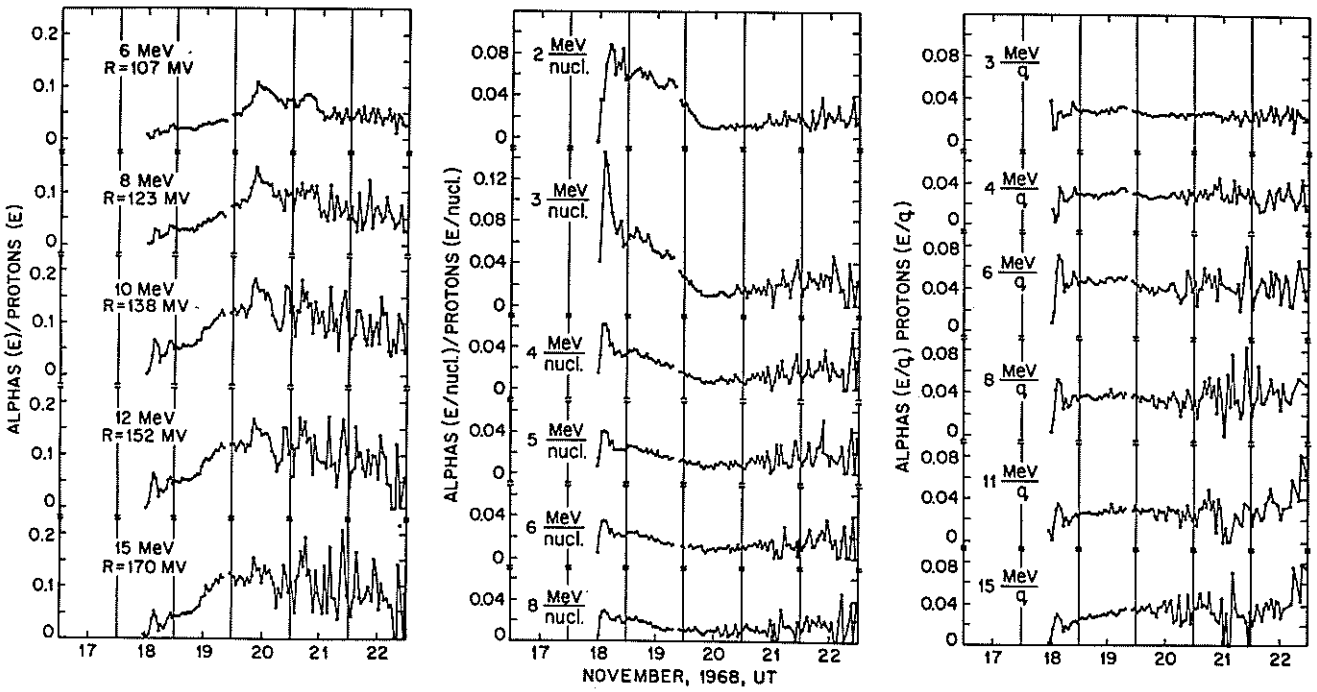

Fig. 3. Alpha to proton ratios plotted as a function of equal particle energy, equal particle energy per nucleon and equal particle energy per charge.

Electron Observations

The electron counting rates measured in three energy channels are plotted in Figure 4. The background counts in each channel are equal to the rates measured during November 17. After subtracting the backgrounds the integral electron fluxes in terms of electrons $(cm^2\ sec\ ster)^{-1}$ can be obtained approximately by multiplying the H1 rates by 57, the H2 rates by 7.2, and the H3 rates by 7.2.

The electron rate onset times on November 18 were energy independent and approximately equal to the proton and alpha particle onset times. The initial sharp enhancement after the electron onsets was seen in all of the electron channels. The electron decay times beginning on November 21 were approximately energy independent and nearly equal to the proton and alpha decay times.

Energetic Storm Particles

The four lowest energy proton channels and the lowest energy alpha particle channel all show approximately steady increases of the particle fluxes up to the time of the sudden commencement (Figures 1 and 2). In particular, the two lowest energy proton channels show flux peaks of several hours duration around the time of the sudden commencement. These energetic storm particle enhancements have often been discussed previously [Axford and Reid, 1963; Rao et al., 1967].

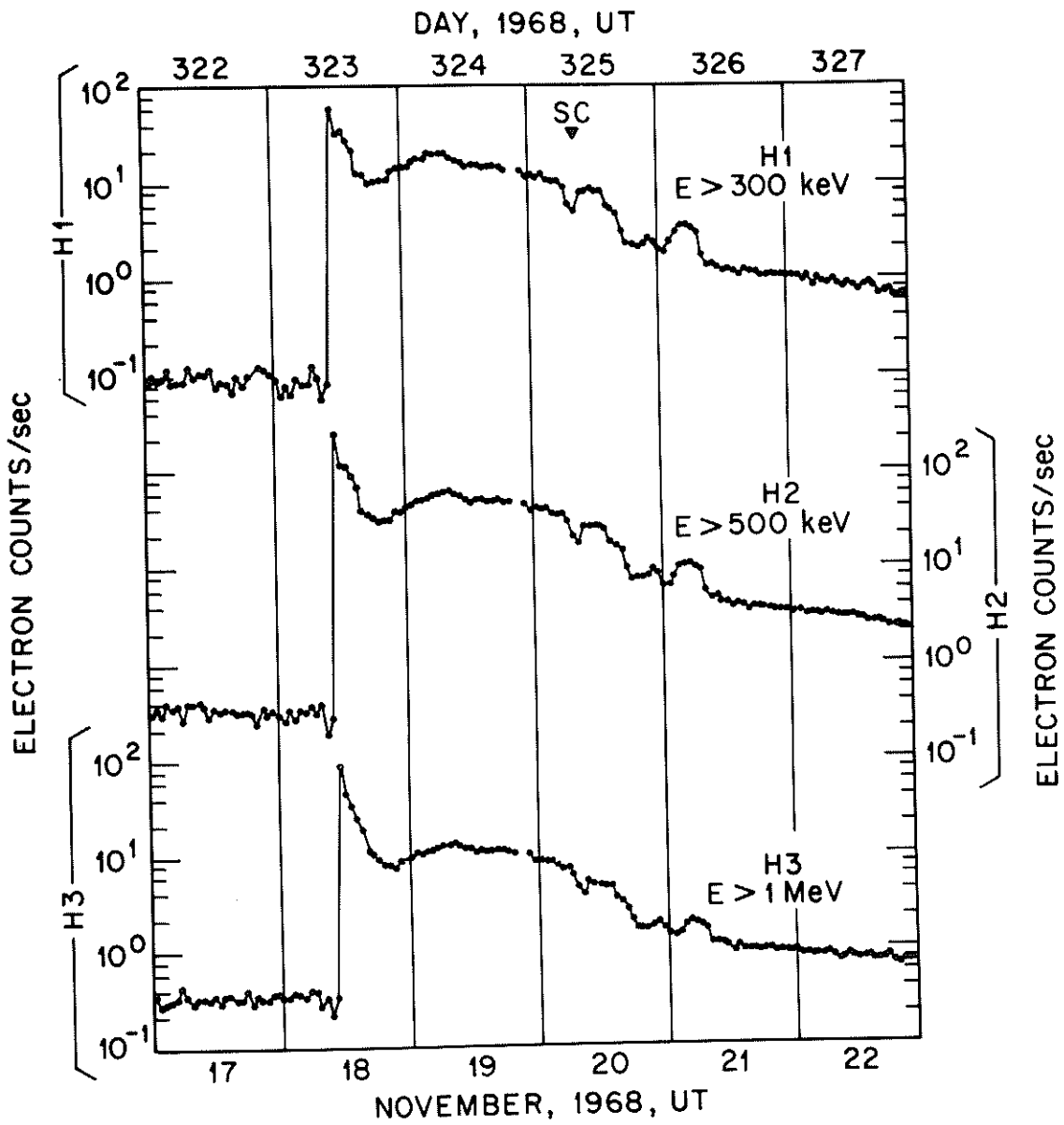

Fig. 4. Electron counting rates measured following the 18 November 1968 solar flare.

Plotted in Figure 5 is each 9.28 second average proton flux measured in five proton energy channels for a three hour interval around the sudden commencement. Clearly observed in the two lowest energy proton fluxes is a sharp, approximately one minute wide peak at the time of the sudden commencement. This peak is not observed in the higher energy fluxes. Immediately following the sudden commencement, a decrease of the proton fluxes is observed in all proton energy channels.

Although a similar narrow enhancement at the time of the sudden commencement was observed in the lowest energy alpha channel, no enhancement was observed in the electron fluxes. The data of Figure 4 indicates clearly that the electron fluxes appear to decrease prior to the sudden commencement and then to increase in intensity after the interplanetary disturbance has passed.

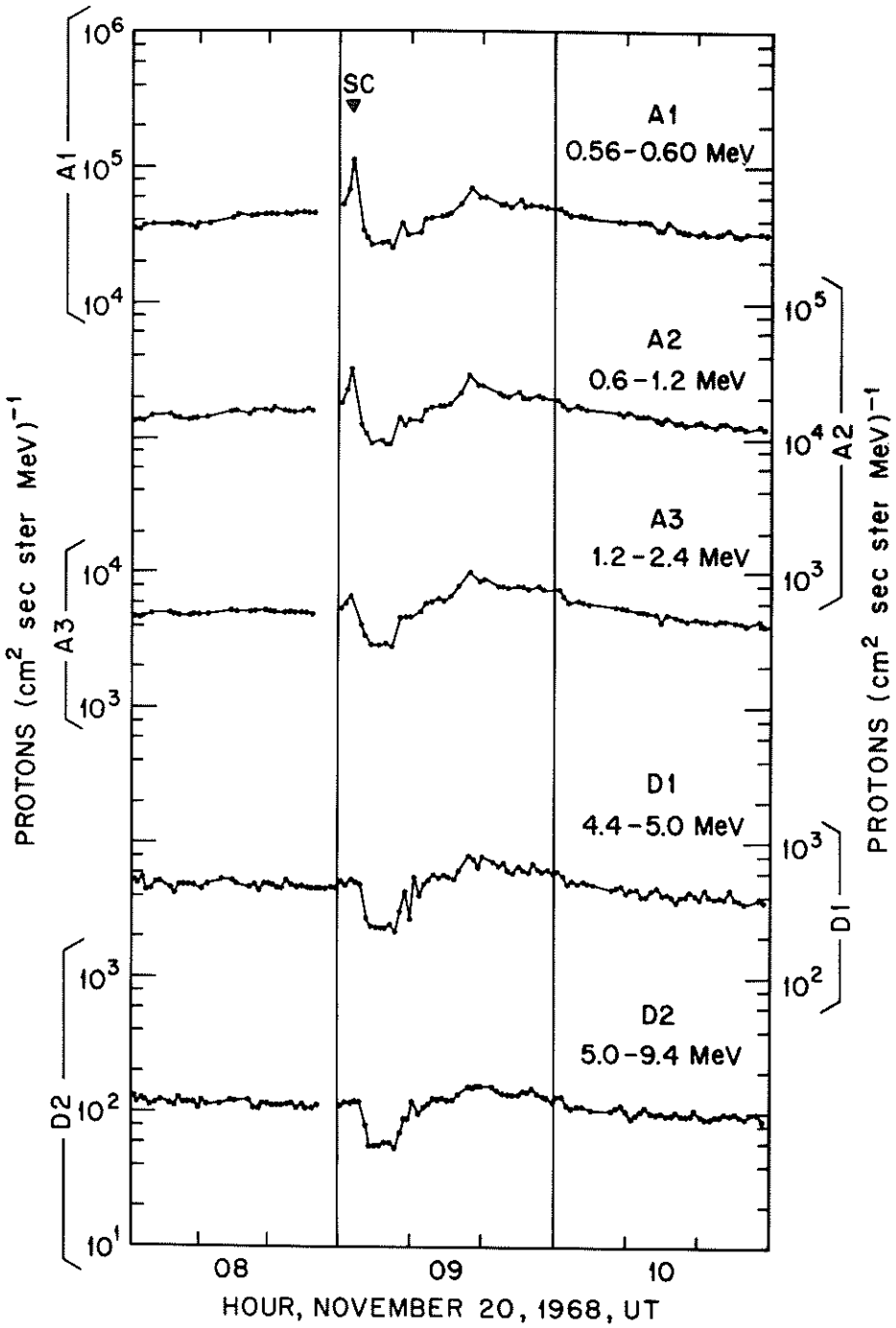

Fig. 5. High time resolution proton data measured during the time of the sudden commencement at 0904 UT, 20 November. Each data point corresponds to a 9.28 second counting average.

Acknowledgements

I thank T. E. Graedel for discussions of the data and C. M. Soltis for computational assistance. The Alert neutron monitor data was kindly supplied by World Data Center A, Upper Atmosphere Geophysics, Boulder, Colorado.

REFERENCES

AXFORD, W. I. and G. C. REID — 1963 — J. Geophys. Res., 68, 1793.

BRYANT, D. A., T. L. CLINE, U. D. DESAI, and F. B. MC DONALD — 1965 — Astrophys. J., 141, 478.

LANZEROTTI, L. J. and T. E. GRAEDEL — To be published.

LANZEROTTI, L. J., H. P. LIE, and G. L. MILLER — 1969 — IEEE Trans. Nucl. Sci., NS-16(1), 343.

LANZEROTTI, L. J. and M. F. ROBBINS — 1969 — Solar Phys., 10, 212.

RAO, U. R., K. G. MC CRACKEN, and R. P. BUKATA — 1967 — J. Geophys. Res., 72, 4325.

"Pioneer 9 Solar Wind Velocity and Electric Field Data 8 November 1968 to 4 January 1969"

by

Ira M. Green and F. L. Scarf
Space Physics Analysis Department
TRW Systems Group, Redondo Beach, California

[The compiler has prepared the following paragraphs from information submitted by the authors.]

Pioneer 9 was launched November 8, 1968. In Figure 1 is shown the trajectory plot of the space probe from launch to January 4, 1969. The position of Pioneer 9 during November 18-20, 1968 is indicated.

Figure 2 presents data from November 8, 1968 - January 4, 1969 from Pioneer 9. Intermittent samples of the peak solar wind velocity in km/sec from the plasma probe are given in the top portion of the graph. Electric field data at the approximate frequency of 100 Hz are given in the center of the graph as the broadband potential amplitude, ϕ, in millivolts. Kp-indices are plotted at the bottom of the graph. Solid triangles indicate the times of ground sudden commencements and open triangles denote sudden impulses.

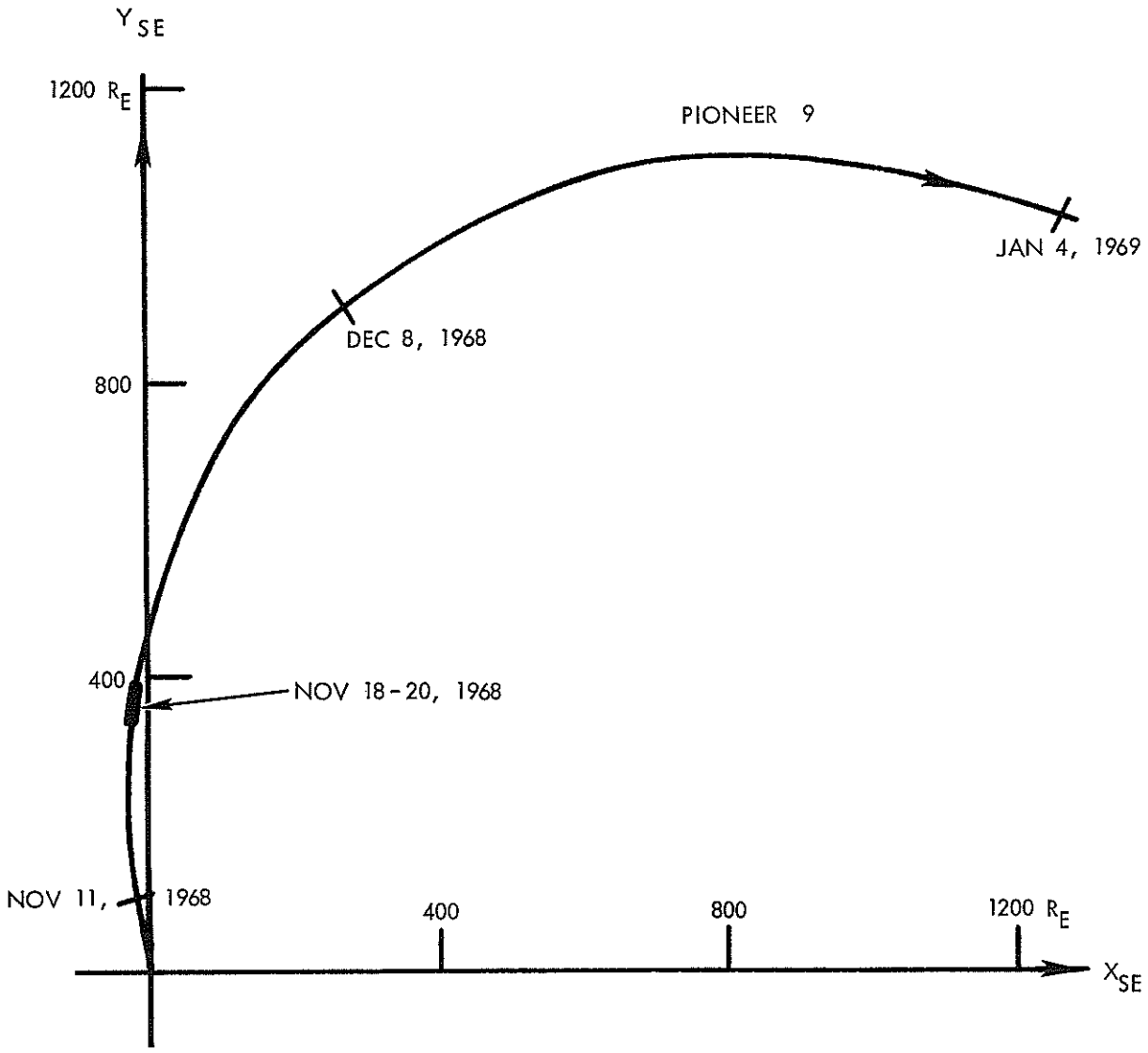

Fig. 1. Trajectory of Pioneer 9, November 8, 1968 to January 4, 1969.

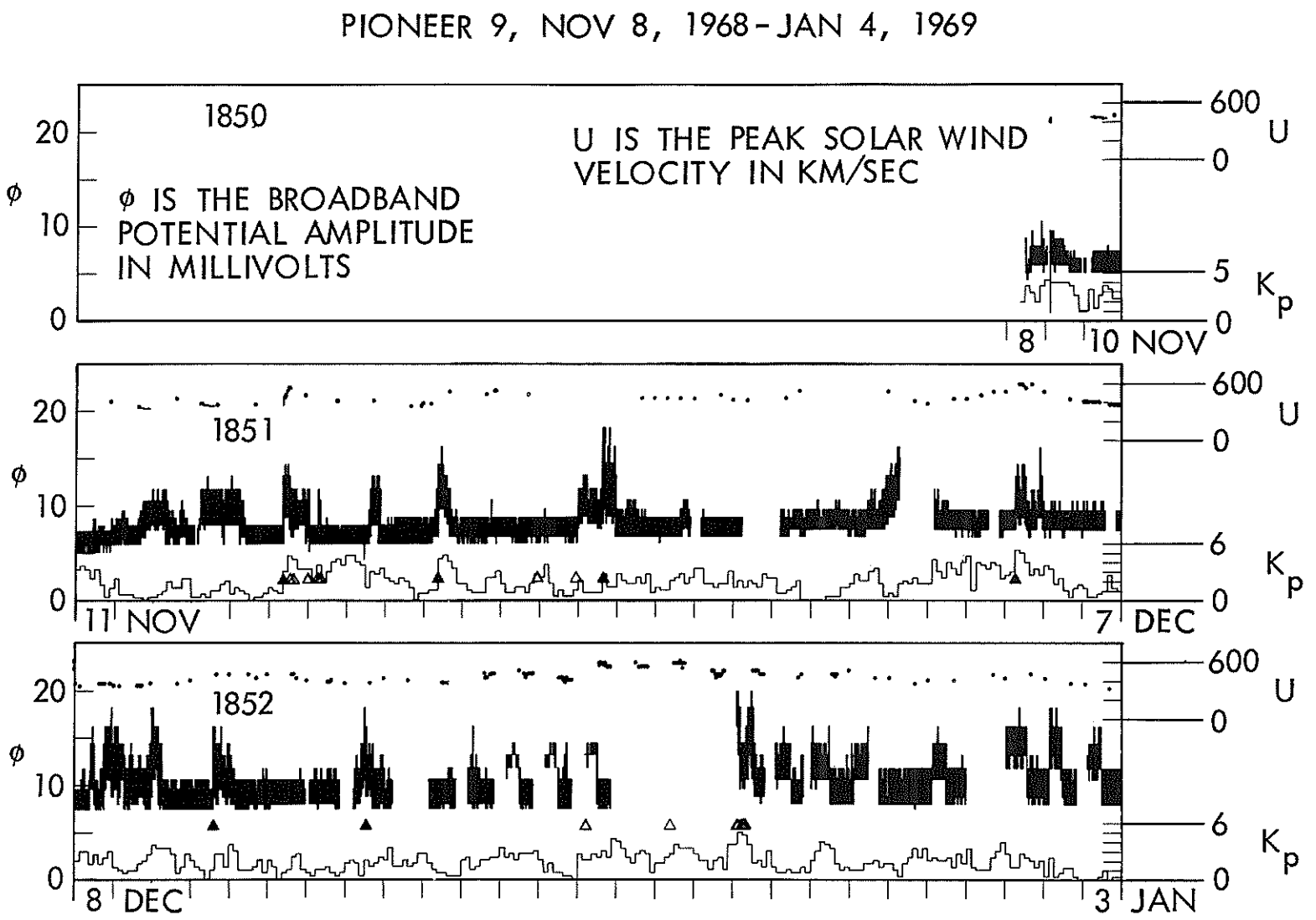

Fig. 2. Solar wind velocity and electric field data from Pioneer 9, November 8, 1968 to January 4, 1969.

6. COSMIC RAYS

"Tabulations and Selected Graphs of Neutron Monitor Observations November 18, 1968"

by

J. Virginia Lincoln
Space Disturbances Laboratory
ESSA Research Laboratories, Boulder, Colorado

One of the outstanding sea-level increases in cosmic ray intensity as observed by neutron monitors was observed on November 18, 1968. Data pertinent to this event are reported.

The data presented were submitted to World Data Center A - Upper Atmosphere Geophysics in keeping with routine submission of data. The cooperation of all the reporting observatories is gratefully acknowledged.

Table 1 presents the hourly values for November 18, 1968 from 43 stations listed in cutoff rigidity order. In Table 2 the stations abbreviations are indicated together with equipment, coordinates, cutoff rigidity, scaling factor, pressure to which corrected, pressure coefficient, mean station pressure, and real count information for each reporting observatory.

Following these hourly values are given in Table 3 the two-minute, five minute, ten-minute or fifteen-minute hourly rates during the period of the increase on November 18, 1968 from 23 stations. All data are pressure corrected except for Calgary and Sulphur Mountain for which uncorrected and pressure hourly rates are given. The headings of each station present the necessary details for interpretation of the data. The stations are in cutoff rigidity order as follows:

Station	Cutoff rigidity	Hourly rate
Thule	0.00	Two-minute
Alert	0.00	Five-minute
Resolute	0.00	" "
Dumont d'Urville	0.01	Fifteen-minute
McMurdo	0.01	Two-minute
South Pole	0.11	" "
Inuvik	0.18	Five-minute
Fort Churchill	0.21	" "
Goose Bay	0.52	" "
Oulu	0.81	" "
Deep River	1.02	" "
Ottawa	1.08	Ten-minute
Calgary	1.09	Five-minute
Sulphur Mountain	1.14	" "
Port aux Francais	1.19	Fifteen-minute
Mt. Washington	1.24	Five-minute
Durham	1.41	" "
Uppsala	1.43	" "
Chicago	1.72	Fifteen-minute
Swarthmore	1.92	Two-minute
Kiel	2.29	Five-minute
Lindau	3.00	Ten-minute
Climax	3.03	Fifteen-minute
Dallas	4.35	Five-minute

A few selected graphs are presented following the tabulations. Figure 1 gives the Victoria superneutron monitor pressure corrected data at five-minute intervals. A tabulation of these data was not available.

Figure 2 gives detail of the onset of the increase as seen on the Deep River superneutron monitor from 1000 to 1200 UT.

In Figure 3 the five-minute data from Goose Bay, Deep River, Inuvik and Alert are shown in percentage deviations for 0900-2400 UT.

Table 1

HOUR	01	02	03	04	05	06	07	08	09	10	11	12
THU	3946	3943	3956	3953	3930	3956	3939	3938	3948	3938	3978	4107
ALE	6408	6400	6440	6396	6410	6441	6434	6411	6413	6398	6414	6611
RES	20301	20261	20362	20239	20213	20206	20307	20203	20323	20264	20287	20919
DUM	1905	1899	1895	1884	1893	1886	1876	1858	1860	1872	1886	1946
MCM	8345	8382	8354	8429	8441	8407	8380	8330	8367	8386	8533	8728
SOU	2003	2003	2026	2033	2017	2033	2007	2011	2019	2023	2106	2205
INU	6032	6041	6016	6034	6027	6011	6035	6026	6013	5987	6018	6247
CHU	5571	5566	5563	5570	5581	5568	5582	5584	5565	5584	5720	5754
GOO	6137	6150	6145	6128	6135	6185	6158	6176	6169	6173	6318	6425
APA	472	479	474	489	477	487	485	488	493	479	477	478
OUL	3322	3325	3333	3315	3313	3304	3315	3333	3311	3300	3327	3343
DEE	6050	6104	6110	6121	6089	6073	6090	6083	6095	6106	6244	6311
OTT	2606	2589	2588	2609	2658	2636	2565	2565	2581	2586	2672	2673
CAL	9978	10012	10003	9952	9966	9963	9949	9923	9939	9969	10240	10484
BEG	22	28	12	10	35	21	8	10	0	0	12	38
SUL	7366	7378	7389	7387	7364	7376	7372	7347	7363	7347	7616	7833
POR	1738	1736	1736	1735	1733	1740	1725	1725	1732	1715	1728	1743
MTW	2002	1998	2026	1995*	1995	2020	2035	2010	2018	2020	2055	2117
DUR	2297	2289	2302	2289	2277	2310	2318	2283	2272	2289	2319	2350
YAK	1004	1000	993	991	986	1008	1002	1015	1003	999	1013	1006
CHI	2166	2185	2170	2191	2192	2175	2163	2212	2205	2193	2232	2218
VIC	5944	5968	5973	5944	5965	5957	5913	5906	5937	5945	6049	6081
SWA	3086	3066	3091	3112	3079	3091	3091	3107	3088	3112	3121	3126
LEE	6604B	6530	6539	6513	6511	6541	6522	6520	6518	6533	6552	6588
KIE	5630	5615	5592	5598	5589	5622	5593	5579	5603	5612	5593	5624
LIN	3474	3445	3444	3450	3438	3436	3448	3442	3453	3440	3451	3458
CLI	3618	3628	3612	3607	3618	3609	3604	3602	3602	3609	3686	3658
HAL	34	48	27	34	46	43	49	23	22	29	34	22
MUN		4931		4902		4868		4902		4888		4888
ZUG		4524		4506		4492		4494		4502		4511
DAL	5736	5721	5737	5727	5733	5736	5746	5732	5759	5761	5768	5768
JUN	54304	54275	54333	54314	54449	54554	54622	54420	54766	54689	54602	54487
WHI	5225	5201	5171	5234	5185	5172	5182	5197	5218	5195	5247	5258
HER	935	933	932	932	931	929	932	941	945	932	924	934
PIC	2296	2286	2281	2272	2265	2284	2280	2276	2278	2275	2281	2275
USH	156	131	145	126	136	156	184	107	132	171	192	150
TBI	1562	1536	1550	1546	1546	1540	1539	1562	1558	1552	1584	1576
ALM	2152	2163	2157	2135	2167	2131	2150	2148	2132	2136	2145	2140
BUE	2724	2774	2798	2749	2760	2722	2752	2831	2756	2746	2773	2776
MIN	3673	3567	3647	3657	3668	3662	3648	3674	3657	3565	3656	3666
CHA	6543	6546	6555	6546	6538	6516	6524	6517	6522	6522	6514	6509
KUL	1178	1172	1191	1195	1178	1191	1193	1194	1186	1180	1190	1198
HUA	1682	1686	1676	1676	1680	1676	1684	1689	1695	1673	1678	1676

Table 1 (Continued)

13	14	15	16	17	18	19	20	21	22	23	24	AVERAGE
3999	3996	3979	3972	3955	3975	3980	3968	3976	3976	3966	3975	3968
6502	6465	6469	6419	6446	6461	6430	6414	6428	6432	6433	6424	6437.5
20435	20442	20447	20354	20291	20387	20241	20383	20380	20389	20321	20420	20348.9
1903	1903	1909	1921	1919	1931	1919	1921	1923	1919	1925	1919	1903
8559	8541	8546	8534	8535	8522	8514	8536	8521	8494	8436	8424	8472
2081	2063	2045	2047	2056	2049	2023	2025	2026	2022	2019	2026	2040
6143	6086	6083	6063	6041	6061	6063	6070	6076	6063	6053	6069	6056.6
5670	5644	5656	5624	5621	5640	5614	5636	5631	5627	5633	5638	5622.6
6299	6233	6219	6208	6225	6237	6202	6231	6226	6232	6228	6230	6211.2
475	468	489	480	488	491	495	495	481	477	466	482	1482.0
3344	3353	3349	3327	3351	3335	3346	3347	3342	3341	3331	3329	3330.6
6228	6189	6152	6137	6133	6116	6082	6076	6106	6092	6111	6121	6125.8
2610	2639	2612	2620	2629	2629	2567	2640	2610	2621	2663	2599	2615.3
10228	10170	10174	10145	10130	10112	10100	10096	10067	10041	10049	10103	10074.7
29	24	11	27	22	13	27	13	16	20	8	28	19.7
7623	7587	7558	7562	7505	7498	7473	7454	7456	7416	7466	7448	7466.0
1748	1732	1731	1745	1740	1749	1744	1740	1744	1758	1759	1763	1739
2086	2050	2026	2037	2018	2006	2011	2011	2020	2028	2038*	2008*	2026
2338	2300	2300	2323	2295	2280	2294	2300	2291	2297	2300	2312	2301
1023	1006	988	1028	1004	1002	995	1002	1003	1010	1018	1003	1004
2204	2229	2234	2208	2223	2218	2226	2211	2199	2211	2178	2198	2201.7
6065	6064	6074	6095	6085	6080	6066	6070	6032	6022	6028	6030	6012.2
3130	3095	3110	3114	3091	3101	3079	3099	3094	3082	3094	3093	3098
6572	6537	6560	6547	6556	6597	6575	6577	6562	6559	6597	6563	6553.0
5609	5613	5601	5625	5609	5629	5614	5630	5637	5634	5639	5645	5613.9
3450	3452	3449	3457	3453	3466	3466	3472	3473	3483	3488	3477	3457
3659	3656	3645	3653	0000	0000	3645	3600	3596	3603	3620	3618	3624.9
22	51	32	30	58	49	43	40	28	29	46	42	36.7
	4858		4850		4897		4898		4937		4896	4893
	4521		4526		4548		4549		4568		4591	4528
5775	5780	5773	5772	5743	5709	5689	5708	5741	5763	5767	5760	5746.0
53890	54005	54814	54631	54314	54556	54566	54808	54602	55237	55168	54999	5455.9
5235	5286	5248	5289	5225	5221	5206	5139	5159	5230	5189	5232	5214
932	934	936	935	926	934	927	929	936	940	938	947	933.9
2278	2280	2280	2281	2286	2289	2289	2288	2296	2297	2312	2314	2285
162	137	165	226	185	183	170	183	192	180	155	169	162.3
1566	1566	1604	1608	1620	0000	0000	0000	0000	0000	0000	0000	1566
2169	2158	2157	2158	2161	2182	2159	2177	2189	2145	2142	2170	2155
2687	2744	2792	2753	2767	2814	2831	2842	2830	2797	2791	2817	2776.1
3584	3544	3537	3564	3664	3679	3666	3650	3682	3681	3680	3677	3658
6510	6512	6517	6521	6536	6528	6553	6555	6566	6573	6577	6586	6536.9
1194	1196	1189	1188	1187	1203	1190	1184	1192	1180	1182	1189	1188.3
1682	1672	1681	1677	1682	1674	1686	1688	1693	1686	1699	1688	1682.5

Table 2

Abbrev.	Station	Equip.	Geographic Coordinates		Cutoff Rigidity	Scaling Factors	Pressure Coefficient	Mean Station Pressure mm HG	Real Counts
THU	Thule	SNM	76.6N	68.8W	0.00	--	0.990 %/mm Hg	730	100 x tabulated
ALE	Alert	SNM	82.3N	62.2W	0.00	--	9.87 %/cm Hg	752	100 x tabulated
RES	Resolute	SNM	74.7N	265.1E	0.00	10	--	--	10 x tabulated
DUM	Dumont d'Urville	SNM	66.4S	140.0E	0.01	200	9.9 %/cm Hg	--	---
MCM	McMurdo	SNM	77.9S	166.6E	0.01	--	0.990 %/mm Hg	730	100 x tabulated
SOU	South Pole	NM	90.0S		0.11	--	-1.000 %/mm Hg	510	100 x tabulated
INU	Inuvik	SNM	68.2N	133.4W	0.18	--	9.87 %/cm Hg	758	100 x tabulated
CHU	Churchill	SNM	58.8N	265.9E	0.21	--	--	1010*	120 x tabulated
GOO	Goose	SNM	53.2N	60.2W	0.52	--	9.87 %/cm Hg	758	100 x tabulated
APA	Apatity	SNM	67.5N	33.3E	0.65	--	-0.68 %/mb	--	---
OUL	Oulu	SNM	65.1N	25.3E	0.81	100	--	--	---
DEE	Deep River	SNM	46.1N	77.3W	1.02	--	9.87 %/cm Hg	747	300 x tabulated
OTT	Ottawa	NM	45.4N	284.4E	1.08	64	--	--	64 x tabulated
CAL	Calgary	SNM	51.1N	114.1W	1.09	--	0.7718%/mb	--	100 x tabulated
BEG	Bergen	NM	60.4N	5.4E	1.13	16	-0.74 %/mb	1010*	16 x tabulated
SUL	Sulphur Mountain	SNM	51.2N	115.6W	1.14	--	0.7665%/mb	--	100 x tabulated
POR	Port aux Francais	SNM	49.2S	70.2E	1.19	--	10.1 %/cm Hg	--	400 x tabulated
MTW	Mt. Washington	NM	44.3N	288.7E	1.24	64	25.4 %/in.Hg	23.800#	x 1.003 normalizes to Jan.66
DUR	Durham	SNM	43.1N	289.2E	1.41	256	-20.8 %/in.Hg	29.940#	---
YAK	Yakutsk	NM	62.0N	129.7E	1.70	--	-0.68 %/mb	--	---
CHI	Chicago	NM	41.8N	87.7W	1.72	10	-0.96 %/mm Hg	750	---
VIC	Victoria	SNM	48.3N	123.2W	1.86	--	--	--	100 x tabulated
SWA	Swarthmore	SNM	39.9N	75.4W	1.92	--	-0.970 %/mm Hg	760	100 x tabulated
LEE	Leeds	SNM	53.8N	01.5W	2.20	--	9.99 %/cm Hg	753	100 x tabulated
KIE	Kiel	SNM	54.3N	10.1E	2.29	--	--	755	100 x tabulated

* mb
\# Inches Hg

Table 2 (Continued)

Abbrev.	Station	Equip.	Geographic Coordinates		Cutoff Rigidity	Scaling Factors	Pressure Coefficient	Mean Station Pressure mm HG	Real Counts
LIN	Lindau	SNM	51.6N	10.1E	3.00	--	--	780	100 x tabulated
CLI	Climax	NM	39.4N	106.2W	3.03	100	-0.96 %/mm Hg	504	---
HAL	Halle	NM	51.3N	11.6E	3.07	--	-9.42 %/cm Hg	750	---
MUN	Munchen	NM	**48.2N	11.6E	4.14	16	-0.96 %/mm Hg	715	---
ZUG	Zugspitze	NM	**47.4N	11.0E	4.24	100	-1.05 %/mm Hg	530	---
DAL	Dallas	SNM	32.6N	96.4W	4.35	--	--	995*	120 x tabulated
JUN	Jungfraujoch	NM	46.6N	8.0E	4.48	100	-0.0096%/mm Hg	482	---
WHI	White Mountain	NM	37.6N	241.8E	4.48	--	-0.76 %/mb	645*	100 x tabulated
HER	Hermanus	SNM	34.3S	19.1E	4.90	100	-0.72 %/mb	1015*	---
PIC	Pic du Midi	SNM	42.6N	0.15E	5.36	--	9.3 %/cm Hg	--	1000 x tabulated
USH	Ushuaia	NM	54.8S	68.3W	5.68	8	--	750	Add 3000
TBI	Tbilisi	NM	42.1N	44.8E	6.67	--	-0.72 %/mb	--	---
ALM	Alma Ata	NM	43.3N	76.9E	6.69	--	-0.72 %/mb	--	---
BUE	Buenos Aires	SNM	34.4S	58.3W	10.63	--	8.75 %/cm Hg	760	32 x tabulated + 320000
MIN	Mina Aguilar	NM	23.1S	65.7W	12.51	--	0.93 %/mm Hg	475	64 x tabulated
CHA	Chacaltaya	SNM	16.2S	68.9W	13.10	--	9.30 %/cm Hg	406	1000 x tabulated
KUL	Kula	SNM	20.4N	203.4E	13.30	--	9.15 %/cm Hg	686	100 x tabulated
HUA	Huancayo	NM	12.0S	75.3W	13.45	100	-0.96 %/mm Hg	518	---

* mb
** Reported Bi-Hourly

Table 3

THULE 76.55N 291.16E GREENLAND

NEUTRON MONITOR NM-64

CORRECTED FOR PRESSURE USING THE GALACTIC PRESSURE COEFFICIENT ONLY

SCALING FACTOR = 100

TWO-MINUTE HOURLY RATES

NOVEMBER 18, 1968

TIME	MINUTES AT END OF INTERVAL														
	00 OR 30	02 32	04 34	06 36	08 38	10 40	12 42	14 44	16 46	18 48	20 50	22 52	24 54	26 56	28 58
1030	1292	1272	1272	1302	1331	1292	1262	1272	1282	1321	1292	1292	1302	1371	1390
1100	1361	1366	1390	1420	1351	1390	1369	1369	1359	1359	1359	1310	1320	1340	1300
1130	1330	1350	1320	1330	1350	1320	1369	1319	1319	1299	1309	1329	1279	1338	1299
1200	1308														

ALERT 82.30N 62.20W CANADA

NEUTRON MONITOR 18-NM-64

REAL COUNTS 100 TIMES TABULATED COUNTS

FIVE-MINUTE BAROMETER CORRECTED HOURLY RATES

NOVEMBER 18, 1968

TIME U.T.	MINUTES AT END OF INTERVAL 05	10	15	20	25	30	35	40	45	50	55	60	AVERAGE
900-1000	6351	6364	6441	6351	6467	6396	6409	6487	6422	6312	6376	6428	6400
1000-1100	6441	6422	6435	6422	6370	6331	6422	6383	6396	6422	6429	6500	6414
1100-1200	6746	6888	6584	6636	6539	6571	6636	6597	6577	6539	6448	6545	6609
1200-1300	6513	6461	6532	6545	6455	6506	6487	6519	6481	6513	6474	6526	6501
1300-1400	6526	6410	6500	6481	6532	6513	6500	6436	6397	6391	6513	6397	6466
1400-1500	6474	6487	6442	6532	6365	6442	6468	6474	6525	6474	6519	6391	6466
1500-1600	6468	6430	6398	6385	6449	6372	6430	6462	6430	6379	6430	6391	6419
1600-1700	6468	6474	6423	6417	6417	6481	6500	6442	6455	6430	6430	6442	6448
1700-1800	6449	6449	6563	6461	6487	6461	6392	6430	6461	6423	6525	6449	6462
1800-1900	6436	6430	6487	6417	6455	6506	6455	6442	6335	6379	6392	6392	6427
1900-2000	6404	6430	6385	6461	6335	6385	6474	6461	6411	6487	6373	6348	6413
2000-2100	6360	6411	6499	6436	6360	6474	6367	6480	6436	6385	6455	6467	6427
2100-2200	6411	6411	6455	6442	6455	6392	6430	6385	6448	6461	6430	6423	6429
2200-2300	6373	6537	6392	6411	6436	6436	6385	6354	6493	6430	6404	6505	6430
2300-2400	6417	6455	6367	6448	6360	6423	6423	6461	6461	6423	6423	6442	6425

RESOLUTE 74.70N 94.98W CANADA

NEUTRON MONITOR 6-NM-64

FIVE-MINUTE BAROMETER CORRECTED RATES

NOVEMBER 18, 1964

TIME-HR.	MINUTE AT END OF INTERVAL 5	10	15	20	25	30	35	40	45	50	55	60
9-10	17167	16898	17283	16703	16778	16855	16745	17056	17036	16886	16682	16552
10-11	17012	17001	16656	16699	17267	16593	16604	16849	16892	16612	16849	17877
11-12	17342	17996	17747	17681	17434	17637	17422	17240	17090	17207	17229	17154
12-13	17218	16727	17099	17087	16967	17032	17247	16990	17001	16947	17151	16938
13-14	17195	17460	17319	17051	16795	16997	16847	16591	16792	17026	17375	16897

Table 3 (Continued)

DUMONT D'URVILLE 66.66S 140.02E ANTARCTICA

NEUTRON MONITOR 9-NM-64

CORRECTED FOR BAROMETRIC PRESSURE

COEFFICIENT 9.9 PER CENT PER CM HG

MULTIPLY INDICATED NUMBERS BY 400

FIFTEEN-MINUTE HOURLY RATES

NOVEMBER 18, 1968

TIME U.T.	MINUTES AT END OF INTERVAL 15	30	45	60
900-1000	230	226	228	227
1000-1100	227	227	225	236
1100-1200	241	235	235	233
1200-1300	232	231	230	229
1300-1400	230	231	229	230

MCMURDO 77.85S 166.72E ANTARCTICA

NEUTRON MONITOR NM-64

CORRECTED FOR PRESSURE USING THE GALACTIC PRESSURE COEFFICIENT ONLY

SCALING FACTOR = 100

TWO-MINUTE HOURLY RATES

NOVEMBER 18, 1968

TIME	MINUTES AT END OF INTERVAL 00 OR 30	02 32	04 34	06 36	08 38	10 40	12 42	14 44	16 46	18 48	20 50	22 52	24 54	26 56	28 58
1030	2812	2770	2855	2759	2824	2786	2750	2848	2813	2900	2886	3087	3089	3167	3123
1100	3020	3077	2970	2989	0000	2991	2947	2962	2917	2910	2917	2917	2892	2930	2903
1130	2940	2909	2924	2930	2924	2909	2930	2944	2930	2924	2868	2878	2892	2909	2851
1200	2847														

SOUTH POLE 89.98S 0.00E ANTARCTICA

NEUTRON MONITOR NM-64

CORRECTED FOR PRESSURE USING THE GALACTIC PRESSURE COEFFICIENT ONLY

SCALING FACTOR = 100

TWO-MINUTE HOURLY RATES

NOVEMBER 18, 1968

TIME	MINUTES AT END OF INTERVAL 00 OR 30	02 32	04 34	06 36	08 38	10 40	12 42	14 44	16 46	18 48	20 50	22 52	24 54	26 56	28 58
1030	670	667	646	688	678	668	657	688	699	720	782	835	824	814	815
1100	815	793	773	794	762	762	752	752	741	741	762	741	752	752	741
1130	752	721	741	731	710	721	710	700	721	700	700	742	690	000	000
1200	700														

Table 3 (Continued)

INUVIK 68.21N 133.43W CANADA

NEUTRON MONITOR 18-NM-64

REAL COUNTS 100 TIMES TABULATED COUNTS

FIVE-MINUTE BAROMETER CORRECTED HOURLY RATES

NOVEMBER 18, 1968

TIME U.T.	MINUTES AT END OF INTERVAL 05	10	15	20	25	30	35	40	45	50	55	60	AVERAGE
900-1000	6009	5972	6009	5966	6003	6027	5990	5972	5972	5942	6003	5948	5984
1000-1100	6046	5985	5973	5997	6022	5979	6004	5955	6004	6052	5991	6230	6020
1100-1200	6425	6388	6327	6266	6260	6236	6224	6193	6205	6236	6102	6077	6245
1200-1300	6120	6211	6144	6181	6199	6114	6163	6120	6108	6132	6169	6053	6143
1300-1400	6114	6047	6041	6078	6065	6126	6053	6126	6114	6078	6132	6078	6088
1400-1500	6090	6102	6126	6053	6114	6138	6035	6120	6060	6035	6065	6023	6080
1500-1600	6072	6144	6090	5993	6114	6054	6102	5981	6096	6023	6017	6090	6065
1600-1700	5993	6060	6108	5999	6048	6090	6017	6066	6054	6023	6035	6023	6043
1700-1800	6150	6042	6060	6017	6017	6017	6126	6120	6060	6036	6060	5999	6059
1800-1900	6060	6024	6108	6011	6036	6060	6060	6048	6084	6096	6030	6126	6062
1900-2000	6054	6078	6000	6108	5963	6108	6108	6156	6102	6048	6036	6054	6068
2000-2100	6126	6012	6036	6120	6114	6138	6102	6102	6084	6024	6084	5994	6078
2100-2200	6108	6066	6102	6114	6054	6048	6078	5994	5994	6126	6030	6042	6063
2200-2300	6048	6072	5988	6090	5988	6036	6012	6180	6066	6084	6054	6042	6055
2300-2400	6042	6144	6060	6096	6030	5964	6120	6060	6090	6012	6120	6108	6070

FORT CHURCHILL 58.75N 265.90E CANADA

NEUTRON MONITOR NM-64

BAROMETER REFERENCE 1010 MILLIBARS

ATTENUATION COEFFICIENT 137.2 MILLIBARS

REAL COUNTS 40 TIMES TABULATED COUNTS

FIVE-MINUTE BAROMETER CORRECTED HOURLY RATES

NOVEMBER 18, 1968

TIME U.T.	MINUTES AT END OF INTERVAL 05	10	15	20	25	30	35	40	45	50	55	60	AVERAGE
900-1000	1400	1393	1384	1399	1400	1391	1383	1395	1400	1403	1395	1408	1396
1000-1100	1412	1419	1398	1408	1421	1382	1396	1414	1398	1418	1542	1554	1430
1100-1200	1491	1471	1450	1444	1437	1421	1424	1432	1432	1415	1419	1427	1438
1200-1300	1434	1434	1411	1425	1427	1408	1422	1428	1393	1413	1413	1403	1418
1300-1400	1401	1400	1416	1416	1433	1411	1412	1416	1399	1412	1411	1406	1411
1400-1500	1407	1424	1426	1419	1405	1411	1424	-	1423	1410	1407	1401	1414

Table 3 (Continued)

GOOSE BAY 53.16N 60.24W CANADA

NEUTRON MONITOR 18-NM-64

REAL COUNTS 100 TIMES TABULATED COUNTS

FIVE-MINUTE BAROMETER CORRECTED HOURLY RATES

NOVEMBER 18, 1968

TIME U.T.	MINUTES AT END OF INTERVAL 05	10	15	20	25	30	35	40	45	50	55	60	AVERAGE
900-1000	6216	6216	6193	6123	6199	6152	6187	6175	6082	6199	6129	6175	6170
1000-1100	6100	6140	6170	6182	6140	6211	6187	6129	6211	6433	7064	6866	6319
1100-1200	6643	6597	6451	6433	6369	6427	6369	6340	6399	6375	6334	6357	6424
1200-1300	6264	6310	6345	6240	6310	6322	6369	6317	6258	6293	6270	6317	6301
1300-1400	6211	6188	6270	6129	6211	6223	6235	6281	6310	6193	6258	6264	6231
1400-1500	6228	6264	6264	6240	6292	6269	6252	6217	6164	6211	6152	6111	6222
1500-1600	6204	6263	6134	6204	6234	6228	6228	6228	6187	6181	6216	6198	6209
1600-1700	6198	6187	6245	6268	6268	6268	6257	6198	6169	6204	6204	6251	6226
1700-1800	6216	6263	6239	6234	6222	6199	6246	6275	6252	6193	6299	6223	6238
1800-1900	6188	6223	6153	6182	6217	6241	6182	6165	6206	6230	6300	6165	6204
1900-2000	6300	6218	6206	6241	6230	6171	6247	6236	6212	6277	6277	6242	6238
2000-2100	6242	6189	6177	6242	6349	6148	6266	6225	6160	6237	6249	6202	6224
2100-2200	6249	6225	6149	6220	6220	6250	6232	6267	6214	6261	6250	6261	6233
2200-2300	6232	6196	6232	6232	6220	6268	6291	6191	6202	6208	6226	6262	6230
2300-2400	6220	6262	6215	6215	6304	6221	6221	6269	6257	6191	6167	6209	6229

OULU 65.00N 25.42E FINLAND

NEUTRON MONITOR 9-NM-64

FIVE-MINUTE BAROMETER CORRECTED HOURLY RATES

NOVEMBER 18, 1968

TIME U.T.	MINUTES AT END OF INTERVAL 05	10	15	20	25	30	35	40	45	50	55	60
800- 900	278	273	276	274	278	280	283	283	276	276	283	275
900-1000	277	278	280	276	276	278	272	273	276	281	278	281
1000-1100	279	282	283	276	280	282	281	277	280	280	282	276
1100-1200	278	276	282	284	283	283	279	284	280	283	277	278
1200-1300	281	276	278	284	283	278	281	281	276	287	281	280
1300-1400	282	286	280	280	286	286	279	280	276	282	278	277
1400-1500	278	283	280	283	281	284	285	282	281	285	282	276
1500-1600	281	286	277	277	283	276	277	282	278	280	276	285
1600-1700	280	276	284	282	284	279	284	276	276	276	286	279
1700-1800	282	285	280	280	278	285	283	284	284	284	283	278
1800-1900	285	278	279	278	279	280	283	288	282	284	281	282

Table 3 (Continued)

DEEP RIVER 46.06N 77.30W CANADA

NEUTRON MONITOR 48-NM-64

REAL COUNTS 300 TIMES TABULATED COUNTS

FIVE-MINUTE BAROMETER CORRECTED HOURLY RATES

NOVEMBER 18, 1968

TIME U.T.	MINUTES AT END OF INTERVAL 05	10	15	20	25	30	35	40	45	50	55	60	AVERAGE
900-1000	6114	6072	6090	6102	6102	6108	6155	6060	6113	6084	6119	6136	6105
1000-1100	6101	6125	6095	6124	6130	6136	6112	6106	6077	6388	6809	6715	6243
1100-1200	6516	6421	6355	6297	6291	6273	6297	6261	6279	6237	6243	6248	6310
1200-1300	6224	6265	6247	6235	6258	6211	6222	6257	6187	6221	6209	6169	6225
1300-1400	6208	6236	6172	6217	6195	6166	6154	6222	6199	6170	6180	6169	6191
1400-1500	6237	6180	6174	6168	6122	6116	6189	6144	6138	6104	6133	6110	6151
1500-1600	6115	6187	6135	6124	6169	6196	6106	6100	6100	6104	6148	6142	6135
1600-1700	6164	6168	6102	6123	6140	6112	6144	6165	6129	6113	6113	6156	6136
1700-1800	6106	6127	6127	6126	6109	6131	6093	6115	6152	6108	6107	6111	6118
1800-1900	6105	6094	6073	6061	6104	6038	6086	6097	6074	6079	6094	6056	6080
1900-2000	6067	6087	6113	6075	6101	6058	6105	6078	6061	6051	6066	6081	6079
2000-2100	6060	6096	6043	6086	6065	6080	6105	6074	6099	6082	6110	6087	6082
2100-2200	6062	6087	6087	6102	6033	6111	6101	6090	6117	6096	6117	6128	6094
2200-2300	6117	6092	6113	6134	6123	6083	6104	6093	6125	6119	6098	6119	6110
2300-2400	6129	6140	6119	6129	6083	6093	6108	6134	6144	6138	6108	6108	6119

OTTAWA 45.40N 75.60W CANADA

2 IGY NEUTRON MONITORS

REAL COUNT 64 TIMES TABULATED COUNTS

TEN-MINUTE BAROMETER CORRECTED RATES

NOVEMBER 18, 1968

TIME U.T.	MINUTES AT END OF INTERVAL 10	20	30	40	50	60
900-1000	87.3	87.1	86.6	86.0	87.1	88.1
1000-1100	89.5	87.1	86.2	87.8	90.3	96.8
1100-1200	91.9	91.7	89.0	92.0	91.7	89.4
1200-1300	91.7	89.3	86.9	87.6	88.2	89.6
1300-1400	88.9	87.2	90.3	90.0	86.7	88.4

Table 3 (Continued)

CALGARY 51.08N 245.91E CANADA

NEUTRON MONITOR 12-NM-64

FIVE-MINUTE UNCORRECTED AND PRESSURE HOURLY RATES

NOVEMBER 18, 1968

UNCORRECTED NEUTRONS, MONITOR A

TIME U.T.	MINUTES AT END OF INTERVAL 05	10	15	20	25	30	35	40	45	50	55	60
000- 100	650	633	636	647	625	636	631	648	627	644	641	636
100- 200	630	654	638	638	639	657	625	641	662	636	642	636
200- 300	638	634	631	636	637	637	648	647	634	632	640	641
300- 400	640	645	636	645	630	638	638	637	641	638	632	634
400- 500	635	639	646	637	643	643	631	645	649	634	645	636
500- 600	645	645	643	639	644	635	639	643	627	635	638	630
600- 700	640	648	630	640	643	637	622	644	645	626	655	641
700- 800	652	647	647	637	634	645	637	640	638	640	641	643
800- 900	651	639	635	637	652	643	651	653	641	641	648	642
900-1000	647	649	644	647	647	655	647	657	655	644	649	651
1000-1100	642	642	648	647	646	647	650	657	651	687	751	743
1100-1200	725	696	689	675	701	668	685	680	684	675	673	680
1200-1300	668	668	664	667	677	685	673	676	674	666	667	677
1300-1400	673	670	667	683	673	667	665	683	684	657	665	661
1400-1500	675	680	681	684	666	658	685	675	670	678	678	674
1500-1600	675	663	666	675	675	674	685	667	676	676	676	680
1600-1700	0	678	681	682	679	682	670	677	678	684	683	671
1700-1800	690	676	677	683	682	673	678	687	668	678	679	681
1800-1900	682	673	657	676	665	671	677	684	666	671	696	679
1900-2000	678	681	673	682	663	686	672	668	681	671	665	668
2000-2100	678	671	666	673	671	673	676	681	677	667	676	664
2100-2200	664	663	660	661	649	668	665	678	658	679	548	667
2200-2300	648	666	670	653	650	657	669	649	668	664	664	650
2300-2400	658	661	648	658	667	651	659	653	662	659	649	651

UNCORRECTED NEUTRONS, MONITOR B

TIME U.T.	MINUTES AT END OF INTERVAL 05	10	15	20	25	30	35	40	45	50	55	60
000- 100	632	636	631	644	635	632	650	636	637	647	635	639
100- 200	641	634	636	636	645	654	631	631	639	637	636	659
200- 300	632	640	637	640	639	630	647	647	632	629	638	645
300- 400	629	637	647	633	644	643	639	621	637	652	642	623
400- 500	642	641	638	650	637	646	631	633	644	629	635	638
500- 600	637	641	633	636	621	630	633	645	647	645	647	635
600- 700	646	636	634	643	643	640	645	633	633	629	637	632
700- 800	636	644	636	639	639	637	632	643	646	638	647	641
800- 900	640	642	652	637	653	645	640	641	642	646	646	639
900-1000	644	649	648	644	648	645	643	657	652	642	638	644
1000-1100	641	659	660	648	652	652	656	644	655	686	757	739
1100-1200	717	702	687	690	690	680	677	683	676	682	669	676
1200-1300	678	661	668	679	680	676	672	675	674	668	678	675
1300-1400	666	676	681	681	686	665	675	664	667	660	678	675
1400-1500	683	663	673	672	669	675	679	680	675	677	687	672
1500-1600	672	680	674	670	688	687	670	674	668	686	682	688
1600-1700	0	666	664	676	675	668	670	681	683	671	673	680
1700-1800	685	672	675	665	682	678	674	670	682	682	675	695
1800-1900	679	674	681	681	679	673	677	673	667	681	687	676
1900-2000	674	689	676	673	676	674	672	665	680	680	670	665
2000-2100	676	660	670	672	660	656	669	665	673	677	671	673
2100-2200	662	660	668	659	661	670	664	655	663	662	656	661
2200-2300	653	667	648	664	663	665	655	649	661	656	651	649
2300-2400	651	660	663	658	653	660	661	646	650	667	654	655

Table 3 (Continued)

TIME U.T.	05	10	15	20	25	30	35	40	45	50	55	60
UNCORRECTED NEUTRONS, MONITOR C						MINUTES AT END OF INTERVAL						
000- 100	627	639	626	642	635	636	632	627	627	637	617	621
100- 200	634	626	625	638	640	640	636	618	634	635	644	629
200- 300	648	634	634	633	636	633	630	647	642	636	643	644
300- 400	639	638	622	631	647	647	631	627	639	627	638	634
400- 500	643	637	628	634	637	630	629	629	637	634	630	631
500- 600	634	632	639	628	643	652	633	625	644	627	634	638
600- 700	641	640	631	634	634	650	633	630	635	639	630	614
700- 800	642	635	646	623	636	628	640	638	629	631	648	644
800- 900	639	638	640	626	626	638	638	639	652	639	647	631
900-1000	641	642	641	649	636	637	643	637	641	643	651	649
1000-1100	645	636	647	636	648	634	632	647	643	676	743	729
1100-1200	719	692	684	694	681	688	681	659	678	683	677	680
1200-1300	674	664	665	666	667	674	667	673	684	660	672	667
1300-1400	664	676	667	670	658	669	678	671	659	672	652	689
1400-1500	662	668	672	655	674	669	666	673	670	678	677	660
1500-1600	669	678	675	670	663	666	678	673	680	664	677	664
1600-1700	0	677	682	668	671	670	661	677	679	667	682	676
1700-1800	665	673	672	673	665	658	677	670	687	669	685	677
1800-1900	668	663	669	655	662	676	678	673	676	675	659	670
1900-2000	668	672	676	681	652	676	684	667	677	668	672	661
2000-2100	677	665	658	665	675	663	668	656	663	667	650	653
2100-2200	674	655	653	662	654	654	667	658	650	659	661	661
2200-2300	661	650	664	650	647	643	650	660	648	657	653	654
2300-2400	642	648	646	640	649	655	655	643	659	640	651	644
UNCORRECTED NEUTRONS, MONITOR D												
000- 100	646	643	633	630	638	644	647	631	642	633	637	645
100- 200	642	642	635	631	649	634	637	640	651	643	645	650
200- 300	653	646	643	635	649	639	640	648	649	640	649	646
300- 400	642	639	638	632	632	650	641	631	638	630	642	630
400- 500	632	645	646	640	631	638	635	631	644	637	645	653
500- 600	637	642	627	650	647	642	645	639	642	646	647	645
600- 700	636	649	638	639	654	634	645	636	637	647	643	644
700- 800	636	645	632	632	625	647	641	634	643	644	640	641
800- 900	645	641	635	642	632	647	641	650	633	648	648	643
900-1000	634	648	644	654	644	655	663	654	654	644	650	657
1000-1100	648	646	656	653	650	637	648	651	650	688	760	742
1100-1200	729	692	703	686	698	701	685	687	674	685	664	681
1200-1300	673	672	684	666	676	671	668	679	683	680	680	679
1300-1400	681	683	680	675	676	666	681	673	671	660	671	685
1400-1500	677	681	678	659	683	681	669	682	680	690	671	674
1500-1600	668	677	676	658	678	676	671	674	680	682	682	677
1600-1700	0	683	682	683	668	672	667	684	690	680	689	689
1700-1800	674	681	701	678	675	682	689	679	670	673	673	685
1800-1900	684	687	672	673	672	675	678	678	675	680	692	682
1900-2000	670	673	675	682	688	681	695	682	690	678	679	680
2000-2100	674	688	684	679	666	668	675	669	661	669	664	662
2100-2200	661	663	659	655	645	657	664	665	659	673	660	659
2200-2300	673	645	668	674	653	658	669	660	652	661	662	665
2300-2400	657	660	677	656	664	653	659	656	653	650	660	653
PRESSURE IN MILLIBARS												
000- 100	8856	8856	8857	8857	8856	8857	8857	8857	8857	8858	8857	8857
100- 200	8858	8857	8856	8856	8855	8856	8856	8856	8856	8850	8855	8855
200- 300	8855	8854	8855	8854	8854	8853	8850	8852	8852	8852	8852	8852
300- 400	8852	8852	8852	8852	8853	8853	8853	8853	8853	8852	8853	8852
400- 500	8852	8853	8854	8854	8854	8850	8852	8852	8851	8849	8851	8850
500- 600	8850	8800	8850	8850	8850	8851	8850	8851	8851	8850	8850	8851
600- 700	8850	8851	8851	8850	8848	8848	8848	8848	8849	8849	8849	8848
700- 800	8847	8845	8845	8845	8844	8844	8843	8843	8843	8842	8842	8841
800- 900	8842	8840	8840	8840	8840	8841	8841	8841	8840	8840	8839	8838
900-1000	8836	8835	8835	8834	8834	8834	8833	8834	8833	8833	8833	8832
1000-1100	8832	8832	8832	8831	8830	8830	8829	8829	8828	8828	8828	8827
1100-1200	8826	8825	8825	8823	8822	8820	8822	8821	8820	8820	8819	8819
1200-1300	8818	8817	8816	8816	8817	8818	8817	8817	8815	8816	8817	8815
1300-1400	8812	8814	8810	8812	8810	8811	8811	8810	8811	8811	8809	8808
1400-1500	8808	8809	8809	8808	8808	8807	8808	8806	8806	8805	8806	8806
1500-1600	8805	8805	8805	8803	8802	8802	8801	8801	8801	8801	8801	8800
1600-1700	0	8801	8799	8801	8800	8799	8798	8796	8795	8794	8790	8793
1700-1800	8793	8793	8794	8793	8793	8793	8794	8794	8790	8791	8793	8794
1800-1900	8793	8796	8798	8800	8798	8798	8795	8797	8795	8796	8794	8794
1900-2000	8794	8794	8795	8795	8795	8794	8794	8794	8796	8796	8798	8800
2000-2100	8800	8802	8801	8800	8802	8803	8803	8804	8807	8806	8807	8809
2100-2200	8808	8813	8816	8817	8817	8816	8816	8817	8817	8818	8819	8819
2200-2300	8818	8819	8821	8822	8823	8821	8823	8825	8827	8828	8827	8831
2300-2400	8830	8832	8834	8835	8836	8837	8837	8838	8838	8839	8840	8842

Table 3 (Continued)

SULPHUR MOUNTAIN 51.20N 115.60W CANADA

NEUTRON MONITOR NM-64
FIVE-MINUTE UNCORRECTED AND PRESSURE HOURLY RATES

NOVEMBER 18, 1968

TIME U.T.	MINUTES AT END OF INTERVAL 05	10	15	20	25	30	35	40	45	50	55	60

LEFT UNIT

TIME U.T.	MINUTES AT END OF INTERVAL 05	10	15	20	25	30	35	40	45	50	55	60
000- 100	203	204	200	203	205	206	204	203	203	199	199	206
100- 200	205	203	204	199	207	204	204	205	203	206	204	203
200- 300	203	204	202	206	202	202	201	201	202	203	202	205
300- 400	205	203	201	203	205	201	201	207	203	202	204	206
400- 500	196	205	202	201	204	206	202	200	201	204	203	201
500- 600	203	200	203	201	199	202	205	200	202	202	204	204
600- 700	201	200	201	204	200	204	201	201	199	201	203	202
700- 800	201	198	201	199	205	203	201	200	204	202	201	204
800- 900	203	201	201	207	202	206	203	201	202	203	201	204
900-1000	202	200	199	205	202	204	205	201	200	204	200	202
1000-1100	205	201	204	200	202	203	203	204	204	214	242	239
1100-1200	225	221	216	218	217	217	211	213	214	212	213	215
1200-1300	209	212	207	214	212	210	210	211	210	209	209	212
1300-1400	211	208	213	208	213	209	210	208	208	208	208	209
1400-1500	206	208	209	209	213	207	207	210	212	209	208	210
1500-1600	210	210	212	215	212	210	209	206	205	211	211	208
1600-1700	209	210	209	208	208	205	211	206	206	209	208	208
1700-1800	208	210	207	211	206	207	208	209	207	204	209	209
1800-1900	208	205	205	207	205	208	207	204	208	205	206	208
1900-2000	208	205	204	205	208	207	208	204	206	206	207	207
2000-2100	204	209	202	207	208	203	205	208	209	207	203	205
2100-2200	202	201	200	202	203	203	205	201	204	206	204	204
2200-2300	203	202	203	200	202	203	205	200	204	204	202	204
2300-2400	205	198	203	198	201	201	204	200	203	199	200	197

CENTER UNIT

TIME U.T.	MINUTES AT END OF INTERVAL 05	10	15	20	25	30	35	40	45	50	55	60
000- 100	225	227	226	226	229	228	227	227	227	226	224	230
100- 200	228	229	226	226	227	227	228	227	225	227	228	229
200- 300	232	231	226	228	226	229	228	224	229	229	227	225
300- 400	229	231	226	229	226	225	226	225	224	223	226	233
400- 500	227	229	226	225	227	228	227	227	226	226	221	225
500- 600	228	224	227	224	225	228	226	226	227	224	230	226
600- 700	224	225	225	229	227	224	227	228	226	227	226	229
700- 800	226	225	225	226	225	224	223	229	225	226	225	227
800- 900	224	229	224	227	226	227	226	224	225	222	232	228
900-1000	223	225	226	226	229	226	228	226	229	225	222	228
1000-1100	227	228	225	230	227	228	226	228	224	238	268	264
1100-1200	256	249	248	242	239	240	241	240	237	239	239	238
1200-1300	236	236	236	235	233	240	235	235	237	236	237	237
1300-1400	224	236	234	236	236	237	237	233	236	237	234	238
1400-1500	232	236	234	234	235	230	235	236	238	236	239	230
1500-1600	236	231	233	236	234	232	235	232	234	232	236	237
1600-1700	233	234	233	236	231	230	232	234	233	235	232	232
1700-1800	238	235	231	231	234	235	231	231	234	234	237	231
1800-1900	234	231	232	234	228	230	229	233	235	229	230	229
1900-2000	229	230	233	226	232	230	231	228	228	233	229	226
2000-2100	231	233	230	230	229	233	226	229	226	227	229	227
2100-2200	226	226	226	230	228	227	227	224	226	226	229	227
2200-2300	227	227	223	227	230	228	230	228	224	224	226	226
2300-2400	230	222	225	223	226	225	221	226	224	229	221	230

Table 3 (Continued)

RIGHT UNIT

TIME U.T.	MINUTES AT END OF INTERVAL 05	10	15	20	25	30	35	40	45	50	55	60
000- 100	205	205	205	205	205	205	206	208	202	203	202	204
100- 200	205	207	203	205	204	202	201	203	204	205	207	203
200- 300	203	209	206	205	205	206	203	207	206	204	202	201
300- 400	206	200	203	199	203	206	204	201	203	203	207	203
400- 500	203	203	205	203	204	203	203	201	207	203	202	201
500- 600	204	201	206	203	204	200	202	204	200	205	206	204
600- 700	206	204	200	205	201	203	202	203	201	202	203	207
700- 800	201	203	201	203	204	203	204	204	200	203	206	203
800- 900	201	202	202	204	204	202	202	203	203	202	204	203
900-1000	202	201	205	202	206	201	201	205	200	204	203	206
1000-1100	204	202	202	208	204	203	205	205	203	217	244	240
1100-1200	226	225	223	218	215	216	220	214	215	212	213	214
1200-1300	214	208	213	213	210	211	211	214	213	209	212	213
1300-1400	213	207	213	210	210	212	211	214	209	210	208	211
1400-1500	212	214	211	210	206	209	212	211	210	209	211	212
1500-1600	211	210	212	212	213	210	212	209	213	208	212	207
1600-1700	210	211	212	209	210	210	213	212	211	209	211	205
1700-1800	213	210	210	208	211	211	208	208	212	209	209	206
1800-1900	206	209	208	211	209	206	204	207	211	211	205	207
1900-2000	208	206	207	207	208	205	209	205	207	206	207	206
2000-2100	209	208	203	209	208	205	204	205	203	203	206	203
2100-2200	203	201	201	206	206	203	204	203	205	207	206	203
2200-2300	205	205	203	206	205	204	204	205	204	200	206	201
2300-2400	203	201	200	201	201	204	204	204	204	205	201	201

PRESSURE IN MILLIBARS

TIME U.T.	MINUTES AT END OF INTERVAL 05	10	15	20	25	30	35	40	45	50	55	60
000- 100	7654	7655	7656	7657	7657	7658	7658	7657	7656	7658	7657	7657
100- 200	7656	7656	7657	7657	7658	7658	7657	7656	7656	7657	7657	7657
200- 300	7656	7656	7656	7657	7658	7659	7659	7660	7660	7661	7661	7662
300- 400	7662	7662	7663	7663	7662	7663	7663	7662	7662	7661	7660	7661
400- 500	7660	7661	7660	7661	7660	7661	7663	7664	7665	7664	7664	7664
500- 600	7664	7664	7665	7663	7663	7663	7664	7665	7664	7663	7664	7665
600- 700	7665	7665	7666	7664	7665	7665	7665	7664	7664	7664	7664	7664
700- 800	7664	7663	7663	7662	7662	7662	7662	7662	7661	7661	7661	7661
800- 900	7662	7663	7662	7662	7662	7662	7662	7660	7661	7661	7661	7660
900-1000	7659	7660	7661	7661	7660	7661	7660	7660	7659	7659	7659	7657
1000-1100	7657	7658	7659	7658	7657	7657	7657	7657	7655	7653	7654	7655
1100-1200	7654	7653	7652	7654	7654	7653	7654	7655	7654	7654	7654	7654
1200-1300	7654	7655	7653	7654	7654	7654	7652	7652	7652	7652	7651	7651
1300-1400	7651	7651	7651	7651	7651	7649	7650	7650	7651	7651	7651	7652
1400-1500	7652	7651	7652	7650	7651	7649	7650	7649	7649	7648	7650	7649
1500-1600	7650	7649	7650	7651	7651	7651	7650	7649	7649	7649	7648	7648
1600-1700	7648	7648	7647	7647	7648	7646	7646	7645	7646	7647	7644	7645
1700-1800	7641	7643	7644	7646	7646	7647	7645	7647	7648	7649	7648	7649
1800-1900	7650	7650	7651	7654	7654	7656	7653	7653	7654	7655	7654	7653
1900-2000	7652	7652	7652	7653	7656	7657	7657	7655	7657	7657	7658	7659
2000-2100	7658	7658	7657	7657	7657	7660	7661	7660	7659	7663	7665	7665
2100-2200	7667	7666	7666	7667	7667	7668	7666	7664	7663	7666	7669	7672
2200-2300	7673	7675	7676	7674	7674	7676	7677	7678	7679	7678	7679	7678
2300-2400	7680	7682	7681	7682	7684	7683	7684	7684	7685	7686	7686	7687

Table 3 (Continued)

PORT AUX FRANCAIS 49.35S 70.25E KERGUELEN IS.

NEUTRON MONITOR 18-NM-64

CORRECTED FOR BAROMETRIC PRESSURE

COEFFICIENT 10.1 PER CENT PER CM HG

MULTIPLY INDICATED NUMBERS BY 400

FIFTEEN-MINUTE HOURLY RATES

NOVEMBER 18, 1968

TIME U.T.	MINUTES AT END OF INTERVAL 05	10	15	20	25	30	35	40	45	50	55	60
900-1000	1429	1427	1429	1444	1429	1439	1423	1403	1427	1424	1427	1444
1000-1100	1439	1445	1437	1431	1445	1421	1433	1436	1431	1444	1456	1452
1100-1200	1461	1473	1447	1466	1448	1448	1455	1443	1457	1447	1457	1441
1200-1300	1454	1474	1429	1465	1456	1454	1467	1451	1463	1452	1442	1452
1300-1400	1456	1445	1432	1441	1438	1447	1448	1456	1442	1444	1447	1452

MT WASHINGTON 44.30N 288.70E NEW HAMPSHIRE

IGY NEUTRON MONITOR

FIVE-MINUTE BAROMETER CORRECTED RATES

NOVEMBER 18, 1968

MONITOR A

TIME U.T.	MINUTES AT END OF INTERVAL 05	10	15	20	25	30	35	40	45	50	55	60
900-1000	8596	8273	8793	8544	8531	8435	8555	8435	8709	8452	8750	8486
1000-1100	8734	8305	8528	8380	8502	8831	8399	8596	8484	8824	9603	9397
1100-1200	9290	9162	8997	8634	9127	8836	8992	8863	8965	8621	9149	8952
1200-1300	8804	9094	9128	8788	8641	8727	8680	9178	8806	8739	8806	8782
1300-1400	8797	8580	8844	8437	8592	8628	8714	8709	8779	8812	8875	8615

MONITOR B

TIME U.T.	MINUTES AT END OF INTERVAL 05	10	15	20	25	30	35	40	45	50	55	60
900-1000	8273	8199	8321	8395	8232	8261	8257	7938	8286	8501	8452	8362
1000-1100	8263	8454	8180	7909	8205	8261	8299	8323	8236	8601	9032	9223
1100-1200	9015	8938	8847	8684	8555	8662	8494	8440	8890	8571	8501	8553
1200-1300	8380	8571	8530	8489	8516	8677	8655	8459	8432	8465	8682	8583
1300-1400	8599	8406	8349	8264	8543	8431	8442	8363	8384	8345	8309	8221

Table 3 (Continued)

DURHAM 43.10N 289.16E NEW HAMPSHIRE

NEUTRON MONITOR NM-64

FIVE-MINUTE BAROMETER CORRECTED RATES

NOVEMBER 18, 1968

MONITOR A

TIME U.T.	MINUTES AT END OF INTERVAL 05	10	15	20	25	30	35	40	45	50	55	60
900-1000	5691	5644	5644	5565	5644	5670	5623	5623	5576	5582	5497	5744
1000-1100	5633	5581	5732	5648	5539	5695	5565	5533	5695	5826	5904	5716
1100-1200	5925	5794	5846	5846	5742	5716	5565	5710	5669	5701	5774	5664
1200-1300	5789	5658	5627	5757	5725	5694	5590	5616	5720	5584	5558	5475
1300-1400	5755	5640	5666	5718	5666	5449	5707	5604	5624	5536	5608	5685

MONITOR B

TIME U.T.	MINUTES AT END OF INTERVAL 05	10	15	20	25	30	35	40	45	50	55	60
900-1000	5586	5539	5434	5539	5487	5460	5387	5361	5471	5476	5339	5429
1000-1100	5424	5528	5471	5439	5460	5382	5486	5585	5408	5617	6087	5820
1100-1200	5716	5716	5690	5559	5350	5611	5539	5658	5486	5622	5669	5455
1200-1300	5476	5423	5470	5522	5595	5382	5564	5564	5564	5610	5532	5657
1300-1400	5496	5589	5408	5563	5485	5526	5526	5655	5547	5562	5505	5453

UPPSALA 59.85N 17.92E SWEDEN

NEUTRON MONITOR, SUM OF 2 NM-IGY SECTIONS

BAROMETRIC COEFFICIENT IS 0.736 PER CENT PER MB

SCALING FACTOR 4

FIVE-MINUTE HOURLY RATES

NOVEMBER 18, 1968

TIME U.T.	MINUTES AT END OF INTERVAL 05	10	15	20	25	30	35	40	45	50	55	60
000- 100	521	515	522	532	501	522	519	519	529	534	516	525
100- 200	526	510	524	495	498	505	554	546	513	493	499	534
200- 300	532	541	501	512	506	510	509	517	494	543	498	517
300- 400	516	512	525	507	528	514	517	515	509	517	506	535
400- 500	547	526	538	517	523	525	525	508	526	506	511	539
500- 600	528	526	542	533	529	515	511	524	537	523	527	531
600- 700	534	511	504	523	517	530	532	527	531	525	526	534
700- 800	502	528	521	491	527	507	544	510	531	534	546	519
800- 900	532	486	532	529	524	503	505	521	525	565	536	523
900-1000	549	536	542	512	522	534	525	521	525	548	529	522
1000-1100	519	527	509	488	506	520	524	515	531	506	538	517
1100-1200	506	530	524	529	534	534	538	546	542	538	540	521
1200-1300	539	560	518	525	532	537	530	537	520	513	525	523
1300-1400	550	522	512	545	502	522	542	535	540	530	501	513
1400-1500	529	548	533	506	550	532	524	533	505	541	551	528
1500-1600	559	560	542	538	523	555	540	523	495	495	532	542
1600-1700	528	505	509	523	533	547	549	495	524	529	541	472
1700-1800	529	524	509	520	558	502	553	491	508	549	515	563
1800-1900	517	518	523	529	526	508	535	534	527	550	545	517
1900-2000	543	524	542	524	508	522	528	538	531	508	511	507
2000-2100	537	535	530	508	539	529	542	553	527	528	534	538
2100-2200	534	534	529	530	503	522	528	530	524	523	498	531
2200-2300	507	534	549	532	526	511	521	536	537	502	504	520
2300-2400	522	524	535	528	520	524	514	519	536	518	527	531

Table 3 (Continued)

CHICAGO 41.83N 272.33E ILLINOIS

IGY TYPE NEUTRON MONITOR

FIFTEEN-MINUTE BAROMETER CORRECTED HOURLY RATES

NOVEMBER 18, 1968

TIME U.T.	MINUTES AT END OF INTERVAL 15	30	45	60
800- 900	546	561	549	544
900-1000	546	546	558	538
1000-1100	544	570	547	567
1100-1200	562	542	558	555
1200-1300	562	550	555	534
1300-1400	566	553	562	545
1400-1500	571	563	558	540
1500-1600	553	549	554	549
1600-1700	552	554	558	555
1700-1800	560	567	547	538
1800-1900	557	564	548	553
1900-2000	556	551	549	

SWARTHMORE 39.90N 284.65E PENNSYLVANIA

NEUTRON MONITOR NM-64

CORRECTED FOR PRESSURE USING THE GALACTIC PRESSURE COEFFICIENT ONLY

SCALING FACTOR = 100

TWO-MINUTE HOURLY RATES

NOVEMBER 18, 1968

TIME	MINUTES AT END OF INTERVAL 00 OR 30	02 32	04 34	06 36	08 38	10 40	12 42	14 44	16 46	18 48	20 50	22 52	24 54	26 56	28 58
1030	1053	1014	1053	1044	1044	1045	1046	1009	1038	1068	1087	1096	1087	1077	1076
1100	1067	1038	1076	1037	1047	1075	1056	1084	1056	1028	1027	1055	1065	1017	1046
1130	1046	1036	1055	1046	1063	1054	1044	1053	1053	1025	1044	1044	1061	1052	1024
1200	1043														

KIEL 54.33N 10.10E GERMANY

NEUTRON MONITOR 18-NM-64

REAL COUNTS 10 TIMES TABULATED COUNTS

FIVE-MINUTE BAROMETER CORRECTED RATES

NOVEMBER 18, 1968

TIME U.T.	MINUTES AT END OF INTERVAL 05	10	15	20	25	30	35	40	45	50	55	60
900-1000	4682	4651	4672	4706	4685	4701	4659	4714	4663	4704	4643	4664
1000-1100	4646	4620	4671	4650	4601	4614	4714	4740	4674	4642	4712	4758
1100-1200	4715	4661	4708	4697	4685	4689	4706	4715	4752	4629	4696	4757
1200-1300	4683	4668	4699	4653	4745	4725	4707	4680	4645	4636	4753	4632
1300-1400	4715	4715	4686	4630	4710	4709	4648	4637	4666	4620	4732	4674
1400-1500	4652	4641	4666	4642	4679	4697	4645	4699	4675	4699	4668	4676

Table 3 (Continued)

LINDAU 51.60N 10.10E GERMANY

NEUTRON MONITOR 18-NM-64

TEN-MINUTE BAROMETER CORRECTED RATES / 100

NOVEMBER 18, 1968

TIME U.T.	MINUTES AT END OF INTERVAL 10	20	30	40	50	60
900-1000	572	571	578	573	573	573
1000-1100	571	574	577	572	575	579
1100-1200	577	576	575	577	578	577
1200-1300	573	575	576	577	575	575
1300-1400	574	577	572	578	574	576

CLIMAX 39.37N 253.82E COLORADO

IGY NEUTRON MONITOR

FIFTEEN-MINUTE BAROMETER CORRECTED HOURLY RATES

NOVEMBER 18, 1968

TIME U.T.	MINUTES AT END OF INTERVAL 15	30	45	60
700- 800		889	908	900
800- 900	902	901	899	902
900-1000	915	904	896	894
1000-1100	907	915	911	949
1100-1200	913	914	917	910
1200-1300	916	910	918	916
1300-1400	913	913	914	914
1400-1500	913	909	912	911
1500-1600	912	917	912	910
1600-1700	917	0	0	0
1700-1800	0	0	903	901
1800-1900	907	910	911	913
1900-2000	899	898	902	

DALLAS 32.78N 96.80W TEXAS

NEUTRON MONITOR NM-64

BAROMETER REFERENCE 995 MILLIBARS

ATTENUATION COEFFICIENT 137.2 MILLIBARS

REAL COUNTS 40 TIMES TABULATED COUNTS

FIVE-MINUTE HOURLY RATES

NOVEMBER 18, 1968

TIME U.T.	MINUTES AT END OF INTERVAL 05	10	15	20	25	30	35	40	45	50	55	60	AVERAGE
900-1000	1437	1452	1438	1440	1456	1439	1441	1440	1426	1441	1428	1442	1440
1000-1100	1435	1439	1415	1434	1443	1433	1435	1453	1452	1464	1462	1440	1442
1100-1200	1459	1429	1442	1451	1441	1439	1436	1438	1443	1444	1432	1452	1442
1200-1300	1451	1452	1435	1451	1436	1449	1437	1455	1440	1433	1436	1449	1444
1300-1400	1433	1450	1434	1453	1433	1441	1450	1446	1439	1450	1452	1460	1445
1400-1500	1460	1433	1440	1447	1444	1446	1447	1450	1445	1442	1433	1436	1443

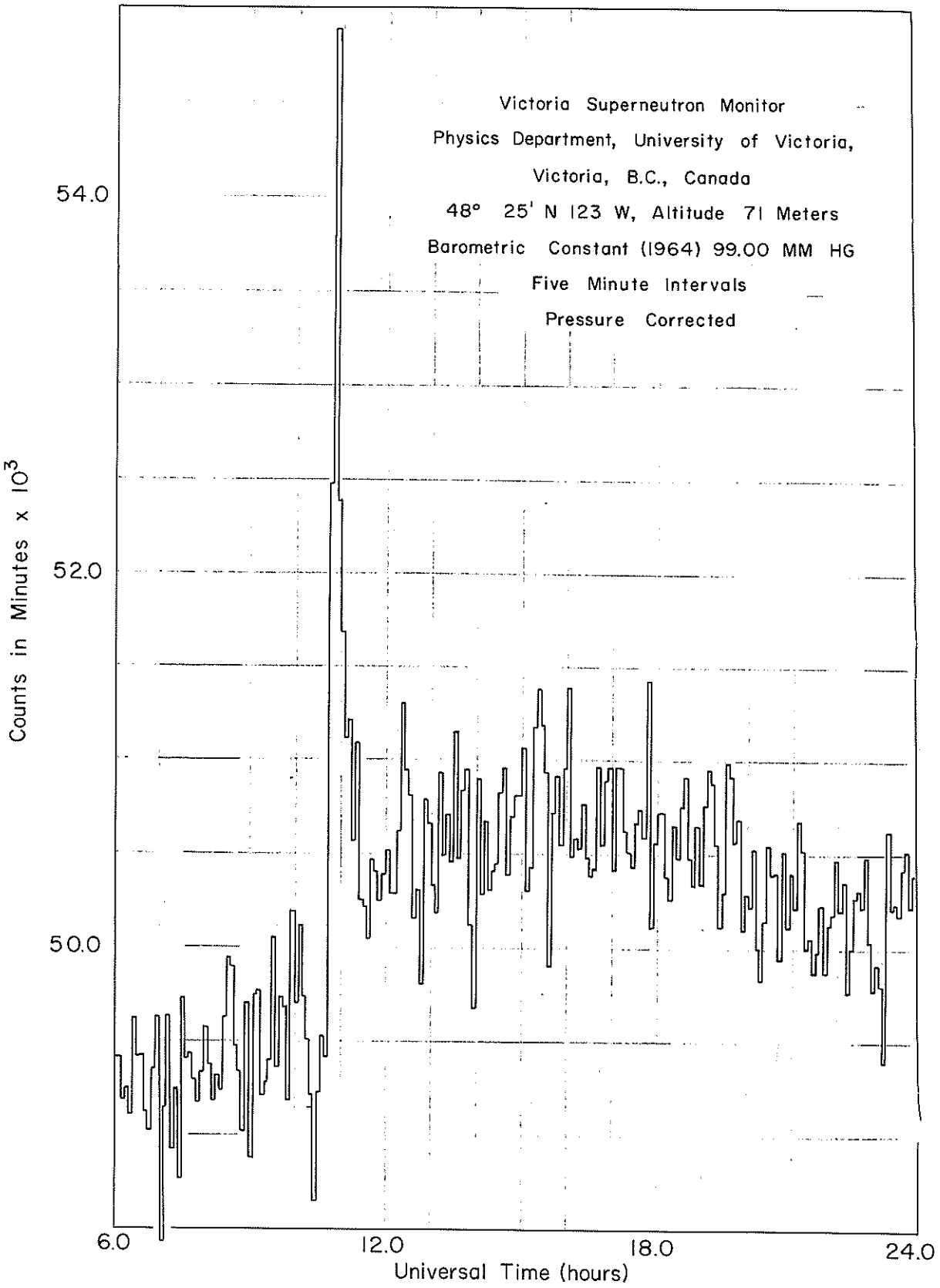

Fig. 1 November 18, 1968

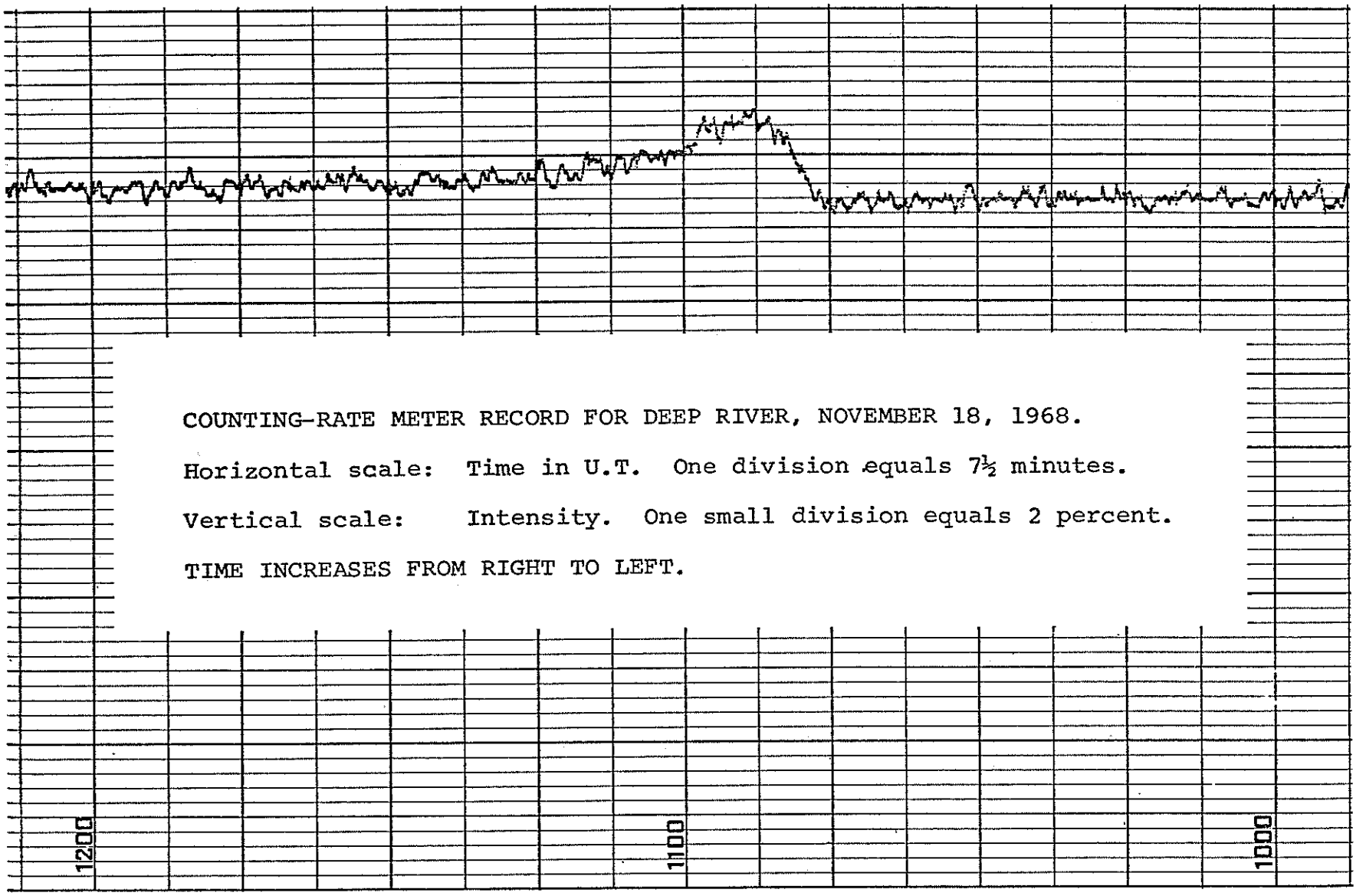

Fig. 2. Onset of cosmic ray increase at Deep River 1000-1200 UT November 18, 1968.

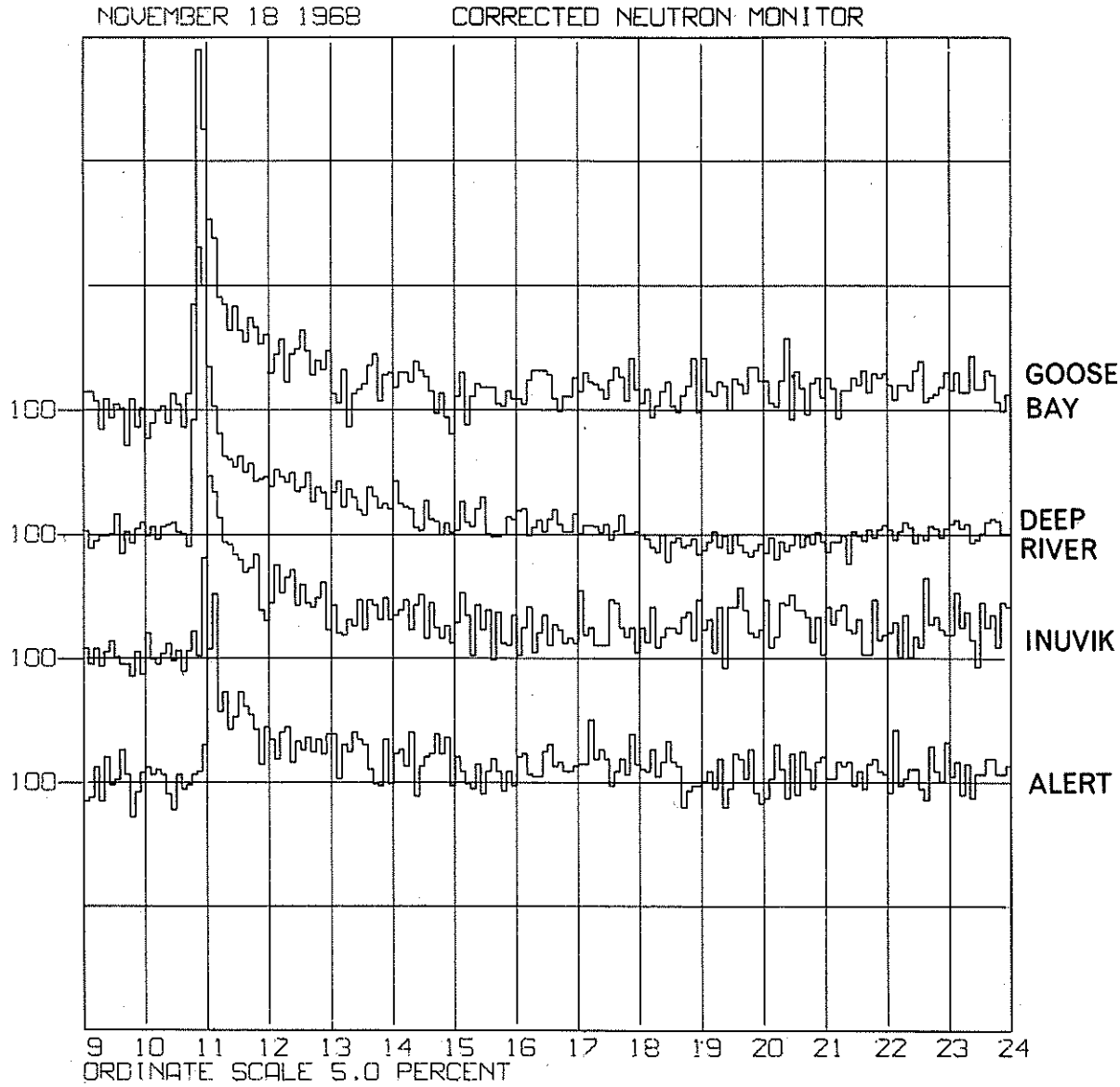

Fig. 3. 5-minute data from Goose Bay, Deep River, Inuvik and Alert 0900-2400 UT November 18, 1968.

"Scintillation Monitor Bologna, Italy 15-Minute Observations"

by

M. Galli
Istituto di Fisica "A. Righi"
Universita Degli Studi di Bologna

Figure 1 presents for November 18-20, 1968 the total ionization (T), the atmospheric pressure at ground level (P), the soft component (M), and the hard components: 45° inclined towards West (W), 45° inclined towards East (E) and vertical cubical coincidences (V).

Table 1 presents the data from the scintillation monitor at Bologna. The tabulated data should be read with a decimal point after the second figure of each number. The numbers are deviations in % units from a fixed value of pressure corrected data at the end of each 15-minute interval.

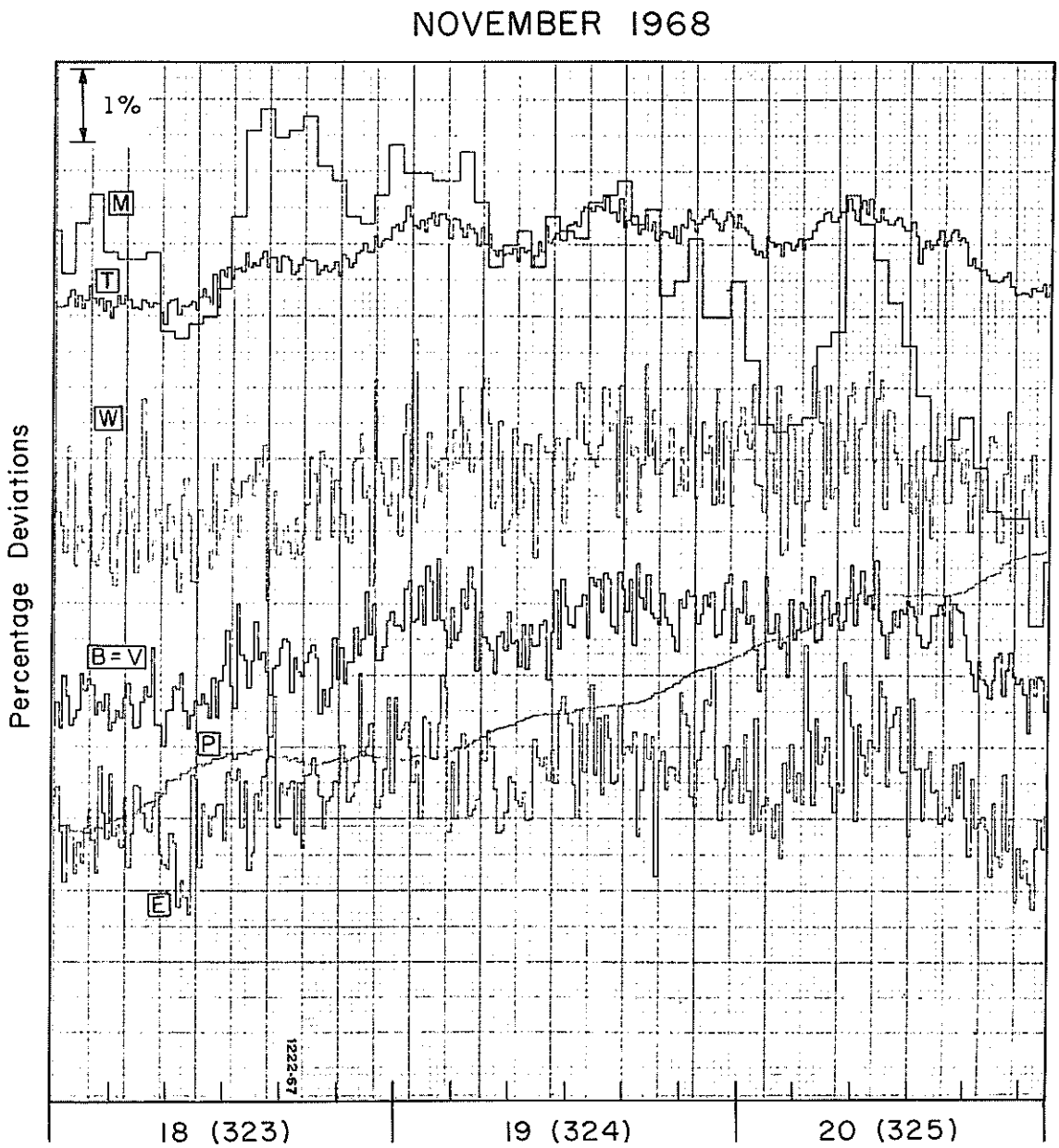

Fig. 1. Scintillation monitor data November 18-20, 1968 at Bologna, Italy.

Table 1

15-MINUTE COSMIC RAY DATA AT BOLOGNA DURING NOVEMBER 18, 1968

Scintillation Monitor for Cosmic Rays
Location Bologna 44.5 N 11.35 E 50 m a.s.l.
Tabulated Deviations in percent units from a fixed value of pressure corrected totals, at the end of each interval

* Total Ionizing Component counts under 5 gr/sqcm *
S.D. 0.084%

* Coincidence counts 45 degrees inclined towards West filtered by 10 cm of lead *
S.D. 0.54%

* Vertical Cubical coincidence counts filtered by 10 cm of lead *
S.D. 0.30%

* Coincidence counts 45 degrees inclined towards East filtered by 10 cm of lead *
S.D. 0.54%

Bar. coeff. 0.20 percent/mb
November 18, 1968

Minutes at End of Interval

U.T. hours	15	30	45	60	Mean	15	30	45	60	Mean	15	30	45	60	Mean	15	30	45	60	Mean
0000-0100	2.19	2.12	2.12	2.15	2.14	2.81	2.25	2.07	1.68	2.20	1.31	1.62	1.26	1.98	1.54	2.31	2.44	1.81	1.11	1.91
0100-0200	2.26	2.36	2.12	2.29	2.25	3.16	2.94	1.51	2.06	2.41	1.70	1.31	1.41	1.53	1.48	1.90	1.72	1.22	1.66	1.62
0200-0300	2.11	2.22	2.42	2.25	2.25	1.82	1.71	2.78	1.57	1.97	2.02	1.79	1.95	1.87	1.90	1.36	1.87	2.13	1.68	1.76
0300-0400	2.15	2.24	2.06	2.21	2.16	1.50	1.74	2.22	3.29	2.18	1.44	1.62	1.51	1.74	1.57	1.22	2.73	2.07	1.70	1.93
0400-0500	1.97	2.13	2.29	2.16	2.13	1.41	1.22	1.96	2.44	1.75	1.23	1.34	1.51	1.41	1.37	2.62	1.74	1.90	1.58	1.96
0500-0600	2.28	2.22	2.11	2.12	2.18	2.70	1.95	2.46	1.40	2.12	1.69	1.89	1.59	1.27	1.61	2.29	1.30	1.79	2.46	1.96
0600-0700	2.09	2.23	2.19	2.13	2.16	2.96	3.82	2.75	1.57	2.77	1.28	1.63	1.84	1.71	1.61	2.42	2.06	1.85	1.81	2.03
0700-0800	2.18	2.16	2.04	1.89	2.06	1.86	2.28	2.05	1.53	1.93	2.38	1.31	1.29	1.01	1.49	2.17	2.37	1.49	1.34	1.84
0800-0900	2.18	2.22	2.24	2.03	2.16	2.36	2.19	1.61	1.15	1.82	1.51	1.52	1.84	1.81	1.67	1.29	1.78	1.65	0.74	1.36
0900-1000	2.15	2.12	2.16	2.20	2.15	2.49	2.73	2.21	1.28	2.17	2.03	1.51	1.24	1.45	1.55	1.13	0.89	0.64	2.61	1.31
1000-1100	2.09	2.26	2.39	2.27	2.25	1.26	2.29	2.08	2.06	1.92	1.64	1.59	1.74	1.60	1.64	2.54	1.31	2.20	2.03	2.02
1100-1200	2.17	2.58	2.13	2.64	2.38	1.47	2.93	1.65	2.03	2.02	1.40	1.97	1.40	1.92	1.67	1.75	2.03	2.18	2.20	2.04
1200-1300	2.55	2.69	2.53	2.67	2.61	2.28	2.14	2.72	2.48	2.40	2.15	2.62	1.85	1.55	2.04	1.69	2.65	2.54	2.52	2.35
1300-1400	2.69	2.61	2.89	2.68	2.72	1.90	2.69	2.66	2.76	2.51	2.98	2.28	2.21	1.83	2.32	2.68	1.87	2.53	1.27	2.08
1400-1500	2.74	2.71	2.81	2.90	2.79	2.49	3.00	2.68	3.19	2.84	2.20	2.74	2.23	2.32	2.37	1.52	2.35	2.10	2.59	2.14
1500-1600	2.68	2.82	2.82	2.62	2.63	1.02	1.74	2.54	1.67	1.74	2.05	1.73	2.11	2.15	2.01	2.82	3.15	3.70	1.86	2.88
1600-1700	2.85	2.83	2.78	2.58	2.76	1.84	2.06	1.83	1.61	1.83	2.39	2.51	2.47	1.77	2.28	2.41	2.32	2.42	2.53	2.42
1700-1800	2.63	2.73	2.82	2.79	2.74	2.17	1.67	1.95	2.37	2.04	2.24	2.05	1.99	2.18	2.11	1.76	2.50	1.58	2.61	2.11
1800-1900	2.77	2.78	2.58	2.64	2.69	3.03	2.79	1.87	3.10	2.69	2.32	2.42	2.25	1.47	2.11	2.62	2.85	2.61	2.31	2.59
1900-2000	2.71	2.63	2.66	2.76	2.69	2.90	2.86	1.91	2.71	2.59	1.81	1.56	1.83	2.52	1.93	1.85	2.25	2.31	2.52	2.23
2000-2100	2.57	2.86	2.80	2.69	2.73	2.59	2.22	1.90	1.83	2.13	1.94	2.39	1.89	2.18	2.10	2.49	3.02	2.78	2.22	2.62
2100-2200	2.75	2.89	2.93	3.02	2.89	2.96	3.01	3.34	2.44	2.93	2.19	2.66	2.28	2.51	2.41	2.30	2.50	4.02	2.86	2.92
2200-2300	2.91	2.90	3.13	2.97	2.97	2.62	1.22	4.10	2.95	2.72	3.16	2.56	2.99	2.21	2.73	3.01	3.33	2.78	2.15	2.81
2300-2400	3.07	3.09	3.07	3.25	3.12	2.78	2.35	2.21	3.00	2.58	2.23	2.40	2.77	2.88	2.57	2.31	2.68	3.69	2.35	2.75

"Events of November 15 to November 22, 1968"

by

John F. Steljes
Atomic Energy of Canada Limited
Chalk River, Ontario, Canada

A figure presents the cosmograms from 1800 UT November 15 to 0600 UT November 22, 1968.

A cosmogram is a projection of the cosmic ray intensity as a function of the spatial angle and time. The anti-solar direction is taken as 0° and the angle increases in the direction of rotation of the earth. The "garden-hose" angle lies between 90° and 180°.

The vertical thickness is proportional to the cosmic ray intensity, zero thickness being equal to the lowest intensity attained by any station during the entire period covered by the cosmograms. A scale of percent is given at the left hand lower corner. Time runs diagonally from the top right to the bottom left of the figure and there is a 12-hour overlap between the adjacent cosmograms.

The paths of the stations are lines extending vertically downwards as is described in a previous publication [Carmichael and Steljes, 1969]. These paths have been omitted here because of the small size of the cosmograms.

The stations used are as follows:

Station	Operated by	Asymptotic angle
Oulu	Finland	4.31 hours
Tixie	U.S.S.R.	10.66
Inuvik	Canada	15.70
Churchill, Canada	U.S.A.	19.01
Goose Bay	Canada	22.43

The stations are those of the "Northern Ring", five in all, and the angles between them are filled in by linear interpolation between simultaneous readings at each station. This type of interpolation is valid if the event is assumed to occur simultaneously at each station as is the case with a Forbush decrease. Each interpolation is judged to be valid for an angle of 30° (2 hours) on each side of the station (after rounding off to the nearest hour). If the separation is greater than this, the intervening portion of the cosmogram is dotted. One dotted portion occurs over Reykjavik and the other over Noril'sk, U.S.S.R.

After interpolation, the data are passed through a triangular filter in the time direction, having weights 1, 2, 3, 2, 1 (operating on hourly values) in order to reduce statistical fluctuations.

In Fig. 1 note the flare increase at 1100 UT on November 18. It was not observed at Oulu and only slightly at Tixie, hence the gap in the "wall" representing the increase. The shape of the "wall" gives a good idea of the way in which the interpolation between stations and the smoothing in the time direction operate. All the cosmograms are on the same scale.

REFERENCE

CARMICHAEL, H. and JOHN F. STELJES 1969 Forbush Decrease and Cosmogram May 25-26, 1967, Data on Solar Event of May 23, 1967 and its Geophysical Effects, World Data Center A, Upper Atmosphere Geophysics Report UAG-5, ESSA, Boulder, Colorado, February 1969, 83-86.

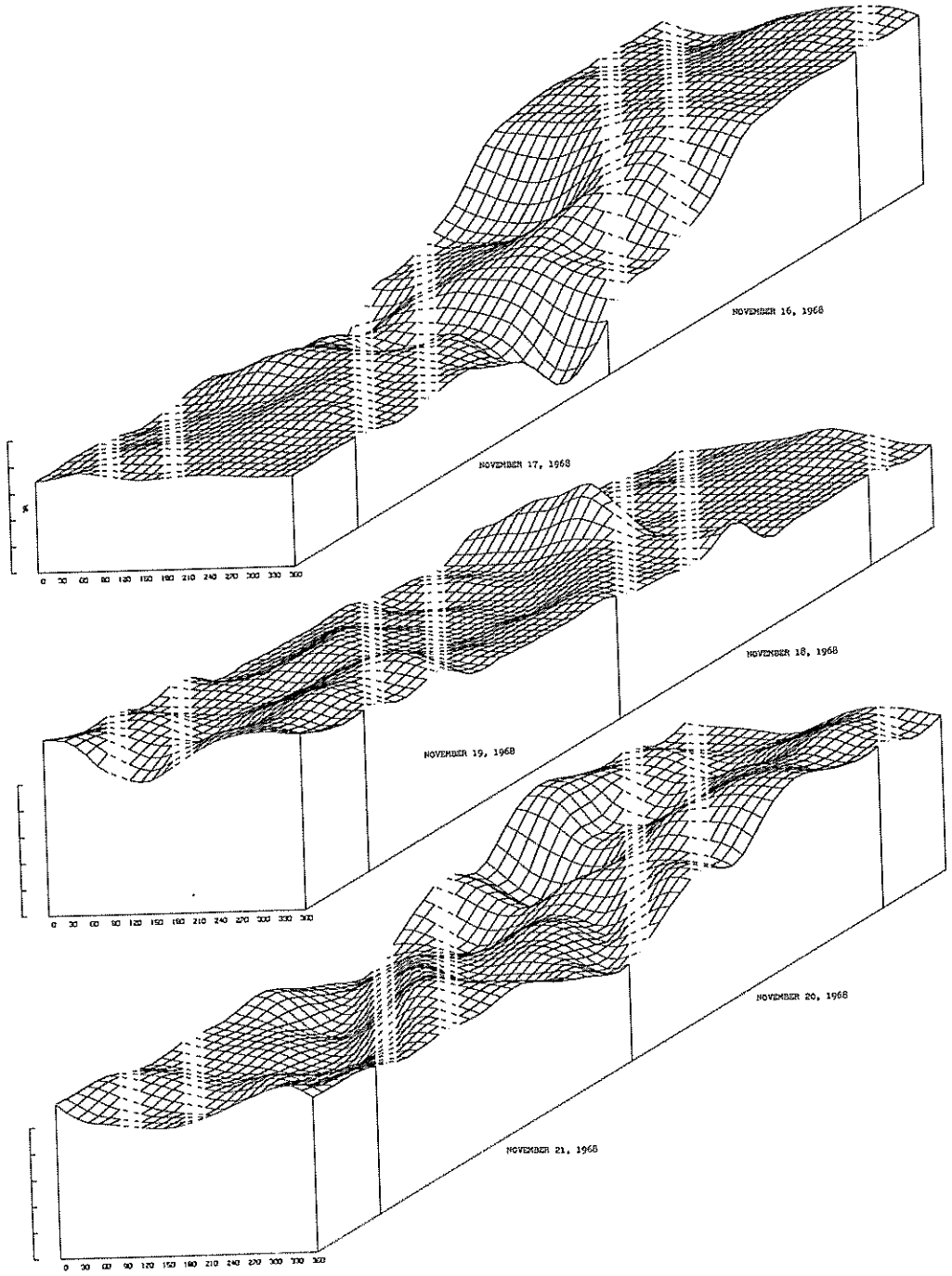

Fig. 1. Cosmograms for the period November 16 to 22, 1968. Note the flare increase at 1100 UT on November 18.

"Asymptotic Directions of Approach Appropriate for the High Energy Solar Proton Event of November 18, 1968"

by

M. A. Shea and D. F. Smart
Air Force Cambridge Research Laboratories
Bedford, Massachusetts

Recent results of Gall [1968] and Gall, et al. [1969] show that the external magnetic sources in the magnetosphere have an appreciable effect on the asymptotic directions of high latitude stations. As a result of the longitudinal asymmetry of the magnetosphere, it becomes apparent that for precise analysis of cosmic-ray data acquired by high latitude neutron monitors the asymptotic directions should be calculated as a function of local station time. In this paper we have calculated the asymptotic directions of approach for selected high latitude neutron monitors for rigidities appropriate to high energy solar cosmic-ray events. All calculations were made for the local station time equivalent to 1100 Universal Time - the time of maximum cosmic-ray intensity as recorded by neutron monitors for the solar cosmic-ray event on November 18, 1968.

The basic computer program of McCracken et al. [1962] where a charged particle of specified momentum per unit charge is traced from a specific location outward through a magnetic field using the Runge-Kutta method of integration, was modified [J. Jimenez, private communication] to include the Williams and Mead [1965] expressions for external sources. The fields from these external sources were vectorily combined with the field of the internal sources as specified by the International Geomagnetic Reference Field, Epoch 1965 [IAGA Commission 2, Working Group 4, 1969].

The magnetic field $\bar{B}$ employed for the calculation of particle trajectories is derived from

$$\bar{B} = \bar{B}_I + \bar{B}_S + \bar{B}_{CS}$$

where

$\bar{B}_I$ = the internal field,

$\bar{B}_S$ = the external field due to currents in the magnetopause, and

$\bar{B}_{CS}$ = the external field due to the current in the neutral sheet of the magnetospheric tail.

The internal field is obtained by

$$\bar{B}_I = \nabla V$$

where the magnetic potential V is obtained by a spherical harmonic expansion

$$V(r,\theta,\phi) = a \sum_{n=o}^{8} \sum_{m=o}^{8} (g_n^m \cos m\phi + h_n^m \sin m\phi)\, P_n^m \cos\theta\, (a/r)^{n+1}$$

with a being the average radius of the earth, g_n^m and h_n^m the coefficients of the internal magnetic field, and r the distance from the geocenter.

The following expressions were used for calculating the external fields:

$$\begin{aligned}\bar{B}_S = {} & (-\bar{g}_1^0 \cos\theta - 2\sqrt{3}\,\bar{g}_2^1\,(r/a)\sin\theta\cos\theta\cos\tau)\,\bar{e}_r \\ & + (\bar{g}_1^0 \sin\theta - \sqrt{3}\,\bar{g}_2^1\,(r/a)\,(2\cos^2\theta - 1)\cos\tau)\,\bar{e}_\theta \\ & + \sqrt{3}\,\bar{g}_2^1\,(r/a)\cos\theta\sin\tau\,\bar{e}_\phi,\end{aligned}$$

with the values used for the coefficients of the external field sources being $\bar{g}_o^1 = -0.2515/(r_b^3)$, $\bar{g}_2^1 = 0.1215/(r_b^4)$ gauss, and

$$\bar{B}_{CS} = (B_x \sin\theta\cos\tau - B_y\cos\theta)\bar{e}_r + (B_x\cos\theta\cos\tau + B_y\sin\theta)\bar{e}_\theta + (-B_x\sin\tau)\bar{e}_\phi$$

where

$$B_x = -2j\,(\theta_2 - \theta_1),$$

$$B_y = 2j\log(r_2/r_1),$$

and e_r, e_θ, e_ϕ are unit vectors in the r, θ, and φ directions with j being the current per unit length in the neutral sheet in electromagnetic units and τ being the geomagnetic time expressed in degrees measured eastward from geomagnetic midnight.

The Williams and Mead parameters to adjust the external field configuration utilized in these calculations are as follows:

r_b (the subsolar point) = 10 R_E (earth radii),

R_1 (the inward termination point of the neutral sheet in the tail) - 10 R_E.

R_2 (the outward termination point of the neutral sheet in the tail) = 40 R_E.

B_{CS} (the tail field associated with the current sheet) adjusted to 40 γ.

The model of the magnetopause used is a surface of revolution about the earth-sun line composed on the day side by a hemisphere of radius of 13.9 R_E centered at -3.5 R_E and extended into the truncated cone whose generators form an angle of 15.3° with the earth-sun line. This model is most appropriate for equinox conditions and does not include seasonal variations or ring currents.

To determine this set of asymptotic directions of approach, an anti-particle of specified rigidity was initiated in the vertical direction at an altitude of 30 km and traced until the trajectory either penetrated the magnetosphere boundary or extended up the tail a distance greater than 25 earth radii. The direction of the velocity vector at the magnetospheric penetration point was calculated in terms of a geocentric coordinate system and the asymptotic direction of approach was determined.

The following tables contain the asymptotic directions of approach for selected high latitude neutron monitors. Negative asymptotic longitudes indicate that the particle velocity vector does not cross the Greenwich meridian. Longitude values larger than 360 degrees are indicative of a large longitudinal drift of the particle as it traverses the magnetic cavity. If the particle orbit intersects the solid earth (i.e. forbidden) it is designated by an R; if the trajectory fails to reach a solution by 15,000 iterative steps, the result is denoted by an F and presumed to be forbidden.

When these results are compared with any of the previous published calculations utilizing only the internal field [Hatton and Carswell, 1963; McCracken, et al., 1965; Shea, et al., 1965; Shea, et al., 1968] significant differences in asymptotic directions are evident at low rigidity values. From our analyses of asymptotic directions calculated using both internal and external sources, we have found that these differences are primarily the result of the addition of external sources to the field in the earth's magnetic cavity. The differences resulting from the use of various internal geomagnetic field models are considerably smaller.

REFERENCES

GALL, RUTH 1968 Daily Variation of the Asymptotic Directions of Cosmic Rays, J. Geophys. Res., 73, 4400.

GALL, RUTH, JAIME JIMENEZ and A. OROZCO 1969 Directions of Approach of Cosmic Rays for High Latitude Stations, J. Geophys. Res., 74, 3529.

HATTON, C. J., and D. A. CARSWELL 1963 Asymptotic Directions of Approach of Vertically Incident Cosmic Rays for 85 Neutron Monitor Stations, Atomic Energy of Canada, Ltd., Report No. AECL-1824, August 1963.

IAGA COMMISSION 2, WORKING GROUP 4 1969 International Geomagnetic Reference Field 1965.0, J. Geophys., Res., 74, 4407.

McCRACKEN, K. G. U. R. RAO, and M. A. SHEA 1962 The Trajectories of Cosmic Rays in a High Simulation of the Geomagnetic Field, Mass. Inst. Technology Tech. Rept. 77, August 1962.

McCRACKEN, K. G., U. R. RAO, B. C. FOWLER M. A. SHEA, and D. F. SMART 1965 Cosmic Ray Tables, IQSY Instruction Manual 10, IQSY Committee, London.

SHEA, M. A, D. F. SMART, and K. G. McCRACKEN — 1965 — A Study of Vertical Cutoff Rigidities Using Sixth Degree Simulations of the Geomagnetic Field, J. Geophys. Res., 70, 4117.

SHEA, M. A., D. F. SMART, K. G. McCRACKEN, and U. R. RAO — 1968 — Supplement to IQSY Instruction Manual 10, Cosmic-Ray Tables, Special Report No. 71, AFCRL 68-0030.

WILLIAMS, D. J., and G. D. MEAD — 1965 — Nightside Magnetosphere Configuration as Obtained from Trapped Electrons at 1100 Kilometers, J. Geophys. Res., 70, 3017.

ALERT, CANADA

Geographic Latitude - 82.50 N
Geographic Longitude - 62.33 W
UT = 1100 LT = 0651
Geomagnetic Time = 1400

Rigidity (GV)	Asymptotic LAT	Asymptotic LONG
20.00	82.74	-23.74
15.00	81.35	-22.78
10.00	80.40	-28.36
5.00	78.37	-19.87
4.00	78.25	-18.83
3.00	76.00	-18.70
2.00	73.08	-16.18
1.00	64.45	-20.10
0.90	62.76	-20.80

RESOLUTE, CANADA

Geographic Latitude - 74.69 N
Geographic Longitude - 94.91 W
UT = 1100 LT = 0440
Geomagnetic Time = 0404

Rigidity (GV)	Asymptotic LAT	Asymptotic LONG
20.00	68.92	-83.44
15.00	66.86	-84.50
10.00	64.24	-88.28
5.00	59.44	-91.69
4.00	57.58	-93.44
3.00	54.40	-95.32
2.00	48.94	-98.42
1.00	34.82	-106.15
0.90	32.08	-107.65

THULE, GREENLAND

Geographic Latitude - 76.55 N
Geographic Longitude - 68.84 W
UT = 1100 LT = 0625
Geomagnetic Time = 0829

Rigidity (GV)	Asymptotic LAT	Asymptotic LONG
20.00	74.34	-42.45
15.00	72.09	-42.96
10.00	70.17	-49.49
5.00	67.93	-50.79
4.00	67.79	-53.74
3.00	65.72	-55.75
2.00	63.70	-58.84
1.00	57.23	-69.84
0.90	56.06	-71.73

VOSTOK, ANTARCTICA

Geographic Latitude - 78.47 S
Geographic Longitude - 106.87 E
UT = 1100 LT = 1807
Geomagnetic Time = 0940

Rigidity (GV)	Asymptotic LAT	Asymptotic LONG
20.00	-69.56	54.58
15.00	-70.31	41.81
10.00	-74.06	33.56
5.00	-70.61	25.22
4.00	-69.75	28.38
3.00	-68.80	19.32
2.00	-64.27	12.73
1.00	-57.50	-2.29
0.90	-56.02	-4.44

DUMONT D'URVILLE, ANTARCTICA

Geographic Latitude - 66.67 S
Geographic Longitude - 140.02 E
UT = 1100 LT = 2020
Geomagnetic Time = 2226

Rigidity (GV)	Asymptotic LAT	Asymptotic LONG
20.00	-67.48	159.20
15.00	-66.60	164.06
10.00	-64.73	170.07
5.00	-60.97	181.73
4.00	-59.30	186.25
3.00	-56.33	192.93
2.00	-49.65	203.68
1.00	-5.76	215.73
0.90	0.00	210.82

McMURDO, ANTARCTICA

Geographic Latitude - 77.85 S
Geographic Longitude - 166.72 E
UT = 1100 LT = 2207
Geomagnetic Time = 0343

Rigidity (GV)	Asymptotic LAT	Asymptotic LONG
20.00	-84.16	291.47
15.00	-79.64	283.14
10.00	-75.80	267.78
5.00	-69.35	271.07
4.00	-68.07	272.56
3.00	-63.76	270.86
2.00	-56.60	272.52
1.00	-41.18	270.60
0.90	-38.24	270.18

WILKES, ANTARCTICA

Geographic Latitude - 66.42 S
Geographic Longitude - 110.45 E
UT = 1100 LT = 1822
Geomagnetic Time = 1733

Rigidity (GV)	Asymptotic LAT	Asymptotic LONG
20.00	-59.00	105.31
15.00	-59.83	103.25
10.00	-61.33	107.12
5.00	-59.10	107.95
4.00	-57.33	109.87
3.00	-57.95	111.12
2.00	-57.64	111.35
1.00	-58.92	119.99
0.90	-59.39	121.88

MIRNY, ANTARCTICA

Geographic Latitude - 66.55 S
Geographic Longitude - 93.00 E
UT = 1100 LT = 1712
Geomagnetic Time = 1514

Rigidity (GV)	Asymptotic LAT	Asymptotic LONG
20.00	-51.11	84.73
15.00	-51.24	79.94
10.00	-54.04	80.35
5.00	-48.34	80.24
4.00	-46.38	83.92
3.00	-45.51	82.38
2.00	-40.59	82.98
1.00	-36.16	86.19
0.90	-35.18	87.13

HEISS ISLAND, USSR

Geographic Latitude - 80.33 N
Geographic Longitude - 57.80 E
UT = 1100 LT = 1451
Geomagnetic Time = 1617

Rigidity	Asymptotic LAT	Asymptotic LONG
20.00	70.83	95.99
15.00	68.78	94.20
10.00	67.41	94.48
5.00	61.58	97.63
4.00	59.95	101.01
3.00	57.77	101.76
2.00	53.34	106.06
1.00	45.98	115.63
0.90	44.40	117.54

SOUTH POLE, ANTARCTICA

Geographic Latitude - 89.98 S
Geographic Longitude - 0.00 E
UT = 1100 LT = 1100
Geomagnetic Time = 0718

Rigidity (GV)	Asymptotic LAT	Asymptotic LONG
20.00	-63.08	5.72
15.00	-58.69	-6.03
10.00	-58.26	-19.50
5.00	-50.04	-18.60
4.00	-50.47	-17.89
3.00	-44.37	-20.26
2.00	-37.84	-17.60
1.00	-20.80	-16.36
0.90	-17.84	-15.59

INUVIK, CANADA

Geographic Latitude - 68.35 N
Geographic Longitude - 133.73 W
UT = 1100 LT = 0205
Geomagnetic Time = 0055

Rigidity (GV)	Asymptotic LAT	Asymptotic LONG
20.00	47.03	-119.94
15.00	42.64	-123.30
10.00	38.84	-125.98
5.00	24.28	-127.63
4.00	19.37	-127.20
3.00	9.71	-132.26
2.00	-4.94	-143.20
1.00	-12.06	-187.94
0.90	-7.97	-197.91

CHURCHILL, CANADA

Geographic Latitude - 58.75 N
Geographic Longitude - 94.09 W
UT = 1100 LT = 0444
Geomagnetic Time = 0450

Rigidity (GV)	Asymptotic LAT	Asymptotic LONG
20.00	41.11	-71.61
15.00	35.94	-72.97
10.00	31.21	-75.70
5.00	19.66	-73.93
4.00	16.58	-72.80
3.00	9.89	-72.46
2.00	-0.21	-69.46
1.00	-20.92	-61.80
0.90	-24.32	-59.73

MAWSON, ANTARCTICA

Geographic Latitude - 67.60 S
Geographic Longitude - 62.88 E
UT = 1100 LT = 1512
Geomagnetic Time = 1246

Rigidity (GV)	Asymptotic LAT	Asymptotic LONG
20.00	-39.82	60.63
15.00	-36.81	54.02
10.00	-39.21	48.44
5.00	-27.59	52.19
4.00	-28.89	54.20
3.00	-20.76	53.38
2.00	-14.73	58.00
1.00	5.85	68.28
0.90	9.46	70.98

SYOWA, ANTARCTICA

Geographic Latitude - 69.03 S
Geographic Longitude - 39.60 E
UT = 1100 LT = 1338
Geomagnetic Time = 1124

Rigidity (GV)	Asymptotic LAT	Asymptotic LONG
20.00	-35.59	46.34
15.00	-29.83	39.78
10.00	-29.27	31.36
5.00	-16.18	38.35
4.00	-16.56	36.46
3.00	-5.38	40.87
2.00	3.60	44.76
1.50	12.77	53.32
1.40	18.72	56.43
1.30	19.22	57.70
1.20	24.92	63.97
1.10	26.56	67.71
1.00	33.18	77.70
0.90	38.14	93.84

GOOSE BAY, CANADA

Geographic Latitude - 53.33 N
Geographic Longitude - 60.42 W
UT = 1100 LT = 0658
Geomagnetic Time = 0743

Rigidity (GV)	Asymptotic LAT	Asymptotic LONG
20.00	35.27	-20.69
15.00	27.02	-20.16
10.00	19.96	-22.99
5.00	7.88	-13.64
4.00	6.06	-12.23
3.00	-2.61	-5.22
2.00	-10.17	7.27
1.50	-17.79	24.06
1.40	-18.27	27.85
1.30	-19.36	34.96
1.20	-19.59	42.13
1.10	-19.41	54.33
1.00	-16.26	68.81
0.90	-5.27	99.50

TIXIE BAY, USSR

Geographic Latitude - 71.55 N
Geographic Longitude - 128.90 E
UT = 1100 LT = 1936
Geomagnetic Time = 1909

Rigidity (GV)	Asymptotic LAT	Asymptotic LONG
20.00	51.46	166.94
15.00	45.93	164.48
10.00	41.73	160.62
5.00	33.26	161.69
4.00	32.23	162.31
3.00	27.98	158.95
2.00	23.95	154.10
1.50	24.05	145.96
1.40	24.45	145.08
1.30	-24.28	145.61
1.20	-32.35	151.78
1.10	-35.74	160.39
1.00	-35.74	171.30
0.90	-31.82	181.58

CAPE SCHMIDT, USSR

Geographic Latitude - 68.87 N
Geographic Longitude - 179.49 W
UT = 1100 LT = 2302
Geomagnetic Time = 2155

Rigidity (GV)	Asymptotic LAT	Asymptotic LONG
20.00	40.43	-151.92
15.00	34.00	-156.61
10.00	30.13	-161.86
5.00	15.55	-164.48
4.00	13.14	-164.89
3.00	5.72	-171.30
2.00	-2.64	-180.54
1.50	-11.40	-174.08
1.40	-11.42	-173.80
1.30	-10.18	-169.83
1.20	-8.68	-169.33
1.10	-5.28	-165.99
1.00	-0.40	-162.67
0.90	7.65	-162.00

APATITY, USSR

Geographic Latitude - 67.55 N
Geographic Longitude - 33.33 E
UT = 1100 LT = 1313
Geomagnetic Time = 1429

Rigidity (GV)	Asymptotic LAT	Asymptotic LONG
20.00	47.26	71.32
15.00	41.62	69.86
10.00	37.98	68.46
5.00	24.17	78.17
4.00	22.44	81.96
3.00	13.31	87.44
2.00	2.91	101.23
1.50	-8.82	118.62
1.40	-9.93	123.19
1.30	-13.51	132.18
1.20	-15.13	141.20
1.10	-17.43	158.08
1.00	-15.31	180.61
0.99	-16.63	180.70
0.98	-18.62	178.97
0.97	-17.51	177.59
0.96	-16.23	176.21
0.95	-15.01	174.86
0.94	-13.89	173.52
0.93	-12.71	172.13
0.92	-11.36	170.53
0.91	-9.49	168.74
0.90	-7.79	166.02

OULU, FINLAND

Geographic Latitude - 65.00 N
Geographic Longitude - 25.40 E
UT = 1100 LT = 1242
Geomagnetic Time = 1357

Rigidity (GV)	Asymptotic LAT	Asymptotic LONG
20.00	42.85	65.26
15.00	36.16	64.14
10.00	31.56	62.54
5.00	16.54	74.64
4.00	14.77	78.31
3.00	4.23	86.81
2.00	-5.98	106.19
1.90	-8.47	110.91
1.80	-11.31	116.19
1.70	-12.07	120.36
1.60	-12.74	126.47
1.50	-15.30	137.10
1.40	-14.90	146.92
1.30	-13.90	161.47
1.20	-11.21	172.28
1.19	-11.85	171.10
1.18	-12.59	169.75
1.17	-13.52	168.14
1.16	-12.18	167.69
1.15	-10.98	166.90
1.14	-9.47	165.97
1.13	-7.54	164.95
1.12	-5.63	163.46
1.11	-3.57	161.74
1.10	-1.44	159.92
1.09	0.50	157.99
1.08	30.76	170.58
1.07	34.47	186.16
1.06	30.92	194.83
1.05	24.87	199.03
1.04	18.02	201.58
1.03	9.55	203.11
1.02	-1.43	202.17
1.01	-16.32	195.54
1.00	-15.04	225.25
0.99	13.66	430.24
0.98	-12.15	298.28
0.97	-15.28	225.98
0.96	5.88	304.82
0.95	1.87	284.44
0.94	10.83	374.26
0.93	3.89	318.50
0.92	-5.43	222.10
0.91	-11.73	175.62
0.90	1.28	200.86

DEEP RIVER, CANADA

Geographic Latitude - 46.10 N
Geographic Longitude - 77.50 W
UT = 1100 LT = 0550
Geomagnetic Time = 0616

Rigidity (GV)	Asymptotic LAT	Asymptotic LONG
20.00	21.85	-41.20
15.00	12.76	-40.44
10.00	4.65	-42.00
5.00	-10.73	-28.06
4.00	-13.17	-23.98
3.00	-21.55	-9.20
2.00	-21.69	21.14
1.90	-20.47	28.80
1.80	-17.82	37.51
1.70	-13.62	44.23
1.60	-8.79	52.93
1.50	2.72	71.26
1.40	20.10	98.96
1.30	16.69	162.29
1.29	-15.04	174.13
1.28	6.64	214.72
1.27	-8.24	184.75
1.26	-8.31	170.94
1.25	20.28	183.78
1.24	11.41	172.75
1.23	8.30	162.06
1.22	23.17	182.01
1.21	R	R
1.20	R	R
1.19	-2.70	221.10
1.18	-14.12	214.60
1.17	3.58	339.18
1.16	4.26	221.62
1.15	-4.47	187.40
1.14	-2.05	177.02
1.13	9.87	208.99
1.12	R	R
1.11	5.37	208.48
1.10	16.78	175.82
1.09	R	R
1.08	8.11	210.16
1.07	R	R
1.06	-5.54	208.42
1.05	F	F
7.47	1.04	398.34
-9.99	1.03	290.23
F	1.02	F
5.35	1.01	397.39
-18.94	1.00	210.20
2.66	0.99	281.28
R	0.98	R
F	0.97	F
17.47	0.96	170.82
R	0.95	R
R	0.94	R
F	0.93	F
R	0.92	R
F	0.91	F
R	0.90	R

SANAE, ANTARCTICA

Geographic Latitude - 70.46 S
Geographic Longitude - 2.49 W
UT = 1100 LT = 1050
Geomagnetic Time = 0932

Rigidity (GV)	Asymptotic LAT	LONG
20.00	-32.43	23.29
15.00	-22.69	18.07
10.00	-15.43	8.72
5.00	-2.07	19.25
4.00	5.00	17.92
3.00	14.18	28.87
2.00	31.80	53.72
1.90	31.90	57.36
1.80	31.24	61.34
1.70	32.96	70.99
1.60	33.68	88.42
1.50	28.96	100.90
1.40	23.53	117.15
1.30	-2.56	154.20
1.20	-4.70	182.46
1.19	6.80	181.02
1.18	18.07	200.63
1.17	-27.64	319.25
1.16	8.46	115.60
1.15	10.99	214.09
1.14	5.52	225.91
1.13	-3.29	210.90
1.12	20.98	222.23
1.11	22.13	215.16
1.10	2.35	400.01
1.09	-27.59	299.40
1.08	8.54	210.24
1.07	11.86	211.18
1.06	-1.20	182.28
1.05	8.24	172.35
1.04	4.12	203.42
1.03	-3.51	168.24
1.02	-9.95	323.81
1.01	11.22	203.95
1.00	-6.55	379.06
0.99	F	F
0.98	-7.28	199.56
0.97	2.77	363.90
0.96	-5.11	347.45
0.95	F	F
0.94	8.62	384.32
0.93	-0.28	194.69
0.92	F	F
0.91	R	R
0.90	R	R

OTTAWA, CANADA

Geographic Latitude = 45.40 N
Geographic Longitude = 75.60 W
UT = 1100 LT = 0558
Geomagnetic Time = 0625

Rigidity (GV)	Asymptotic Lat	Long
20.00	21.02	-38.00
15.00	11.60	-36.86
10.00	3.13	-38.15
5.00	-12.13	-22.70
4.00	-14.48	-18.12
3.00	-22.16	-1.17
2.00	-18.30	33.23
1.90	-15.91	41.44
1.80	-10.92	52.12
1.70	-3.87	61.30
1.60	3.90	73.31
1.50	22.33	109.01
1.49	24.57	116.19
1.48	26.40	124.10
1.47	27.53	133.21
1.46	27.75	142.56
1.45	26.92	151.44
1.44	24.83	159.91
1.43	21.84	167.47
1.42	25.26	166.70
1.41	22.35	164.55
1.40	16.46	161.67
1.39	8.59	158.18
1.38	-9.80	184.68
1.37	-0.95	231.32
1.36	R	R
1.35	-18.12	224.20
1.34	-5.27	171.05
1.33	-8.07	257.14
1.32	5.42	168.99
1.31	-28.56	253.58
1.30	R	R
1.29	R	R
1.28	1.26	154.10
1.27	11.16	187.45
1.26	1.07	413.65
1.25	-11.60	199.29
1.24	-12.40	213.80
1.23	F	F
1.22	-7.22	190.17
1.21	-9.30	283.69
1.20	7.27	215.96
1.19	-8.13	266.55
1.18	-2.19	174.34
1.17	4.71	200.98
1.16	R	R
1.15	F	F
1.14	0.13	198.79
1.13	F	F
1.12	-8.18	361.70
1.11	-13.12	185.07
1.10	-12.81	332.88
1.09	-15.71	344.63
1.08	F	F
1.07	-10.34	282.33
1.06	R	R
1.05	R	R
1.04	F	F
1.03	F	F
1.02	F	F
1.01	F	F
1.00	F	F

CALGARY, CANADA

Geographic Latitude = 51.08 N
Geographic Longitude = 114.09 W
UT = 1100 LT = 0324
Geomagnetic Time = 0317

Rigidity (GV)	Asymptotic Lat	Asymptotic Long
20.00	19.46	-90.17
15.00	11.40	-92.20
10.00	4.99	-94.86
5.00	-13.88	-85.75
4.00	-17.02	-81.44
3.00	-26.93	-70.58
2.00	-31.10	-38.63
1.90	-30.40	-30.06
1.80	-27.90	-22.58
1.70	-24.69	-16.78
1.60	-20.29	-6.30
1.50	-9.33	8.81
1.40	2.63	22.55
1.30	32.05	90.29
1.29	27.15	122.47
1.28	10.19	152.89
1.27	-19.06	146.53
1.26	14.40	202.72
1.25	-11.56	179.69
1.24	-23.90	282.13
1.23	-11.16	156.43
1.22	4.84	218.91
1.21	-4.68	365.24
1.20	-9.12	180.34
1.19	6.82	169.14
1.18	R	R
1.17	-5.52	215.36
1.16	-2.05	429.57
1.15	F	F
1.14	12.46	170.17
1.13	-4.47	222.91
1.12	-13.57	353.60
1.11	-2.15	375.72
1.10	-5.35	284.00
1.09	-5.58	300.33
1.08	-21.14	290.99
1.07	-5.38	391.11
1.06	F	F
1.05	1.53	216.28
1.04	R	R
1.03	R	R
1.02	-10.09	322.24
1.01	F	F
1.00	R	R
0.99	F	F
0.98	R	R
0.97	F	F
0.96	F	F
0.95	F	F

PORT AUX FRANCAIS

Geographic Latitude = 49.35 S
Geographic Longitude = 70.22 E
UT = 1100 LT = 1541
Geomagnetic Time = 1442

Rigidity (GV)	Asymptotic Lat	Asymptotic Long
20.00	-15.40	86.86
15.00	-8.47	84.81
10.00	-5.21	83.06
5.00	14.91	98.04
4.00	16.28	101.87
3.00	29.31	120.25
2.00	28.64	159.78
1.90	26.96	165.91
1.80	26.80	174.95
1.70	22.30	176.27
1.60	15.42	173.37
1.50	-7.86	174.83
1.49	-12.68	180.14
1.48	-14.03	185.81
1.47	-13.08	191.34
1.46	-10.30	196.78
1.45	-7.06	203.32
1.44	-2.03	209.90
1.43	4.98	216.89
1.42	14.81	223.56
1.41	13.26	236.64
1.40	-2.38	252.48
1.39	7.15	334.54
1.38	-0.39	234.60
1.37	10.38	418.87
1.36	-8.74	300.38
1.35	-6.19	359.69
1.34	-12.70	406.50
1.33	R	R
1.32	-18.84	327.57
1.31	-10.03	392.31
1.30	R	R
1.29	R	R
1.28	4.17	395.44
1.27	-5.82	261.22
1.26	-24.00	307.06
1.25	-20.22	296.53
1.24	-3.74	364.71
1.23	1.85	254.86
1.22	-22.04	358.99
1.21	F	F
1.20	-13.62	207.99
1.19	-2.67	414.82
1.18	-4.37	221.50
1.17	-10.47	232.03
1.16	-7.66	361.69
1.15	F	F
1.14	F	F
1.13	F	F
1.12	F	F
1.11	F	F
1.10	F	F

DURHAM, U.S.A.

Geographic Latitude = 43.10 N
Geographic Longitude = 70.84 W
UT = 1100 LT = 0617
Geomagnetic Time = 0647

Rigidity (GV)	Asymptotic Lat	Asymptotic Long
20.00	18.00	-29.37
15.00	7.58	-27.12
10.00	-2.14	-27.04
5.00	-16.52	-5.79
4.00	-18.23	1.26
3.00	-20.66	27.39
2.50	-14.68	43.53
2.40	-12.30	50.91
2.30	-8.01	59.89
2.20	-1.60	68.87
2.10	5.39	77.28
2.00	12.04	87.86
1.90	21.51	110.83
1.80	25.73	164.57
1.79	21.23	165.19
1.78	11.98	164.73
1.77	-11.06	177.96
1.76	12.62	220.41
1.75	14.02	400.99
1.74	-13.05	199.46
1.73	12.82	181.15
1.72	-0.94	152.93
1.71	2.51	200.46
1.70	5.02	322.06
1.69	6.15	196.59
1.68	13.61	190.05
1.67	-6.93	212.76
1.66	R	R
1.65	R	R
1.64	R	R
1.63	R	R
1.62	-17.03	209.37
1.61	1.04	305.68
1.60	R	R
1.59	23.06	185.43
1.58	3.03	181.72
1.57	-24.85	212.80
1.56	-14.67	274.53
1.55	5.15	356.24
1.54	-17.25	227.31
1.53	-17.86	364.47
1.52	5.78	195.00
1.51	-5.97	299.24
1.50	7.87	214.37
1.49	R	R
1.48	-15.40	327.98
1.47	F	F
1.46	-15.74	281.03
1.45	-16.65	199.84
1.44	F	F
1.43	F	F
1.42	20.01	92.30
1.41	R	R
1.40	F	F
1.39	F	F
1.38	F	F
1.37	F	F
1.36	9.07	109.00
1.35	-15.04	218.77
1.34	F	F
1.33	F	F
1.32	R	R
1.31	F	F
1.30	R	R

CHICAGO, U.S.A.

Geographic Latitude = 41.83 N
Geographic Longitude = 87.67 W
UT = 1100 LT = 0509
Geomagnetic Time = 0529

Rigidity (GV)	Asymptotic Lat	Asymptotic Long
20.00	11.54	-51.57
15.00	1.21	-50.33
10.00	-8.04	-50.40
5.00	-24.29	-25.58
4.00	-24.93	-16.06
3.00	-21.56	16.76
2.90	-19.56	19.72
2.80	-17.40	22.64
2.70	-15.04	26.27
2.60	-12.23	31.27
2.50	-8.03	38.56
2.40	-0.83	48.76
2.30	10.55	62.02
2.20	24.22	81.37
2.10	31.08	114.67
2.00	15.33	148.05
1.99	-12.61	153.27
1.98	-14.63	178.94
1.97	16.14	216.29
1.96	6.42	148.16
1.95	14.73	59.52
1.94	2.77	197.99
1.93	14.37	197.41
1.92	-8.22	206.85
1.91	7.10	197.44
1.90	18.77	176.41
1.89	13.76	189.55
1.88	R	R
1.87	R	R
1.86	9.87	88.31
1.85	R	R
1.84	R	R
1.83	5.69	188.06
1.82	-18.24	289.02
1.81	-4.89	276.42
1.80	-23.80	246.63
1.79	-4.67	-188.34
1.78	-1.81	342.24
1.77	-13.83	305.52
1.76	R	R
1.75	9.29	87.40
1.74	R	R
1.73	-17.41	306.55
1.72	R	R
1.71	R	R
1.70	R	R
1.69	F	F
1.68	-8.59	321.03
1.67	F	F
1.66	F	F
1.65	F	F
1.64	R	R
1.63	F	F
1.62	R	R
1.61	R	R
1.60	F	F

VICTORIA, CANADA

Geographic Latitude = 48.50 N
Geographic Longitude = 123.42 W
UT = 1100 LT = 0246
Geomagnetic Time = 0237

Rigidity (GV)	Asymptotic Lat	Asymptotic Long
20.00	11.05	-96.81
15.00	1.07	-98.34
10.00	-6.96	-100.30
5.00	-27.65	-78.56
4.00	-29.04	-68.62
3.00	-28.44	-32.01
2.90	-26.55	-28.84
2.80	-24.54	-25.41
2.70	-22.44	-21.12
2.60	-19.70	-14.96
2.50	-15.00	-6.22
2.40	-6.35	5.29
2.30	7.10	19.38
2.20	22.23	40.32
2.10	27.92	81.30
2.09	26.81	87.80
2.08	25.02	95.08
2.07	22.32	103.10
2.06	18.41	111.93
2.05	12.84	121.97
2.04	5.09	133.14
2.03	-5.42	146.90
2.02	-14.64	169.66
2.01	23.49	87.16
2.00	6.44	222.99
1.99	-0.76	349.58
1.98	-4.81	152.31
1.97	14.58	373.25
1.96	5.59	383.50
1.95	-13.92	304.60
1.94	-4.46	346.40
1.93	-16.80	327.56
1.92	R	R
1.91	R	R
1.90	-6.60	368.44
1.89	F	F
1.88	F	F
1.87	3.16	182.52
1.86	R	R
1.85	-10.35	229.74
1.84	-5.99	352.52
1.83	-2.84	381.18
1.82	R	R
1.81	F	R
1.80	R	R
1.79	-9.89	375.08
1.78	R	R
1.77	R	R
1.76	R	R
1.75	R	R
1.74	F	F
1.73	-8.94	364.04
1.72	F	F
1.71	F	F
1.70	F	F
1.69	F	F
1.68	F	F
1.67	F	F
1.66	F	F
1.65	R	R

LEEDS, ENGLAND

Geographic Latitude = 53.82 N
Geographic Longitude = 1.55 W
UT = 1100 LT = 1054
Geomagnetic Time = 1157

Rigidity (GV)	Asymptotic Lat	Asymptotic Long
20.00	26.14	47.24
15.00	14.74	49.34
10.00	4.20	51.01
5.00	-10.94	82.39
4.00	-11.33	97.14
3.00	-1.84	144.02
2.90	3.40	151.32
2.80	8.94	155.22
2.70	23.72	158.11
2.60	26.91	174.75
2.50	17.64	196.26
2.40	-4.56	243.61
2.39	-24.02	298.75
2.38	5.20	58.88
2.37	2.09	330.05
2.36	5.72	156.43
2.35	13.31	381.70
2.34	18.12	122.00
2.33	8.69	108.47
2.32	16.82	183.83
2.31	F	F
2.30	R	R
2.29	R	R
2.28	R	R
2.27	R	R
2.26	22.18	73.40
2.25	18.41	69.63
2.24	R	R
2.23	0.42	203.70
2.22	-4.93	330.03
2.21	F	F
2.20	20.11	111.30
2.19	-13.87	308.68
2.18	7.40	396.36
2.17	-1.26	372.30
2.16	R	R
2.15	6.56	395.01
2.14	12.78	55.66
2.13	R	R
2.12	R	R
2.11	14.56	132.75
2.10	-3.71	395.74
2.09	R	R
2.08	F	F
2.07	-18.50	240.53
2.06	F	F
2.05	R	R
2.04	-6.22	252.47
2.03	R	R
2.02	R	R
2.01	R	R
2.00	R	R
1.99	F	F
1.98	R	R
1.97	F	F
1.96	F	F
1.95	R	R

DALLAS, U.S.A.

Geographic Latitude = 32.78 N
Geographic Longitude = 96.80 W
UT = 1100 LT = 0433
Geomagnetic Time = 0450

Rigidity (GV)	Asymptotic Lat	Asymptotic Long	Rigidity (GV)	Asymptotic Lat	Asymptotic Long
20.00	-6.77	-51.06	4.41	17.94	172.53
15.00	-20.71	-43.25	4.40	2.76	204.24
10.00	-31.12	-27.06	4.39	-7.18	234.48
9.00	-30.03	-22.15	4.38	12.93	194.93
8.00	-27.44	-15.73	4.37	12.41	186.34
7.00	-23.63	-4.97	4.36	R	R
6.00	-15.53	17.40	4.35	1.55	228.41
5.00	27.20	74.45	4.34	R	R
4.90	32.13	94.06	4.33	-9.16	224.81
4.80	25.21	123.39	4.32	15.04	175.63
4.70	-18.73	178.86	4.31	-6.41	243.78
4.69	-9.76	200.43	4.30	R	R
4.68	3.94	246.74	4.29	-6.70	247.03
4.67	-10.82	219.19	4.28	4.25	213.42
4.66	-26.80	295.90	4.27	7.08	56.27
4.65	-5.36	314.25	4.26	R	R
4.64	-9.14	394.14	4.25	R	R
4.63	-13.25	229.72	4.24	6.53	132.05
4.62	7.13	146.95	4.23	R	R
4.61	-3.35	145.73	4.22	R	R
4.60	-3.82	180.28	4.21	11.01	186.28
4.59	-11.45	250.77	4.20	-12.01	224.01
4.58	-12.36	243.14	4.19	-4.56	217.95
4.57	-1.19	146.56	4.18	-8.42	320.32
4.56	8.56	222.78	4.17	R	R
4.55	17.74	195.69	4.16	R	R
4.54	2.02	168.00	4.15	R	R
4.53	19.39	190.72	4.14	R	R
4.52	13.53	207.92	4.13	R	R
4.51	4.96	151.79	4.12	-18.08	321.69
4.50	R	R	4.11	R	R
4.49	R	R	4.10	R	R
4.48	R	R	4.09	R	R
4.47	R	R	4.08	18.17	103.31
4.46	R	R	4.07	R	R
4.45	R	R	4.06	R	R
4.44	R	R	4.05	R	R
4.43	20.36	168.49	4.04	R	R
4.42	13.02	95.25	4.03	R	R

4.02 - 3.85 all reentrant trajectories

[Permission to reprint the following article has been given by the authors and the "Antarctic Journal of the United States".]

Investigations of Cosmic Ray Intensity Variations in Antarctica

MARTIN A. POMERANTZ *and* SHAKTI P. DUGGAL

Bartol Research Foundation of The Franklin Institute

The emission by the sun of nuclear particles having energies as high as several hundred MeV is a rare occurrence which, on the average, happens only once every two years. Thus, although the data recorded at the antarctic cosmic ray stations continue to provide the basis for a number of unique analytical studies in which galactic particles serve as probes for investigating the solar-controlled electromagnetic conditions in interplanetary space, the arrival from the sun of "newborn" cosmic rays having sufficient energy to propagate their effects through the earth's atmosphere is by far the most spectacular phenomenon that we can hope to observe with ground-based detectors. Two such events occurred during 1968: on September 29 and on November 18. The magnitude of the first was too small to permit extensive analysis (solar-particle intensity less than one percent above the galactic cosmic ray background). However, the second was sufficiently unusual to warrant detailed description here.

It is interesting to recollect that earlier theories of propagation precluded the arrival of solar particles at polar stations. However, cosmic ray flux increases have been observed during every so-called "ground level event," and, in fact, their magnitude has generally been greater than that at lower-latitude stations having directions of viewing in the equatorial plane. Studies of these events have revealed that diffusion mechanisms play an important role in the transport of particles from the sun to the earth (Pomerantz *and* Duggal, 1961; Pomerantz *et al.*, 1961a, b, c; Pomerantz *and* Duggal, 1962; Baird *et al.*, 1967).

The November 18, 1968 event is the first in which direct impact of solar particles in the polar regions has been observed with the new, high counting-rate neutron monitors. The earlier instruments would not have provided the high resolution required for the quantitative analysis that has led to the conclusion that the dominant mode of propagation in this case was guidance directly from the sun along magnetic lines of force. Fig. 1 shows the intensity of solar cosmic rays as recorded by the Bartol neutron monitors at McMurdo and South Pole Stations, as well as at the arctic station at Thule, Greenland, and at Swarthmore, where the particles arrive from the equatorial plane. Because of its altitude, the South Pole detector responds to lower-energy particles than the other stations, hence the magnitude of the increase is enhanced.

The most striking feature is the sharp rise time, in marked contrast to the slower-developing previous events, particularly the last one (January 28, 1967), described in this journal (Pomerantz, 1968). Maximum intensity was attained 15 min after onset, and the major activity subsided in about 2 hours. This event occurred while a cosmic ray storm was in progress, and was associated with a relatively minor (1B) limb flare at N21° W87° on the solar disk. The spectrum, deduced from an analysis of data from 18 stations, was of the form k exp(−P/550), where P is the magnetic rigidity in units of MV.

After normalizing the data to remove the effects of differences in altitude and geomagnetic threshold rigidity, a large variance remains in the magnitude of the increase as recorded at different stations near the peak of this event. For example, the percentage increase observed at Thule (76.6°N. 291.6°E.) was twice that at Alert (82.5°N. 297.7°E.), while no enhancement was recorded at the Soviet station at Tiksi Bay (71.6°N. 128.9°E.).

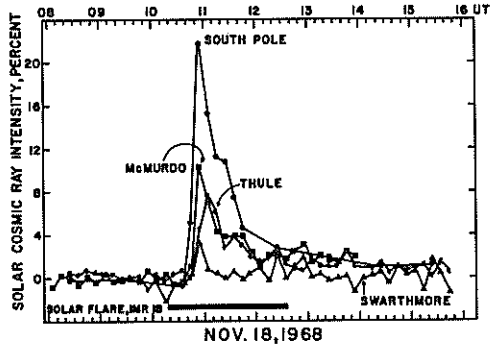

Figure 1. (above). Solar cosmic ray event of November 18, 1968, as observed by Bartol neutron monitor stations. The ordinates are percentage increase in intensity above the galactic cosmic ray background. South Pole Station recorded the largest flux detected anywhere on the earth's surface.

Figure 2 (below). For each station from which data were available, X represents its geographic location, O is the asymptotic direction of viewing of its detector, and the number indicates the percentage enhancement (appropriately normalized to remove the effects of altitude and geomagnetic cutoff differences) above the galactic cosmic ray background. The axis of symmetry, +, represents the position of the apparent source, which is 50° west of the sun-earth line, corresponding to the garden-hose angle characterizing the Archimedean spiral structure of the interplanetary magnetic field.

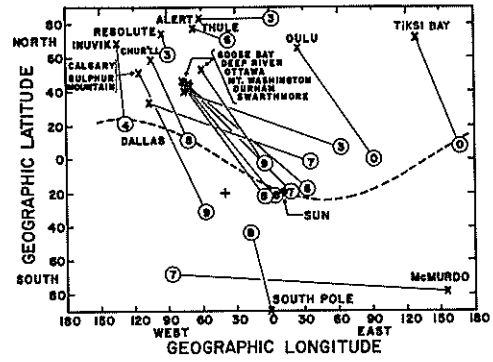

In Fig. 2, the normalized maximum percentage increases during a 20-min interval are indicated in circles representing the approximate asymptotic directions of arrival of the solar particles to which the detectors at the specified locations (X) respond. Our analysis reveals that the intensity increase was symmetric with respect to a point on the celestial sphere with geographic coordinates 20°S. 40°W. This location was 50° west of the position of the sun at that time, which conforms with the Archimedean spiral structure of the interplanetary magnetic field and confirms that the solar particles were magnetically guided from the source. Because of the rapid decrease in the flux to a low level shortly after the maximum, it is not possible to determine when diffusion ultimately became the principal propagation mechanism.

References

Baird, G. A., G. G. Bell, S. P. Duggal, *and* M. A. Pomerantz. 1967. Neutron monitor observations of high-energy solar particles during the new cycle. *Solar Physics,* 2: 491-501.

Pomerantz, M. A. *and* S. P. Duggal. 1961. Unusual increase in the cosmic ray intensity on November 20, 1960. *Journal of the Franklin Institute,* 271: 327-335.

Pomerantz, M. A., S. P. Duggal, *and* K. Nagashima. 1961a. Observations near the North and South Poles of bursts of cosmic rays from the sun. *Journal of the Franklin Institute,* 271: 317-326.

Pomerantz, M. A., S. P. Duggal, *and* K. Nagashima. 1961b. Solar-produced cosmic rays near the North and South Poles. *Physical Review Letters,* 6: 123-125.

Pomerantz, M. A., S. P. Duggal, *and* K. Nagashima. 1961c. The unusual cosmic ray intensity increases on November 12, 1960. *Space Research,* II: 788-802.

Pomerantz, M. A. *and* S. P. Duggal. 1962. Anisotropy in solar particles incident on polar regions during July 1961. *Journal of the Franklin Institute,* 273: 242-248.

Pomerantz, M. A. 1968. Investigations of cosmic ray intensity variations in Antarctica. *Antarctic Journal of the U.S.,* III(5): 252-253.

ANTARCTIC JOURNAL

Reprinted from *Antarctic Journal of the United States,* vol. IV, no. 5.

"Observations in the Arctic and Antarctic of the 18 November 1968 Solar Cosmic Ray Event"

by

A. D. Goedeke and A. J. Masley
Space Sciences Department
McDonnell Douglas Astronautics Company - Western Division
Santa Monica, California, U.S.A.

ABSTRACT

One of the largest solar proton events during the present broad solar maximum period occurred on 18 November 1968. The only visible flare that could be associated with the particle emission was a 1B flare that was in progress at 1030 UT, 18 November, located at N22 W87 in McMath Plage Region 9760. Type IV radio emission, of intensity 3, occurred between 1026 UT and 1034 UT. Type II emission was present between 1026 UT and 1050 UT. At about 1045 UT, the Deep River and Sulphur Mountain neutron monitors indicated an increasing counting rate. The Sulphur Mountain super neutron monitor registered a 12% maximum increase at about 1052 UT; by 1130 UT, the counting rate was down to 4% above normal. The relativistic particle intensity increase at ground commenced a few minutes before increased counting rates were observed on VELA and the ATS-I satellites. The first increase in the flux of $21 \leq E_p \leq 70$ Mev observed by ATS-I occurred between 1050 UT and 1100 UT. The 30 and 50 MHz riometers at McMurdo Sound, Antarctica, registered the onset of polar cap absorption at about 1055 UT. The propagation time between the sun and earth for Gev protons was about 16 minutes; for low energy protons, the delay time was about 21 minutes. The peak 30 MHz absorption was 12.5 dB at 1330 UT.

Introduction

The solar cosmic ray event of 18 November 1968 was observed in space by particle detectors on such satellites as IMP-E, OGO-5 (1968-14A), ATS-I (1966-110A) and 1963-38C. It was also observed by ground-based instruments, including neutron monitors and polar-based riometers. The riometer data to be reported here were taken at the McDonnell Douglas Astronautics Company's (hereafter referred to as MDAC) Geophysical Observatories and were briefly discussed by Masley, et al. [1969].

The MDAC Antarctic Geophysical Observatory (77°51'S, 166°43'E) at McMurdo Sound began operation in February, 1962. The magnetically conjugate Arctic Observatory (68°49'N, 93°26'W) at Shepherd Bay, N.W.T., Canada, began operation in August, 1963. These stations, at geomagnetic latitudes of 80°, are located inside the polar cap regions, removed poleward from the auroral zones to minimize auroral interference and geomagnetic cutoffs. These stations include 30 and 50 MHz riometers, 27 kHz spherics receivers, magnetometers which monitor the horizontal component, and photometers at 3914 Å and 5577 Å.

Discussion

During its passage across the solar disk, McMath Plage Region 9760 was very inactive, producing no flares of importance 2 or greater until 18 November. The only visible flare that could be associated with the energetic proton emission was of importance 1B. It was in progress at 1030 UT, and located at N21 W87. However, due to the limb position its classification was probably underestimated. Type II solar radio emission was observed between 1026 UT and 1105 UT; Type IV was present between 1026 UT and 1050 UT.

According to the "provisional solar proton event" information in the ESSA Solar-Geophysical Data Report, No. 292, dated December 1968, the counting rates of the Deep River and Sulphur Mountain neutron monitors began to increase at 1045 UT, and recorded a maximum increase of 12% at 1052 UT. Table I lists the onset times for various physical events.

Table I - Event Onset Times on 18 November 1968

Event	Onset Time (UT)
Flare	1030 E (in progress)
SCNA	1024
Type II	1026.5
Type IV	1026.5
Neutron Monitors	1045
ATS-I ($E_p \geq 21$ Mev)	∿1050
30 MHz Riometer Absorption (McMurdo)	∿1055
Pioneer 8 ($E_p \geq 13.9$ Mev)	1113
Pioneer 9 ($E_p \geq 13.9$ Mev)	1116

According to Křivský and Švestka [1969], the main acceleration process occurs simultaneously with the phase of the fast separation of the bright flare ribbons (which coincides with the hard x-ray burst and the peak of the microwave radio flux). As this separation was observed to occur between 1029 UT and 1031 UT, the propagation time for relativistic protons was about 16 minutes; for protons of $E \leq 70$ Mev, approximately 21 minutes.

As is shown in the top half of Figure 1, 30 MHz riometer absorption could be identified to commence at McMurdo Sound, Antarctica, at about 1055 UT. Due to the presence of Type IV solar radio noise, an earlier time could not be determined. Shepherd Bay was experiencing day/night effects. The McMurdo absorption increased very rapidly, reaching a first peak of 9.8 dB at 1224 UT, only 1.5 hours after onset. It then proceeded to drop to about 6 dB in 20 minutes, and then rapidly increased to the maximum absorption of 12.5 dB at 1330 UT. Between 1330 UT and about 1900 UT, the absorption decreased from 12.5 dB to 6 dB, exhibiting large rapid fluctuations. The magnetometer trace of the horizontal component exhibited the same rapid time variation but was out of phase with the 30 MHz absorption by about 2 minutes. After 1900 UT the absorption began a gradual increase, reached a broad maximum of about 8 dB, and began to decay at 1600 UT, 19 November, reaching 1 dB at 2000 UT, 20 November. Three days later it returned to normal.

As can be seen in the lower half of Figure 1, the flux of protons of energies between 5 Mev $\leq E_p \leq$ 21 Mev and 21 Mev $\leq E_p \leq$ 70 Mev, as observed by ATS-I [Blake, private communication], also exhibited the same structure as the riometer absorption early in the event. The peaks of the proton flux profiles correspond with the riometer absorption peaks. These same variations were also observed by K. A. Anderson's ionization chamber and scatter counter on IMP-E [private communication].

Acknowledgement

We are indebted to the Office of Antarctic Programs, National Science Foundation, for its support of the work under Contract NSF C-393. This work was supported in part by the McDonnell Douglas Independent Research and Development Program. We thank J. W. McDonough, G. C. Nelson, and our station operators for their assistance in data reduction and overall program operation. Also, we acknowledge the cooperation of the Canadian Government for allowing us to operate our northern station.

REFERENCES

KŘIVSKÝ, L., and Z. ŠVESTKA 1969 The Solar Proton Flares of June and November 1968 and February 1969, presented at the COSPAR Panel on Polar Cap Experiments Meeting, Prague, May, 1969.

MASLEY, A. J., J. W. MCDONOUGH, and G. C. NELSON 1969 The 1968 Solar Cosmic Ray Events, Trans. Amer. Geophys. Union, 50, 304.

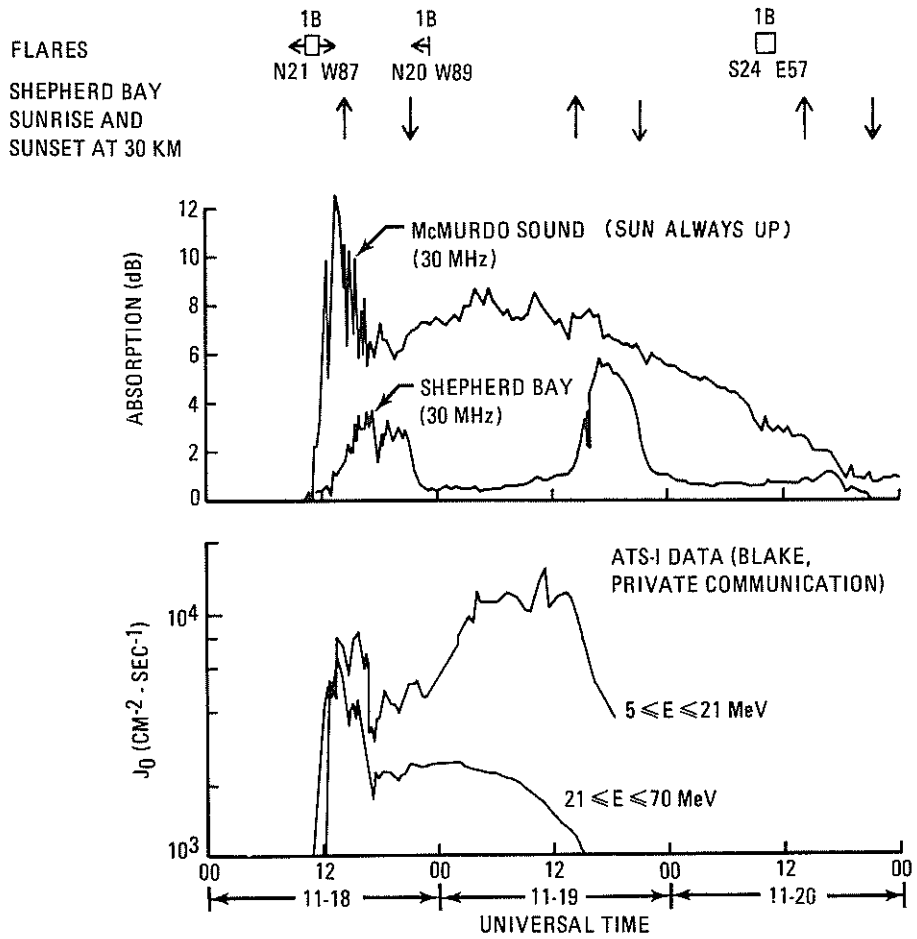
FLARES
SHEPHERD BAY
SUNRISE AND
SUNSET AT 30 KM
1B
N21 W87
1B
N20 W89
1B
S24 E57
ABSORPTION (dB)
McMURDO SOUND (SUN ALWAYS UP)
(30 MHz)
SHEPHERD BAY
(30 MHz)
ATS-I DATA (BLAKE,
PRIVATE COMMUNICATION)
J_0 (CM^{-2} · SEC^{-1})
5 ≤ E ≤ 21 MeV
21 ≤ E ≤ 70 MeV
11-18
11-19
11-20
UNIVERSAL TIME

"Comparison of Transpolar VLF Measurements with Riometer Measurements Made Within the Polar Cap During the PCA Event November 18, 1968"

by

K. Rinnert
Max-Planck-Institut für Aeronomie, Lindau/Harz, Germany

The VLF signal of the transmitter NPG/NLK (18.6 kHz) is continuously monitored at Lindau/Harz (German Federal Republic). The propagation path - with total length of 8,100 km - passes the arctic polar cap and reaches approximately at midway its geomagnetically most northern latitude of 82° Near this point is the riometer site at Godhavn. The cosmic noise of 30.5 MHz is received by a 2-element-Yagi-antenna directed to the zenith. These measurements are carried out by the ionospheric laboratory of the Danish Technical High School Lyngby in cooperation with the Max-Planck Institute for Aeronomy Lindau.

The Figure shows the comparison of these recordings during the solar proton event of November 18, 1968.

At the top there is a representation of the changes of solar illumination along the propagation path NPG-Lindau. The great circle arc is scaled as the ordinate, the upper and lower border correspond to the position of the transmitter NPG and to the receiver, respectively. The dashed line marks the location of the riometer site at Godhavn and the dotted lines represent the intersection points of the propagation path with the zone of maximum auroral frequency. The curves show the situation of the terminator at a height of 75 km taking into account a screening height of 30 km above the propagation path. The hatched regions represent nighttime conditions, that is, the solar zenith angle is greater than 96.5°.

In the middle the cosmic noise recordings from Godhavn, Greenland (30.5 MHz) are shown. The diode-current is recorded on a linear scale. At this time of the year the sun above Godhavn reaches its smallest zenith angle of 92° at about 16 hours UT. The increase of absorption caused by the proton impact starts at about 1135 UT. The riometer shows the biggest effect during "daytime conditions" in the lower ionosphere. During nighttime conditions there is a relatively small enhancement of absorption. Four days after the beginning of the effect the diurnal variations are normal again.

The recordings at the bottom of the figure represent the field strength (logarithmic scale) and the phase of the 18.6 kHz signal from NPG at Lindau. At 1040 UT on November 18, the signal strength decreases rapidly, by at least 25 dB, beyond a certain threshold and the phase detection stays. Up to the morning hours of the 20th of November the signal remains near this lower limit whereas the diurnal phase change is quite normal even on the 19th. The field strength increases slowly during the following days.

The attenuation of the VLF propagation during nighttime conditions especially is a very sensitive indicator for additional ionization in low altitudes as it is produced by high-energetic protons in the polar cap [Lange-Hesse and Rinnert, 1969]. The recovery of the nighttime field strength takes about 10 days with a time constant of about 3 dB per day. The phase is not very much affected, i.e., the diurnal changes are quite normal even if the absorption is still increased [Rinnert, 1967].

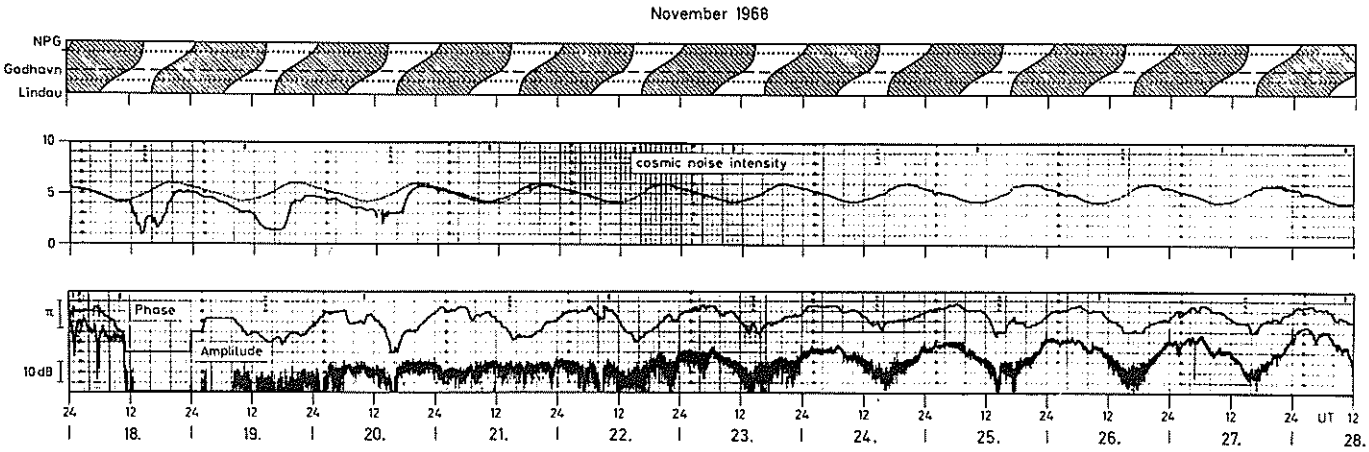

Fig. 1. Solar illumination, 30.5 MHz cosmic noise recordings at Godhavn, and amplitude and phase recordings of NPG (18.6 kHZ) at Lindau, November 18-27, 1968.

REFERENCES

RINNERT, K. 1967 Die Beeinträchtigung transpolarer Längstwellenausbreitung durch die solaren Protonen- und Plasma-Niederschläge am 3./4. September 1966, Kleinheubacher Berichte, Band 12, 261-264.

LANGE-HESSE, G. and K. RINNERT 1969 The reliability of transpolar VLF-measurements as a method to forecast HF-propagation disturbances, AGARD Conference Proceedings No. 49.

"Ionospheric Absorption Around November 18, 1968"

by

H. Schwentek
Max-Planck-Institut für Aeronomie, D 3411 Lindau (FRG)

The measurement of ionospheric absorption by field-strength recordings on the frequencies 2.61, 2.77 [Schwentek, 1966] and 6.09 MHz over paths of about 300 km, and by a riometer, the corner reflector antenna of which is directed to the Pole star [Schwentek, in press], showed mainly a sudden shortwave fadeout on November 18, 1968 as indicated in Table 1. The effect was very strong so that during its maximum the signal strengths of 2.61, 2.77 and 6.09 MHz were zero (total blackout). The cosmic noise record was disturbed by a solar radio burst occurring for a certain time interval during the fadeout.

Table 1

Characteristic data of the ionospheric effect (shortwave fadeout) on November 18, 1968 observed at Lindau (FRG; 51°39'N; 10°7.5'E). U = unreliable; N = value cannot be determined; d = distance.

Start UT	Maximum UT	End UT	Type	Absorption Δ L(dB)	Frequency (MHz)	Method	Remarks	d km
1026	N	U1230	S-SWF	> 15	2.61	A3	total blackout	296
1026	N	1206	S-SWF	> 13	2.77	A3	"	300
1027	N	1224	S-SWF	> 25	6.09	A3	"	339
1026	N (1100?)	1224	S-SWF	N (>2.0)	27.6	A2	partly disturbed	-

With the exception of the quoted SID on November 18 (Table 1) the riometer showed no clear effect during the daylight hours. However, the data obtained in the interval 18-20, and 20-22 MET (= UT + 1 h) indicate a small enhancement of absorption (Table 2) on November 18 to 20 (see also Figure 1 in the contribution by K. Rinnert on page 86 of this Report.

Table 2

Mean absorption L(27.6 MHz) in dB with regard to the quiet day curve in the interval 18-20 h and 20-22 h MET for the period November 15 to 26, 1968.

Date	Nov. 15	16	17	18	19	20	21	22	23	24	25	26
18-20 h	-0.05	0.10	0.05	0.14	0.05	0.16	0.04	0.02	0.05	-0.06	-0.03	-0.02
20-22 h	0.02	0.08	0.02	0.13	0.09	0.08	0.03	0.03	0.07	0.06	0.07	0.03

REFERENCES

SCHWENTEK, H. 1966 Annales de Géophysique 22, 276-288.

SCHWENTEK, H. and E. H. GRUSCHWITZ J. Atm. Terr. Phys., in press.

"Radio Propagation Quality Indices November 15-30, 1968"

by

B. Beckmann
Fernmeldtechnisches Zentralamt
Deutsche Bundespost, Darmstadt, G.F.R.

The table presents radio propagation quality indices prepared from observations of the transmission frequency ranges at three azimuths for both day and night radio propagation conditions. The observations were made at Lüchow 53.0°N, 11.2°E from selected transmitters located in the three areas: U.S.A., South America and East Asia. The only evidence of disturbance following the November 18 proton event is the slight decrease in quality, which does not reach storm level, for the night of November 19. A quality index of "6" represents normal conditions and values less than "6" are indicative of disturbance.

Radio Propagation Quality Indices
derived from observations of the transmission frequency range

November 1968

Date	USA - Germany		South America - Germany		East Asia - Germany	
	Day	Night	Day	Night	Day	Night
1	3.0	2.0	5.0	4.8	5.4	4.0
2	3.2	2.8	5.0	4.2	4.2	4.2
3	3.2	2.0	4.6	3.8	5.0	4.0
4	4.2	2.4	4.6	4.4	4.8	5.0
5	3.8	3.0	5.0	3.8	5.0	3.8
6	4.6	4.0	5.8	5.2	5.4	4.8
7	4.4	4.2	5.2	5.0	5.4	5.0
8	4.8	3.8	5.4	5.6	6.4	5.8
9	4.8	3.8	5.2	4.6	6.2	4.6
10	5.0	4.8	5.2	5.8	5.6	4.6
11	6.0	4.6	6.0	5.0	6.6	5.6
12	5.6	4.0	5.2	5.0	6.2	5.0
13	5.8	5.4	5.4	6.0	6.2	5.4
14	6.2	5.4	5.8	5.8	6.4	5.4
15	6.6	7.0	5.8	5.6	6.2	5.0
16	7.2	8.0	6.2	6.2	5.6	6.4
17	5.6	5.0	5.4	6.0	5.4	5.6
18	4.6	4.4	5.2	4.6	5.6	5.0
19	6.2	5.0	6.0	4.8	5.4	5.0
20	7.0	6.4	6.6	7.0	6.6	6.4
21	6.6	6.8	7.0	7.4	6.4	5.6
22	6.8	7.0	7.2	6.2	6.4	5.8
23	7.8	7.8	6.8	6.4	6.6	5.6
24	8.2	9.0	6.2	6.2	7.4	6.8
25	8.2	9.0	7.4	7.6	6.6	5.8
26	8.0	7.6	7.4	7.6	6.2	6.2
27	7.6	7.6	7.0	7.2	7.0	6.8
28	7.0	6.8	8.0	7.2	6.4	7.2
29	8.0	7.6	6.8	7.0	6.2	5.6
30	7.0	6.6	6.6	6.4	6.4	5.2

8. GEOMAGNETIC ACTIVITY

"Note on 'On the Solar and Geomagnetic Events of October-November 1968' by M. C. Ballario in World Data Center A - Upper Atmosphere Geophysics Report UAG-8, March 1970."

by

J. Virginia Lincoln
Space Disturbances Laboratory
ESSA Research Laboratories, Boulder, Colorado

This paper by M. C. Ballario covers the period of this Report UAG-9. She states:

"The importance 2 flare of November 12 is followed by very quiet geomagnetic conditions. On the contrary, the sc geomagnetic disturbance of November 20 might be due to the importance 1 proton flare, since there are no correlated CMPs of positive plages."

The flare referred to by M. C. Ballario is that from the IAU Quarterly Bulletin on Solar Activity of November 20, 1968, maximum at 0131 UT, position 21S 63E, importance 1N with remark U=close and somewhat parallel bright filaments (|| or Y shape), in McMath region 9780. She associated with this flare the geomagnetic storm of November 20 with Kp maximum about 1330 UT, Kp maximum value of 5- and delay time Δt_h from flare to storm about 12 hours.

"Equatorial Dst"

by

M. Sugiura and S. J. Cain
Goddard Space Flight Center
Greenbelt, Md.

The Figure presents the hourly equatorial Dst for November 10 to December 10, 1968. The Kp indices for the same period are also plotted on the Figure and the sudden commencements are indicated.

The table below is reproduced from the NASA Report X-612-70-3, Goddard Space Flight Center, Greenbelt, Maryland, January 1970 entitled "Provisional Hourly Values of Equatorial Dst for 1968" by M. Sugiura and S. J. Cain.

NOVEMBER 1968

UNIT=GAMMAS

DAY	1	2	3	4	5	6	7	8	9	10	11	12	13	14	15	16	17	18	19	20	21	22	23	24
																							S.M.T.	
1	-138	-121	-113	-109	-109	-106	-108	-107	-101	-87	-77	-69	-89	-111	-88	-124	-128	-131	-129	-159	-154	-183	-210	-192
2	-164	-172	-171	-173	-157	-156	-156	-156	-153	-123	-127	-120	-116	-109	-105	-97	-95	-79	-61	-56	-59	-67	-81	-91
3	-99	-108	-114	-103	-100	-101	-97	-90	-86	-82	-75	-71	-61	-67	-70	-71	-66	-59	-63	-66	-67	-70	-73	-69
4	-65	-62	-61	-61	-57	-45	-47	-57	-61	-54	-46	-41	-47	-51	-52	-50	-46	-43	-43	-41	-48	-46	-40	-42
5	-44	-44	-45	-43	-44	-44	-46	-47	-46	-45	-43	-39	-35	-33	-31	-35	-35	-34	-25	-25	-27	-27	-29	-26
6	-25	-23	-26	-30	-23	-29	-30	-28	-25	-23	-23	-25	-25	-22	-21	-20	-19	-17	-12	-15	-18	-13	-13	-28
7	-37	-34	-38	-43	-46	-53	-44	-39	-35	-35	-36	-41	-39	-39	-30	-24	-23	-23	-24	-21	-18	-18	-18	-20
8	-19	-19	-19	-21	-21	-24	-27	-25	-25	-26	-26	-23	-33	-29	-32	-32	-29	-27	-20	-21	-30	-32	-34	-36
9	-38	-36	-31	-32	-30	-23	-21	-20	-24	-22	-25	-18	-18	-29	-35	-36	-33	-26	-23	-21	-19	-20	-20	-18
10	-20	-19	-19	-20	-20	-25	-28	-29	-27	-27	-27	-23	-21	-18	-13	-18	-22	-25	-27	-24	-27	-29	-28	-27
11	-22	-26	-32	-28	-29	-32	-34	-29	-25	-28	-29	-30	-32	-26	-23	-23	-21	-23	-20	-15	-15	-16	-17	-18
12	-18	-14	-15	-16	-17	-13	-18	-16	-13	-13	-14	-16	-15	-15	-12	-8	-8	-6	-4	-4	-4	-3	-3	-4
13	-3	-2	1	1	-1	-4	-3	-2	3	1	-0	-1	-0	2	2	-1	-4	-4	-1	-3	-11	-11	-7	-6
14	-7	-6	-6	-2	1	-0	-0	3	5	4	5	6	8	12	13	10	9	3	7	6	6	-3	4	9
15	9	10	8	10	10	10	9	3	3	2	1	2	3	2	1	-0	-3	-2	-1	1	0	1	1	1
16	1	1	0	1	-1	-0	0	1	6	20	27	37	37	33	49	50	49	43	42	33	19	5	-5	8
17	6	-3	3	1	1	-3	-10	-7	-14	-15	-11	-9	-5	-2	-11	-22	-29	-42	-42	-44	-57	-65	-66	-61
18	-54	-50	-53	-59	-61	-63	-67	-70	-67	-53	-48	-46	-43	-37	-29	-25	-14	-8	-11	-13	-15	-22	-27	-27
19	-28	-23	-24	-27	-30	-34	-35	-30	-23	-17	-16	-18	-19	-13	-11	-9	-7	-4	-4	-8	-12	-10	-7	-4
20	-5	-3	-6	-18	-17	-15	-4	-2	-3	18	21	17	12	-3	-20	-36	-33	-37	-40	-39	-31	-24	-19	-18
21	-17	-14	-15	-19	-22	-21	-20	-24	-29	-27	-26	-25	-24	-21	-19	-20	-24	-25	-28	-23	-18	-18	-23	-22
22	-20	-19	-17	-15	-13	-11	-14	-16	-19	-20	-16	-13	-11	-10	-5	-1	-0	1	3	-1	-1	-3	-3	-1
23	-0	-2	-5	-8	-10	-6	-3	-6	-8	-12	-11	-10	-8	-3	-1	2	4	8	10	9	8	8	11	16
24	20	22	19	16	14	15	17	18	19	19	17	17	15	15	13	19	29	28	25	24	25	25	24	21
25	16	12	14	16	18	17	15	18	18	13	8	6	3	-2	1	-1	-3	-0	-3	-7	-3	-1	-1	-1
26	1	3	5	5	6	10	10	9	4	0	-3	2	4	7	4	-0	-3	-3	1	-2	-3	1	-4	-6
27	-0	-4	-3	-5	-6	-3	-4	-8	-9	-9	-5	-4	-1	0	3	1	3	6	8	-7	-11	-10	-5	-7
28	-9	-4	-4	-4	-2	0	3	1	-3	-8	-12	-12	-9	-4	-3	-3	-3	1	-7	-2	5	13	8	7
29	8	10	12	10	5	6	5	2	1	1	-3	0	-1	-5	-5	-4	0	1	2	3	5	4	4	4
30	4	6	5	2	1	4	7	8	8	5	6	6	1	-0	1	1	3	2	-1	-1	-3	1	1	-3

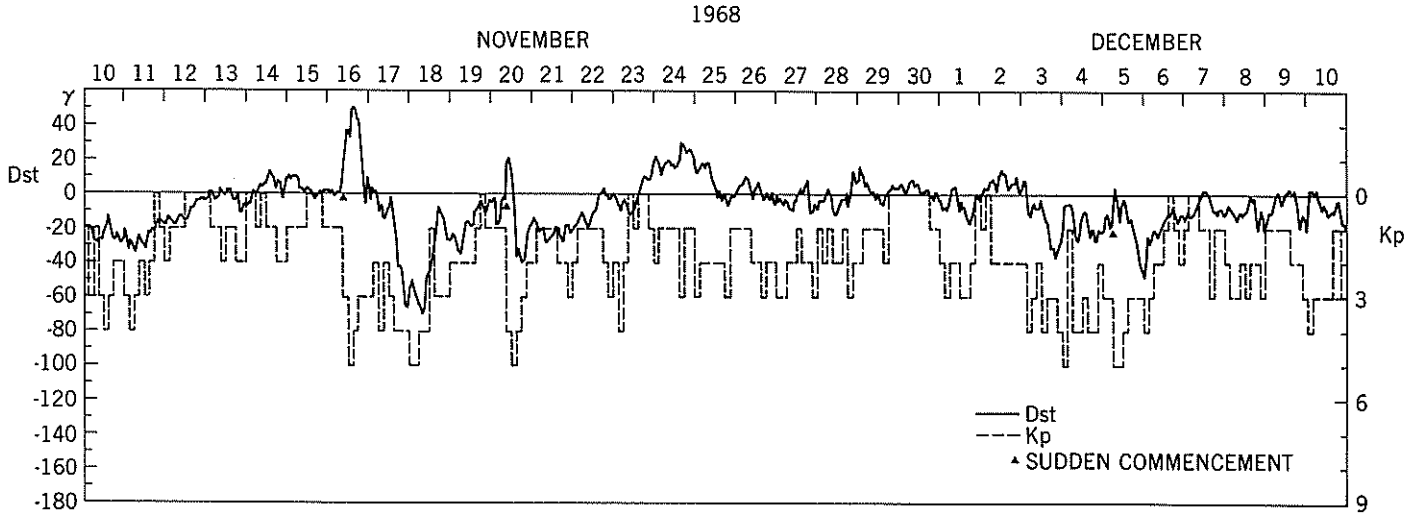

Fig. 1. Hourly equatorial Dst November 10 - December 10, 1968.

"Geomagnetic Disturbances During the Period November 16-21, 1968 Associated with the McMath Plage Regions 9760, 9772 and 9780"

by

K. Kawasaki and S.-I. Akasofu
Geophysical Institute, University of Alaska
College, Alaska 99701

ABSTRACT

A compilation of magnetograms of selected observatories for the period November 16-21, 1968 is presented. The period covered includes a large Forbush decrease in cosmic rays which began during November 16, 1968 and the intense cosmic ray increase of November 18, 1968. The Forbush decrease and the geomagnetic storm of November 16/18, 1968 were probably associated with the McMath plage region 9772 and the solar cosmic ray increase and the weak geomagnetic storm of November 20/21, 1968 with the plage region 9760.

Major si are identified for this moderately disturbed period.

Magnetograms compiled from observatories widely dispersed in longitude show that the period November 16-21, 1968 was only moderately disturbed. A moderate Forbush decrease and a solar proton event were also observed during this period [Venkatarangan, et al., 1969; "Solar-Geophysical Data", January 1969]. It is of interest to study in detail the geomagnetic disturbances and to identify the probable regions producing the enhanced geomagnetic activity.

Table 1 is a summary of the geomagnetic activity in terms of the three-hourly Kp indices and sum of Kp during the period. The indices for the three days prior to November 16 are also tabulated and show only minor activity was recorded on November 14 and 15, both being designated as International Quiet Days.

Table 1

1968	THREE HOURLY KP INDICES								KP SUM
November 13	0+	1-	1	2	1+	1+	2+	2+	11+
November 14	0+	0+	1-	0+	1	1	2-	2	7+
November 15	1-	1+	1	1-	0	0+	0+	1-	5
November 16	1+	1	1-	3	5-	4+	3+	3+	22-
November 17	3+	2	4-	2	3	4	4+	4-	26
November 18	5-	5-	4	4-	1+	3	3-	3+	27+
November 19	2+	2	2-	2+	2	1+	0	1-	12+
November 20	1-	1	1	4+	5-	4	3+	2-	21-
November 21	2-	1	1-	1-	1-	2+	2+	3	12+

Table 2 is a list of 27 flares numbered consecutively which occurred during the period November 13-21, 1968 and which were reported to be of Importance ≥ 1 by at least one observatory. The flares of the three days prior to November 16 are included to allow for the transit time between the beginning of a flare and the subsequent arrival of flare particles at the orbit of the earth.

There were only four major regions of flare activity - McMath plage regions 9760, 9768, 9772 and 9780, which will be designated as M9760, M9768, M9772 and M9780. M9768 produced only one of the 27 flares. M9760 was first observed on the eastern limb of the sun on November 4 and passed out of the field of view on the western limb on November 18. M9772 appeared on the eastern limb on November 13; it did not pass out of view during the interval studied. M9780 was first noted near the eastern limb on November 19.

Table 2

FLARE NUMBER	DATE: 1968	START UT	PLAGE REGION	APPROXIMATE LATITUDE & MERIDIAN DISTANCE	IMPORTANCE
1	November 13	0015	M9760	N18, W15	1B
2	November 13	0910	M9772	N24, E90	1B
3	November 13	1103	M9760	N19, W21	1B
4	November 13	1248	M9760	N19, W21	1B
5	November 13	1411	M9772	N18, E82	1B
6	November 13	1716	M9760	N17, W28	1N
7	November 14	2038	M9772	N13, E65	1F
8	November 14	2148	M9760	N19, W45	1F
9	November 14	2254	M9772	N14, E66	1F
10	November 15	1030	M9772	N14, E60	1B
11	November 15	1520	M9768	N10, E05	1B
12	November 16	0033	M9760	N17, W65	1N
13	November 16	0127	M9772	N13, E52	1F
14	November 16	2154	M9760	N16, W65	1N
15	November 16	2359	M9760	N20, W67	1N
16	November 17	0103	M9760	N17, W67	1N
17	November 17	0244	M9760	N13, W67	1B
18	November 17	0707	M9772	N10, E35	1B
19	November 18	0747	M9772	N11, E19	1F
20	November 18	1026	M9760	N20, W90	1B
21	November 18	1504	M9772	N11, E15	1F
22	November 19	0141	M9780	S17, E85	1N
23	November 20	0118	M9780	S18, E60	1N
24	November 20	0925	M9780	S24, E57	1B
25	November 20	1215	M9780	S20, E55	1N
26	November 20	1956	M9780	S17, E58	1N
27	November 21	0031	M9772	N14, W18	1B

The consensus of solar observatories is that all the flares during the period November 13-21, 1968 associated with the above mentioned plage regions were of Importance $\leq$ 1; however, two of the flares were reported to be of Importance 2 by one of the observatories in each case. They are listed as 10 and 20 in Table 2. These flares may be responsible for the geomagnetic storms of November 16/18 and 20/21.

Figure 1 illustrates the H-component magnetic record of Honolulu, the probable interval of arrival of flare particles for the flares listed in Table 2, and the identifiable si during the period November 16-21, 1968. The numbers from 1 through 27 for the flares are the same as in the enumeration scheme of Table 2. The dashed portion represents the first 20 hours <u>after</u> the flare was sighted; the solid portion represents the next 52 hours. The interval of 20-72 hours from

flare sighting is the most probable for a flare to produce identifiable si and ssc observed at the surface of the earth; the average time is about 40 hours [Akasofu and Yoshida, 1967].

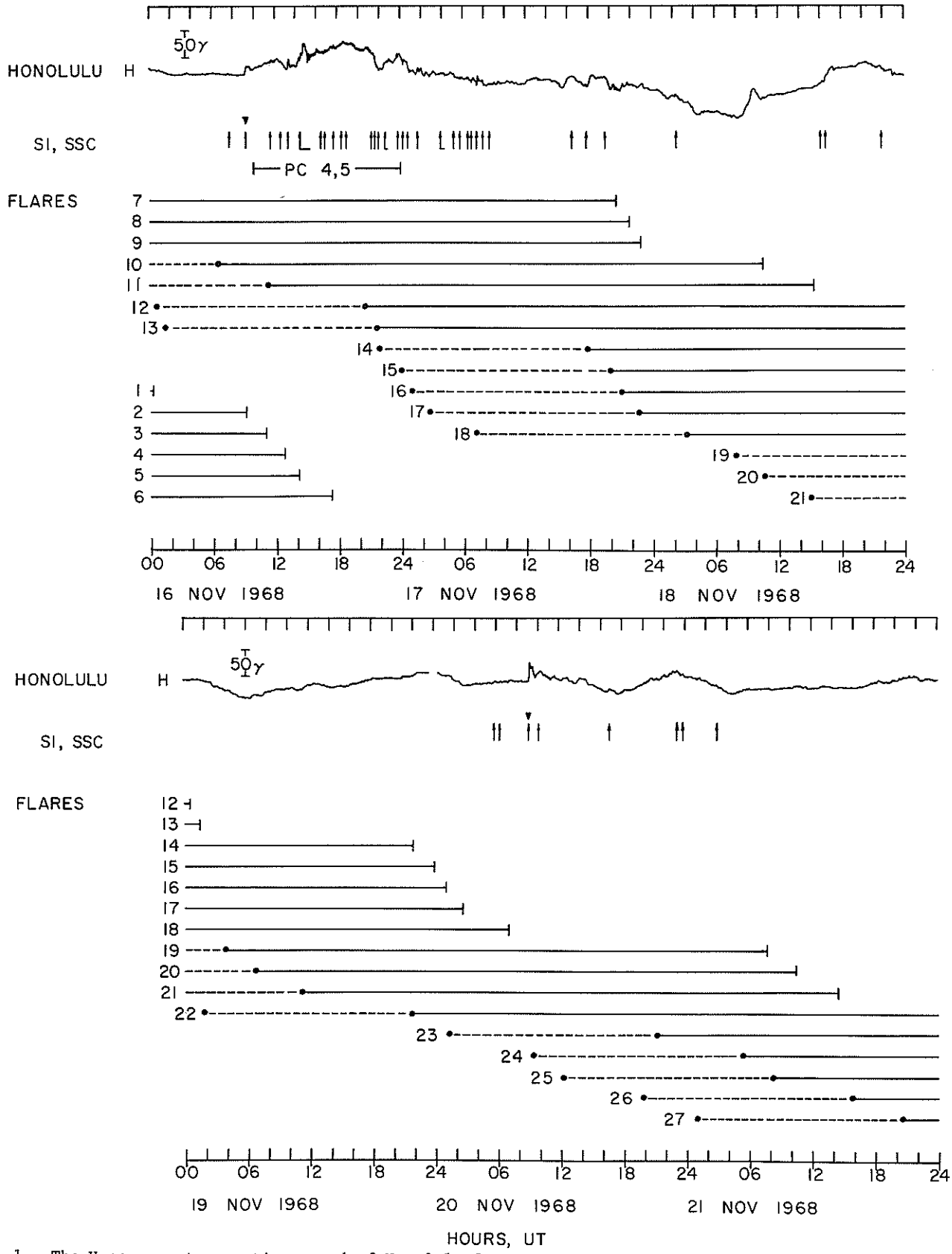

Fig. 1. The H-component magnetic record of Honolulu for the period November 16-21, 1968. The major si are indicated by arrows and reported ssc by triangles over arrows. Dotted and solid horizontal lines represent the first 20 hours and the next 52 hours, respectively, after flares of Importance ≥1 were observed. The numbers from 1 through 27 identifying the flares are the same as those in Table 2.

Only two geomagnetic storms were reported during the interval. Figures 2a through 7b are a compilation of magnetic records from sets of high and low latitude stations which show the development of the two storms; unfortunately, Siberian data were not available at the date of writing.

The first geomagnetic storm began with a small ssc at 0916 UT on November 16. The ssc was followed by a number of complicated worldwide geomagnetic disturbances. Thus, it is inferred that the solar wind flow behind the shock wave, which passed near the earth at 0916 UT, was quite "turbulent" or "structured". The "turbulent" flow lasted until about 07 UT on November 17 [Yoshida and Akasofu, 1966]. It is interesting to note that it is this period when the flux of the galactic cosmic rays decreased by an amount of about 7%.

Flares 1 through 6 are unlikely to be the cause of the disturbed period of November 16/18; they were of minor importance and the transit times for their particles were improbably long. Flare 10 of the region M9772 was of sufficient intensity and its particles had enough transit time to have caused the ssc and storm of November 16/18; however, Flares 7, 8, 9 and 11 cannot entirely be excluded as the cause of the ssc while Flares 7, 8, 9, 11, 12 and 13 cannot be excluded as the cause of the main phase decrease.

As mentioned previously, the initial part of the November 16/18 geomagnetic storm was very complex. At low latitudes a number of si were observed and at both high and low latitudes, large micropulsations were in evidence. Although Flare 10 probably caused the ssc of November 16 and possibly the si that followed, some of the si during the initial phase may have been caused by Flares 7 through 9 and 11 through 13. The observed Forbush decrease and plasma cloud transit time to ssc were more or less characteristic of a far eastern flare [Akasofu and Yoshida, 1967; Haurwitz, et al., 1965], which is further confirmation that Flare 10 was responsible for the storm of November 16/18.

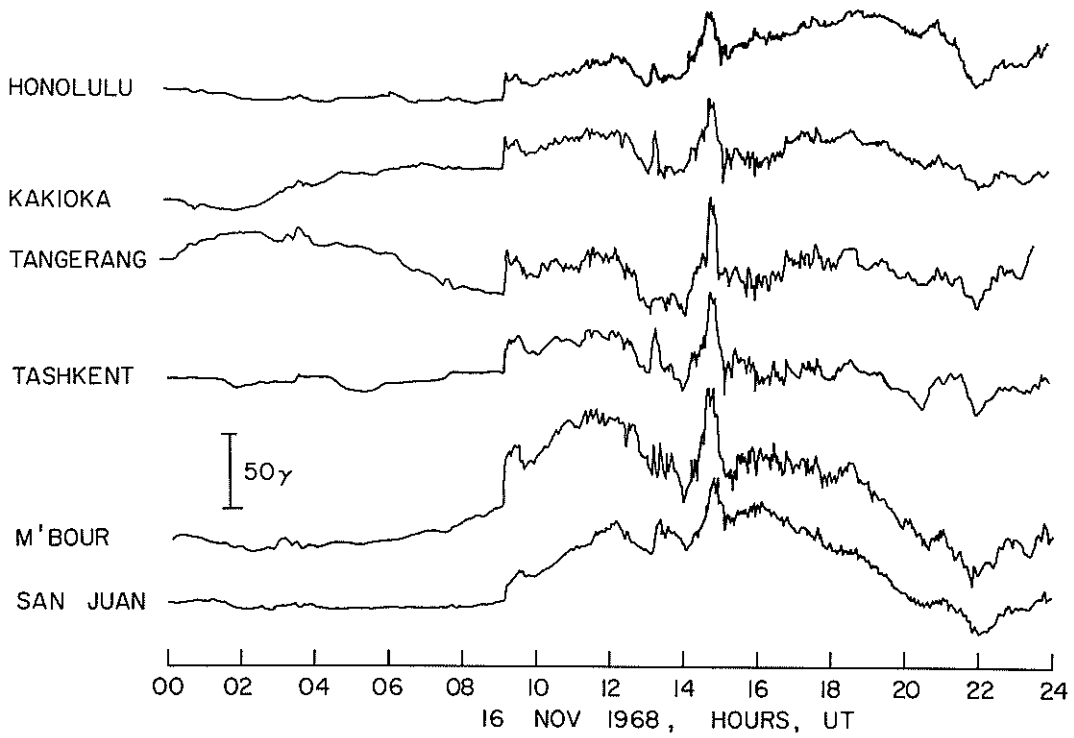

Fig. 2a. H-component magnetic records of six low latitude stations for November 16, 1968.

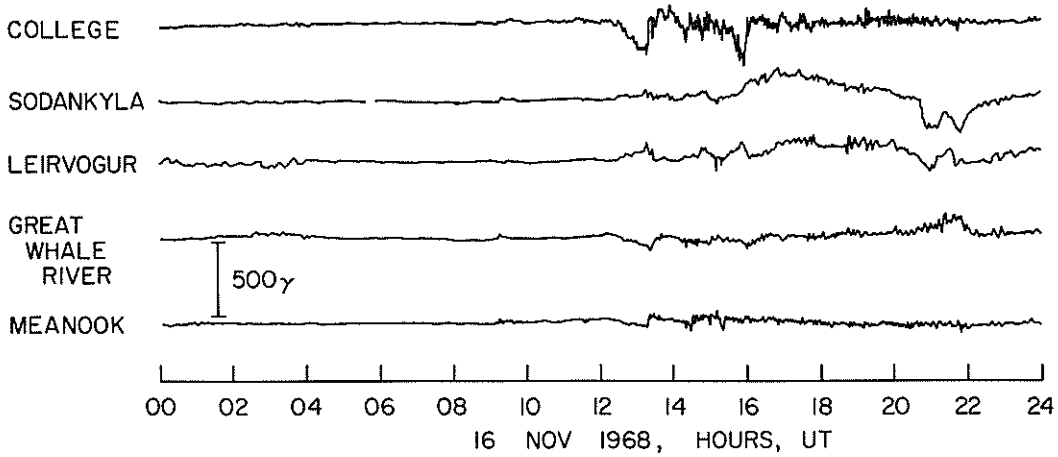

Fig. 2b. H-component magnetic records of five high latitude stations for November 16, 1968.

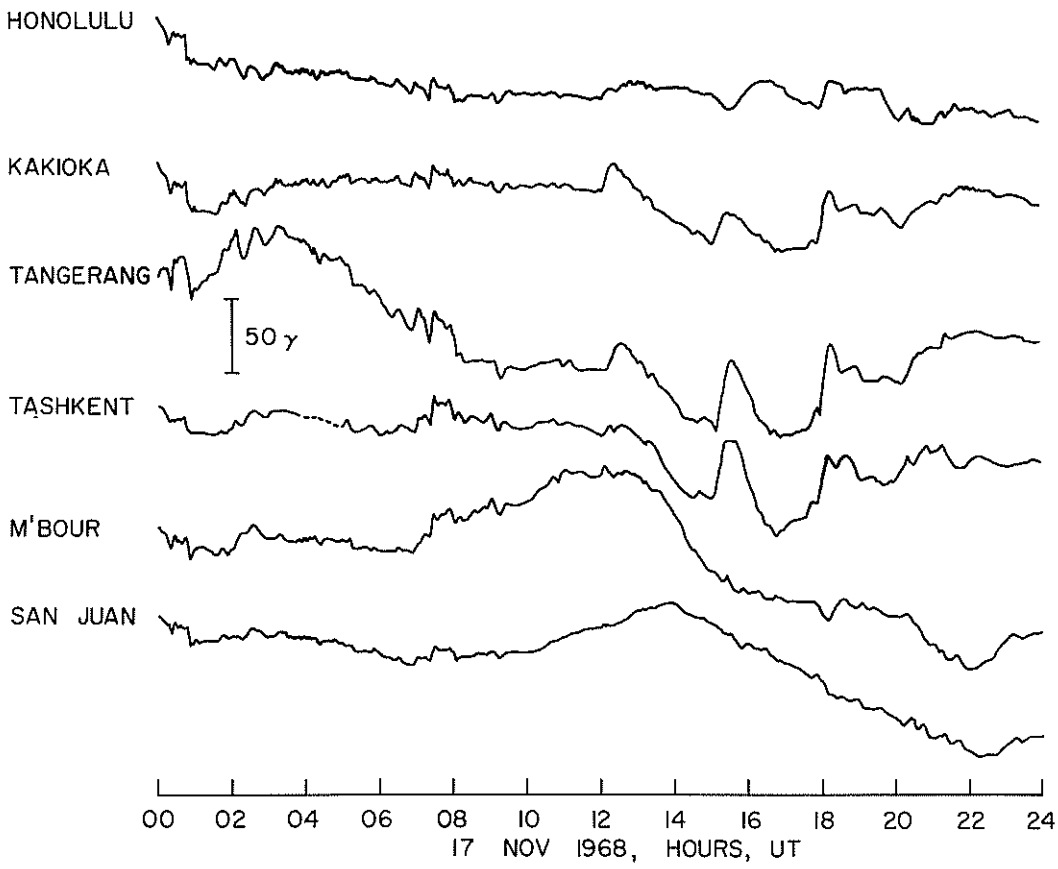

Fig. 3a. H-component magnetic records of six low latitude stations for November 17, 1968.

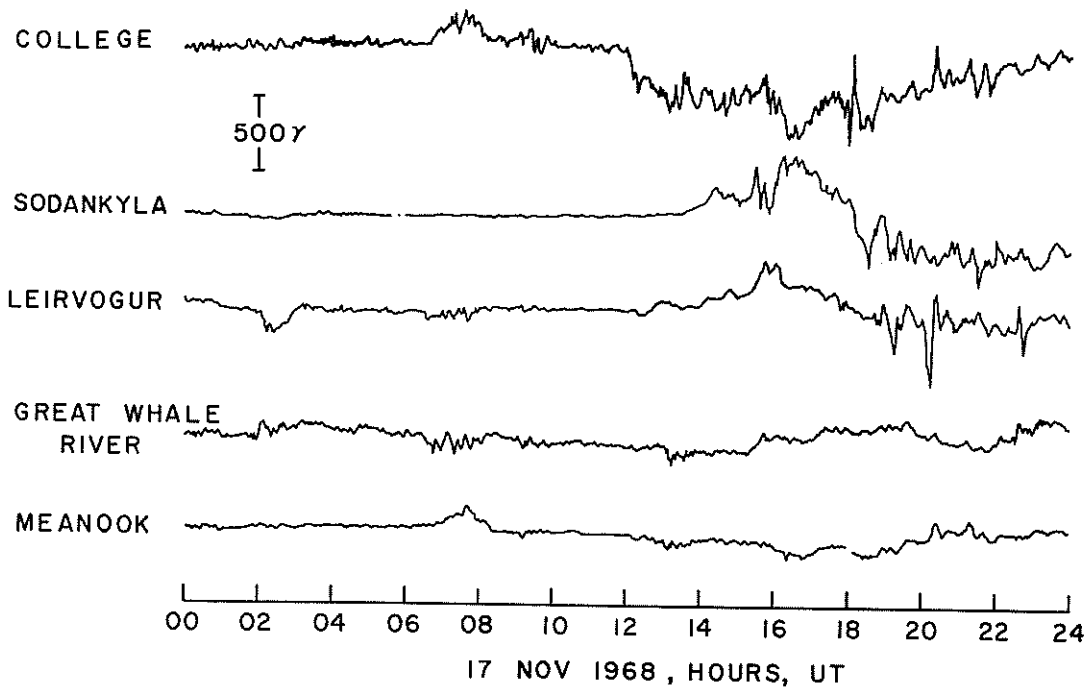

Fig. 3b. H-component magnetic records of five high latitude stations for November 17, 1968.

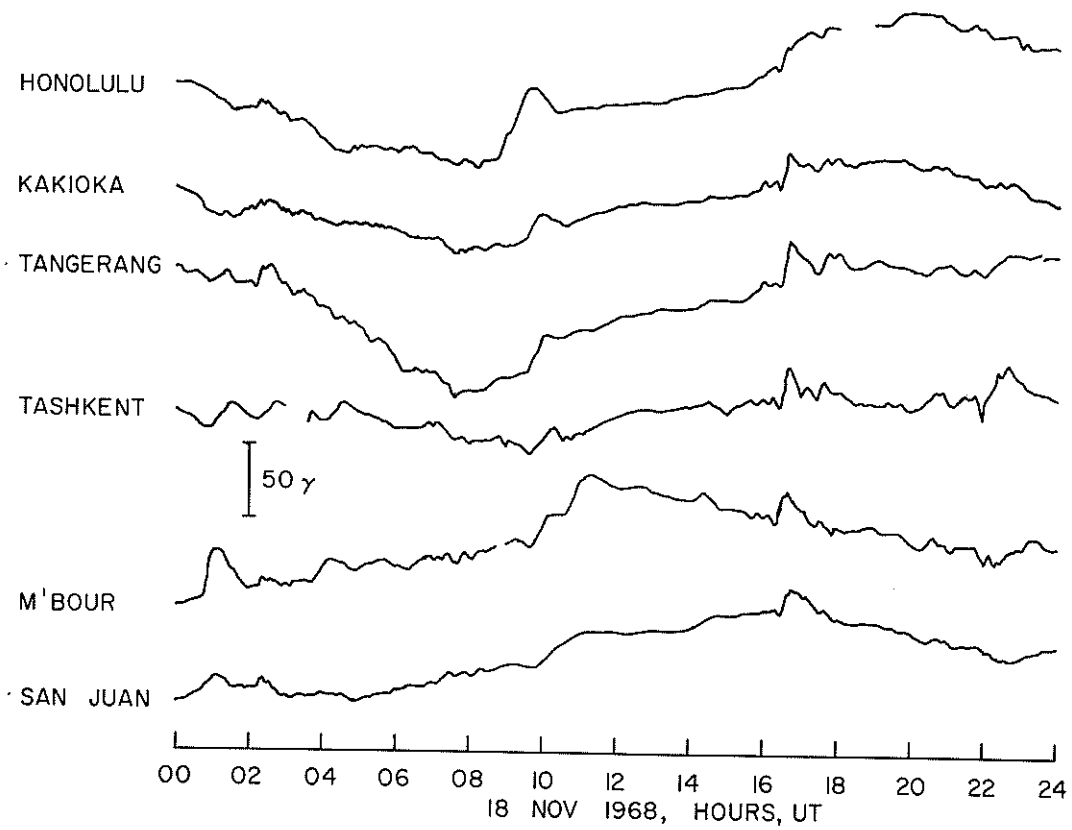

Fig. 4a. H-component magnetic records of six low latitude stations for November 18, 1968.

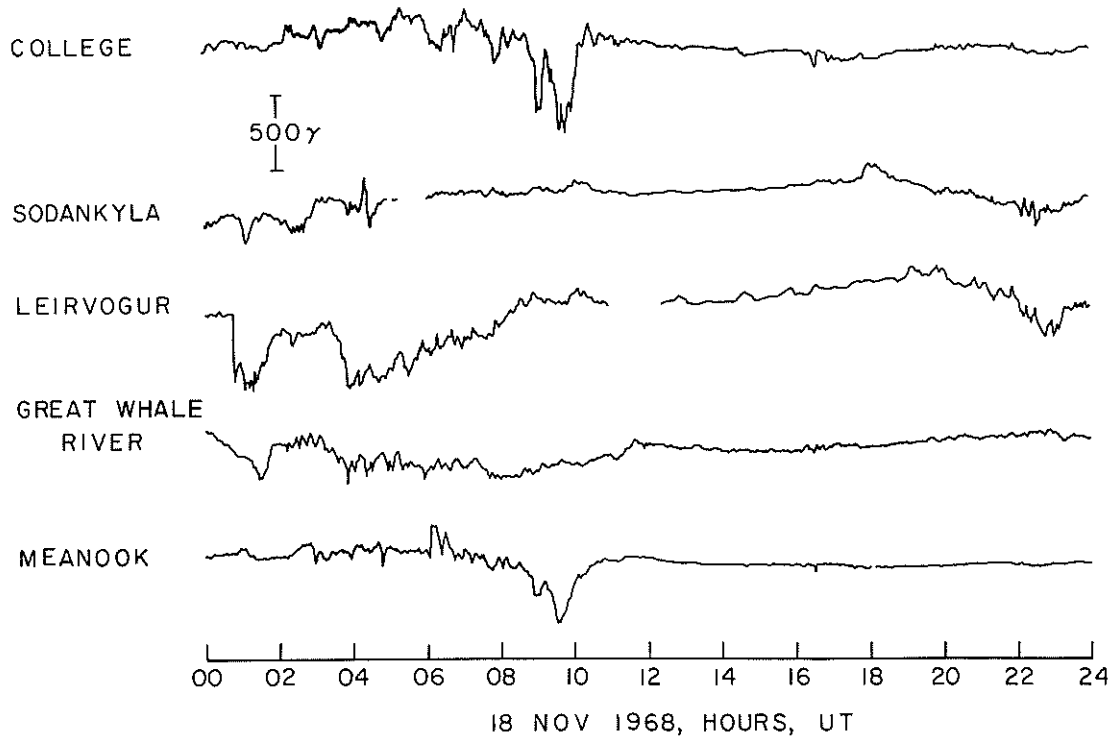

Fig. 4b. H-component magnetic records of five high latitude stations for November 18, 1968.

The decrease in the H-component associated with this disturbed period began about 1200 UT, November 17 reaching a minimum of about 100 gammas around 20 UT November 17; by 1200 UT of November 18 the storm was well in its recovery phase. Three rather large positive bays were recorded at low latitude stations in the Asian sector (Figures 3a and 4b). Bays are known to occur when intense polar substorms are in progress along the midnight sector of the auroral oval. The records for high latitudes, Figures 3b and 4b, although lacking Siberian data, indicate polar substorms were in progress during the main and recovery phases of the storm.

These polar substorms were especially intense when the ring current became asymmetric. This can be seen particularly during the recovery phase of the storm when the high latitude stations whose records were available were in a favorable position to record polar substorms along the midnight portion of the auroral oval. This rough direct correlation between polar substorms and ring current asymmetry is less evident during the main phase decrease probably due to the lack of Siberian data.

Flares 14 through 18 did not appear to have produced significant geomagnetic activity except possibly for the few si which occurred during the latter part of November 17 and November 18.

At approximately 1630 UT on November 18, a fairly isolated large si was observed (Figure 4a). The simultaneous high latitude records (Figure 4b) show very little disturbance. This event might be classified as the beginning of a magnetic storm which did not develop a main phase, but its rise was quite gradual (~ 20 minutes). This large si could have been caused by any one of the Flares 14 through 18. However, its large amplitude is suggestive of a central meridian flare [Akasofu and Yoshida, 1967]. Of the Flares 14 through 18, Number 18 occurred closest to the central meridian. No noticeable Forbush decrease was associated with the si ["Solar-Geophysical Data", January, 1969].

By the latter part of November 19, the geomagnetic storm which began on November 16 had fully recovered (Figures 5a and b) and this relatively quiet condition continued through the early part of November 20 (Figures 6a and b).

The second geomagnetic storm of the period of study began with a large ssc at 0904 UT on November 20 (Figures 6a and b). Note a "precursor"-like si activity which preceded the ssc. The

main phase decrease began about 13 UT reaching about 100 gammas some six to ten hours after ssc; by midday of November 21 recovery was well underway (Figures 7a and b).

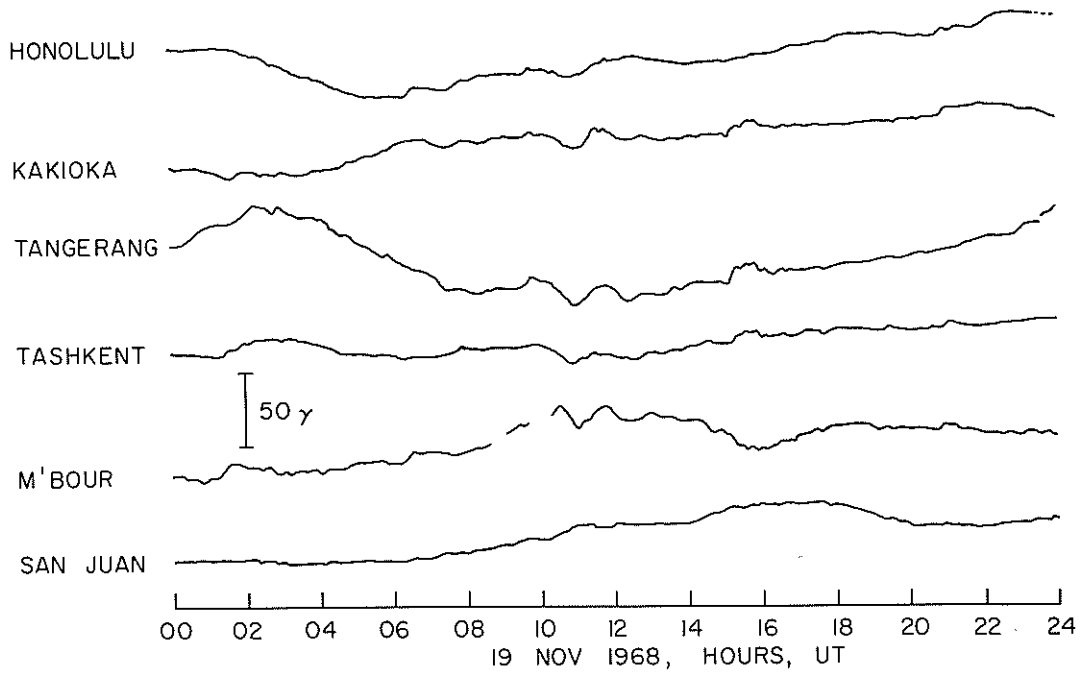

Fig. 5a. H-component magnetic records of six low latitude stations for November 19, 1968.

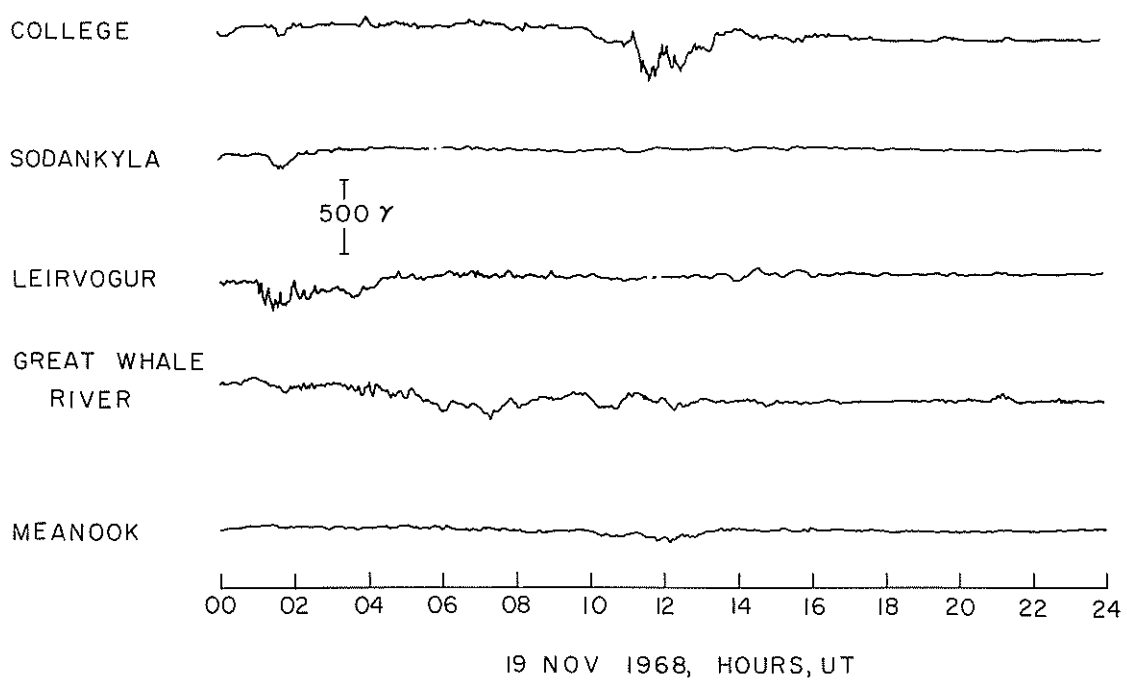

Fig. 5b. H-component magnetic records of five high latitude stations for November 19, 1968.

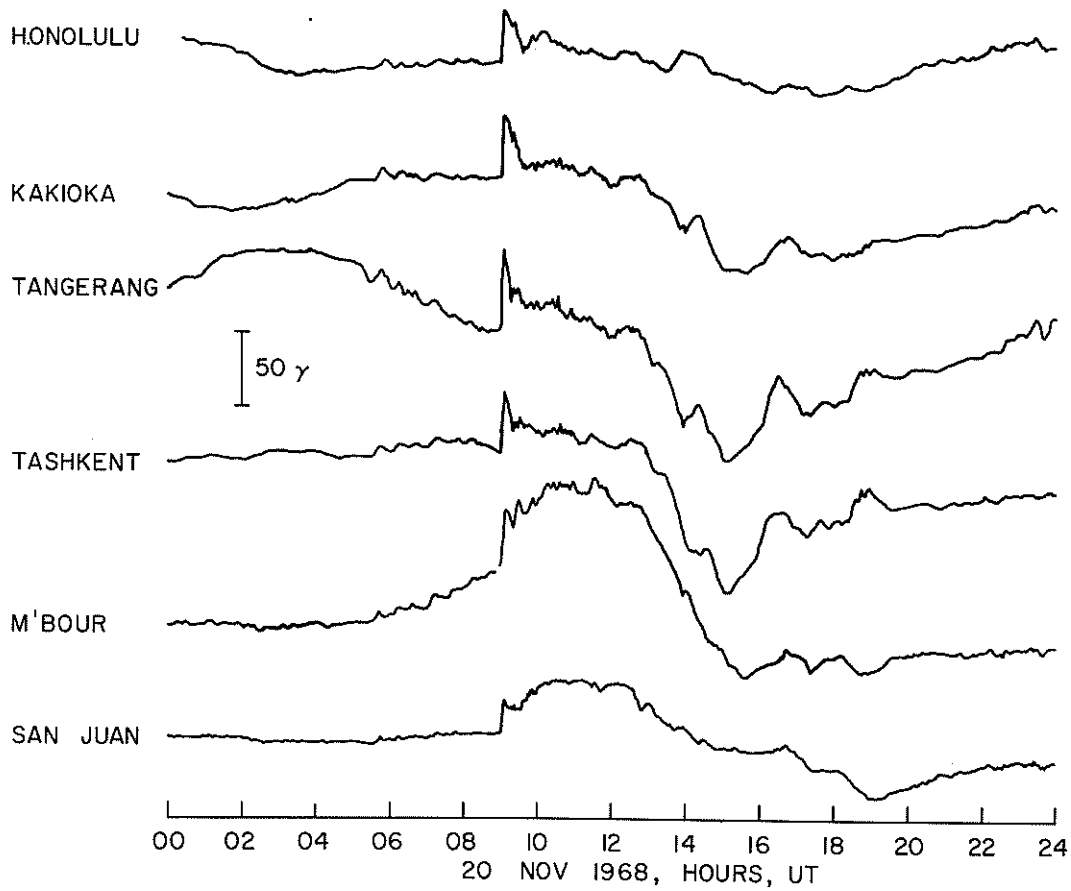

Fig. 6a. H-component magnetic records of six low latitude stations for November 20, 1968.

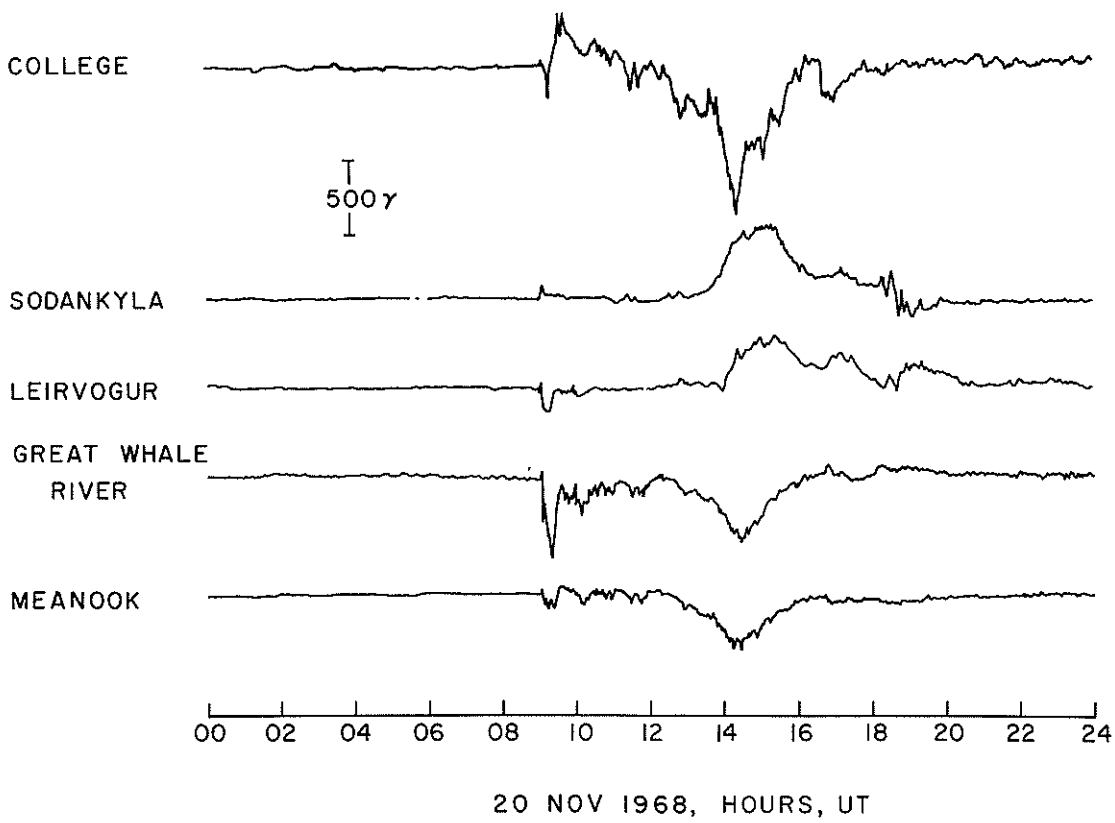

Fig. 6b. H-component magnetic records of five high latitude stations for November 20, 1968.

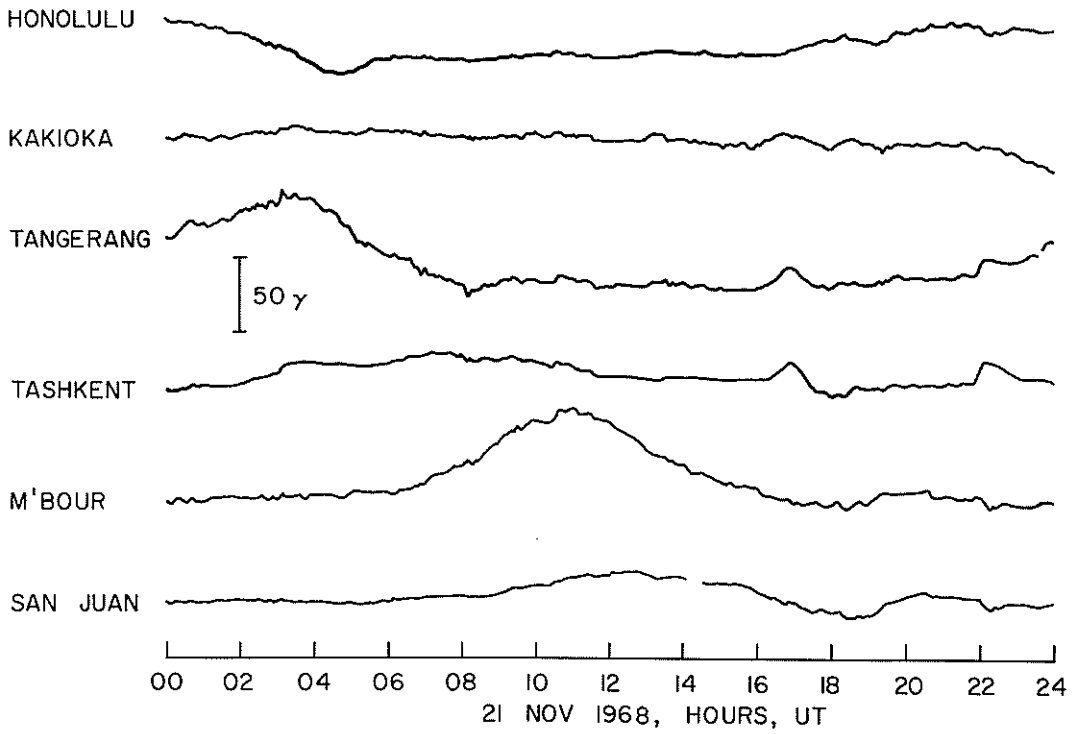

Fig. 7a. H-component magnetic records of six low latitude stations for November 21, 1968.

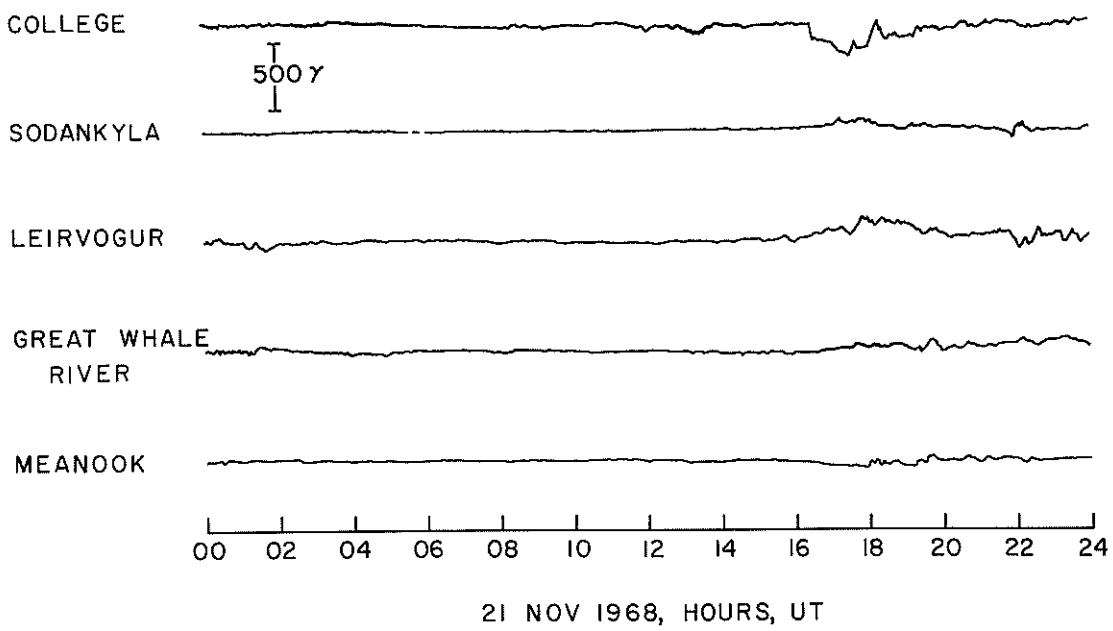

Fig. 7b. H-component magnetic records of five high latitude stations for November 21, 1968.

The growth of the main phase was observed in the afternoon-evening sector (Kakioka (22 LT), Tangerang (20 LT), Tashkent (18 LT) and M'Bour (12 LT)). However, it was not observed in the morning sector (Honolulu (03 LT) and San Juan (09 LT)). San Juan observed the later part of the main phase after 16 UT, when it moved into the afternoon sector. However, by the time Honolulu reached the afternoon sector, the main phase was near the end of its recovery. Thus, no large main phase decrease was observed at Honolulu during this brief storm.

Of the remaining flares (Numbers 19 through 27) only Flares 19 through 22 were likely to have caused the ssc of the second geomagnetic storm. The amplitude of the ssc and the accompanying Forbush decrease (about 4%) were more indicative of a central meridian or eastern limb flare rather than a western limb flare. However, the central and eastern limb Flares 19, 21 and 22 were not intense. Flare 20 although not significantly more intense optically was associated with large increases in solar protons and x-rays among others [Venkatarangan, et al., 1969]. Moreover, the high latitude magnetic records (Figure 6b) show significant polar substorm activity at the time of ssc and return currents from the high latitudes may have enhanced the amplitude of the ssc at low latitudes. Thus, it is likely the western limb Flare 20 of M9760 was responsible for the geomagnetic storm of November 20/21, 1968.

Flares 23 through 27 appear to have produced only minor worldwide magnetic disturbances during the latter part of the period under study.

Acknowledgement

National Science Foundation Grant GA-1703 and the efficient service of Mr. W. Paulishak of World Data Center A for Geomagnetism in providing magnetograms made this study possible.

REFERENCES

AKASOFU, S.-I. and S. YOSHIDA 1967 The structure of the solar plasma flow generated by solar flares, Planet. Space Sci., 15, 39-47.

HAURWITZ, M. W., S. YOSHIDA, and S.-I. AKASOFU 1965 Interplanetary magnetic field asymmetries and their effects on polar cap absorption events and Forbush decreases, J. Geophys. Res., 70, 2977-2988.

VENKATARANGAN, P., D. VENKATESAN, and J. A. VAN ALLEN 1969 Solar flare increases in cosmic ray intensity on November 18, 1968; February 25, 1969; and March 30, 1969, U. of Iowa Report, 69-47.

YOSHIDA, S. and S.-I. AKASOFU 1966 The development of the Forbush decrease and the geomagnetic storm fields, Planet. Space Sci., 14, 979-986.

USCOMM-ESSA-ASHEVILLE-4-25-70-1100

Upper Atmosphere Geophysics Report UAG-1
"IQSY Night Airglow Data" by L. L. Smith, F. E. Roach, and J. M. McKennan of Aeronomy Laboratory, ESSA Research Laboratories, July 1968, single copy price $1.75.

Upper Atmosphere Geophysics Report UAG-2
"A Reevaluation of Solar Flares, 1964-66" by Helen W. Dodson and E. Ruth Hedeman of McMath-Hulbert Observatory, The University of Michigan, August 1968, single copy price 30 cents.

Upper Atmosphere Geophysics Report UAG-3
"Observations of Jupiter's Sporadic Radio Emission in the Range 7.6-41MHz, 6 July 1966 through 8 September 1968" by James W. Warwick and George A. Dulk, Department of Astro-Geophysics, University of Colorado, October 1968, single copy price 30 cents.

Upper Atmosphere Geophysics Report UAG-4
"Abbreviated Calendar Record 1966-67" by J. Virginia Lincoln, Hope I. Leighton and Dorothy K. Kropp of Aeronomy and Space Data Center, Space Disturbances Laboratory, ESSA Research Laboratories, January 1969, single copy price $1.25.

Upper Atmosphere Geophysics Report UAG-5
"Data on Solar Event of May 23, 1967 and its Geophysical Effects" compiled by J. Virginia Lincoln, World Data Center A, Upper Atmosphere Geophysics, ESSA, February 1969, single copy price 65 cents.

Upper Atmosphere Geophysics Report UAG-6
"International Geophysical Calendars 1957-1969" by A. H. Shapley and J. Virginia Lincoln, ESSA Research Laboratories, March 1969, single copy price 30 cents.

Upper Atmosphere Geophysics Report UAG-7
"Observations of the Solar Electron Corona: February 1964 - January 1968" by Richard T. Hansen, High Altitude Observatory, Boulder, Colorado and Kamuela, Hawaii, October 1969, single copy price 15 cents.

Upper Atmosphere Geophysics Report UAG-8
"Data on Solar Geophysical Activity October 24 - November 6, 1968" compiled by J. Virginia Lincoln, World Data Center A, Upper Atmosphere Geophysics, ESSA, March 1970, single copy price $1.75.